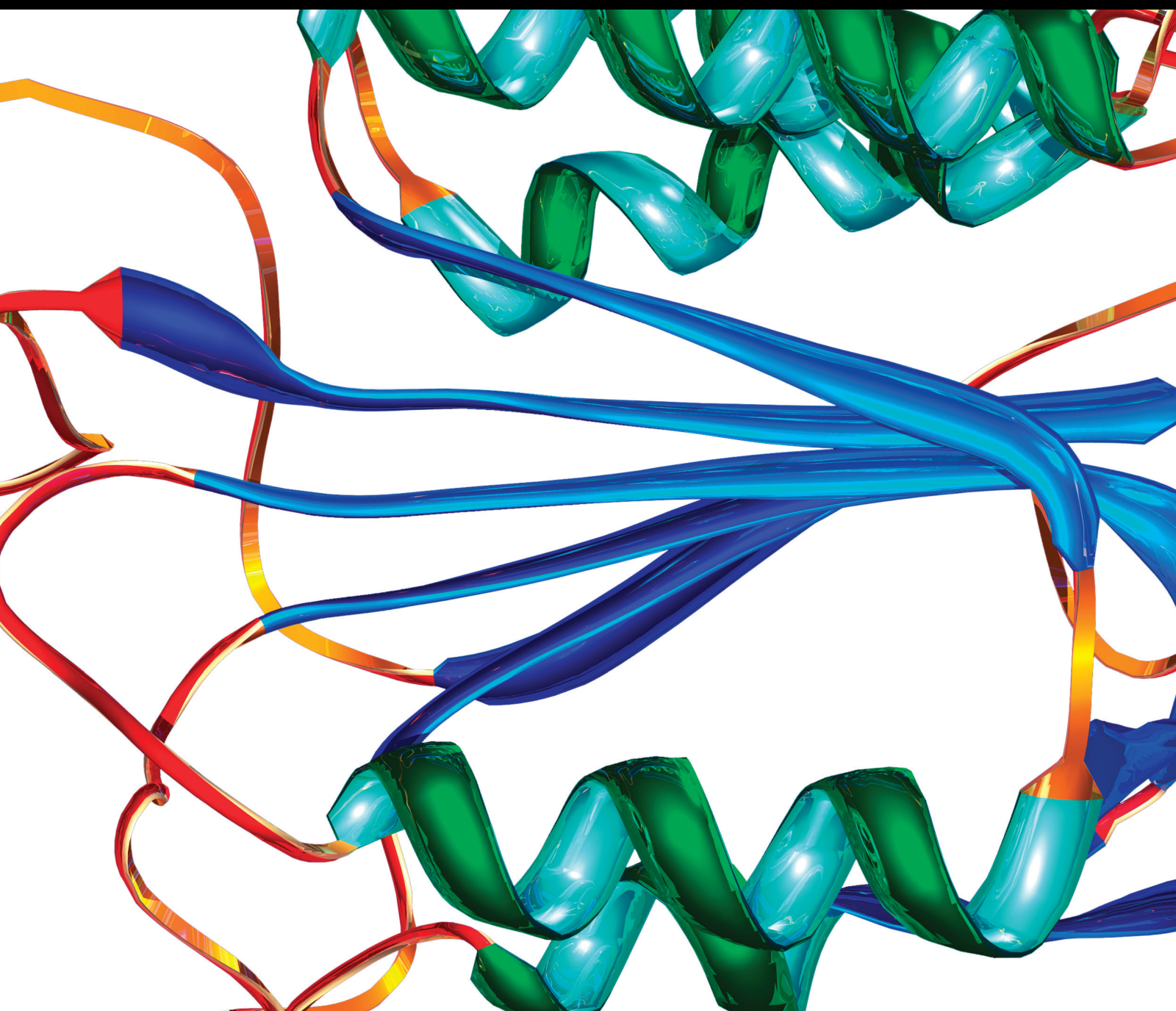


# Epigenetic Markers in Health and Diseases

Lead Guest Editor: Andrea Maugeri

Guest Editors: Antonella Agodi, Martina Barchitta, and Damjan Glavač





---

# **Epigenetic Markers in Health and Diseases**

Disease Markers

---

## **Epigenetic Markers in Health and Diseases**

Lead Guest Editor: Andrea Maugeri

Guest Editors: Antonella Agodi, Martina Barchitta,  
and Damjan Glavač



---

Copyright © 2021 Hindawi Limited. All rights reserved.

This is a special issue published in "Disease Markers." All articles are open access articles distributed under the Creative Commons Attribution License, which permits unrestricted use, distribution, and reproduction in any medium, provided the original work is properly cited.

# Chief Editor

Paola Gazzaniga, Italy

## Associate Editors

Donald H. Chace , USA  
Mariann Harangi, Hungary  
Hubertus Himmerich , United Kingdom  
Yi-Chia Huang , Taiwan  
Giuseppe Murdaca , Italy  
Irene Rebelo , Portugal

## Academic Editors

Muhammad Abdel Ghafar, Egypt  
George Agrogiannis, Greece  
Mojgan Alaeddini, Iran  
Atif Ali Hashmi , Pakistan  
Cornelia Amalinei , Romania  
Pasquale Ambrosino , Italy  
Paul Ashwood, USA  
Faryal Mehwish Awan , Pakistan  
Atif Baig , Malaysia  
Valeria Barresi , Italy  
Lalit Batra , USA  
Francesca Belardinilli, Italy  
Elisa Belluzzi , Italy  
Laura Bergantini , Italy  
Sourav Bhattacharya, USA  
Anna Birková , Slovakia  
Giulia Bivona , Italy  
Luisella Bocchio-Chiavetto , Italy  
Francesco Paolo Busardó , Italy  
Andrea Cabrera-Pastor , Spain  
Paolo Cameli , Italy  
Chiara Caselli , Italy  
Jin Chai, China  
Qixing Chen, China  
Shaoqiu Chen, USA  
Xiangmei Chen, China  
Carlo Chiarla , Italy  
Marcello Ciaccio , Italy  
Luciano Colangelo , Italy  
Alexandru Corlateanu, Moldova  
Miriana D'Alessandro , Saint Vincent and the Grenadines  
Waaqo B. Daddacha, USA  
Xi-jian Dai , China  
Maria Dalamaga , Greece

Serena Del Turco , Italy  
Jiang Du, USA  
Xing Du , China  
Benoit Dugue , France  
Paulina Dumnicka , Poland  
Nashwa El-Khazragy , Egypt  
Zhe Fan , China  
Rudy Foddis, Italy  
Serena Fragiotta , Italy  
Helge Frieling , Germany  
Alain J. Gelibter, Italy  
Matteo Giulietti , Italy  
Damjan Glavač , Slovenia  
Alvaro González , Spain  
Rohit Gundamaraju, USA  
Emilia Hadziyannis , Greece  
Michael Hawkes, Canada  
Shih-Ping Hsu , Taiwan  
Menghao Huang , USA  
Shu-Hong Huang , China  
Xuan Huang , China  
Ding-Sheng Jiang , China  
Esteban Jorge Galarza , Mexico  
Mohamed Gomaa Kamel, Japan  
Michalis V. Karamouzis, Greece  
Muhammad Babar Khawar, Pakistan  
Young-Kug Kim , Republic of Korea  
Mallikarjuna Korivi , China  
Arun Kumar , India  
Jinan Li , USA  
Peng-fei Li , China  
Yiping Li , China  
Michael Lichtenauer , Austria  
Daniela Ligi, Italy  
Hui Liu, China  
Jin-Hui Liu, China  
Ying Liu , USA  
Zhengwen Liu , China  
César López-Camarillo, Mexico  
Xin Luo , USA  
Zhiwen Luo, China  
Valentina Magri, Italy  
Michele Malaguarnera , Italy  
Erminia Manfrin , Italy  
Utpender Manne, USA

Alexander G. Mathioudakis, United Kingdom

Andrea Maugeri , Italy

Prasenjit Mitra , India

Ekansh Mittal , USA

Hiroshi Miyamoto , USA

Naoshad Muhammad , USA

Chiara Nicolazzo , Italy

Xing Niu , China

Dong Pan , USA

Dr.Krupakar Parthasarathy, India

Robert Pichler , Austria

Dimitri Poddighe , Kazakhstan

Roberta Rizzo , Italy

Maddalena Ruggieri, Italy

Tamal Sadhukhan, USA

Pier P. Sainaghi , Italy

Cristian Scheau, Romania

Jens-Christian Schewe, Germany

Alexandra Scholze , Denmark

Shabana , Pakistan

Anja Hviid Simonsen , Denmark

Eric A. Singer , USA

Daniele Sola , Italy

Timo Sorsa , Finland

Yaying Sun , China

Mohammad Tarique , USA

Jayaraman Tharmalingam, USA

Sowjanya Thatikonda , USA

Stamatios E. Theocharis , Greece

Tilman Todenhöfer , Germany

Anil Tomar, India

Alok Tripathi, India

Drenka Trivanović , Germany

Natacha Turck , Switzerland

Azizah Ugusman , Malaysia

Shailendra K. Verma, USA

Aristidis S. Veskoukis, Greece

Arianna Vignini, Italy

Jincheng Wang, Japan

Zhongqiu Xie, USA

Yuzhen Xu, China

Zhijie Xu , China

Guan-Jun Yang , China

Yan Yang , USA

Chengwu Zeng , China

Jun Zhang Zhang , USA

Qun Zhang, China

Changli Zhou , USA

Heng Zhou , China

Jian-Guo Zhou, China

## Contents

---

**The Relationship between Body Mass Index, Obesity, and LINE-1 Methylation: A Cross-Sectional Study on Women from Southern Italy**

Andrea Maugeri , Martina Barchitta , Roberta Magnano San Lio , Giuliana Favara , Claudia La Mastra, Maria Clara La Rosa, and Antonella Agodi 

Research Article (7 pages), Article ID 9910878, Volume 2021 (2021)

**Identification of an m6A-Related Signature as Biomarker for Hepatocellular Carcinoma Prognosis and Correlates with Sorafenib and Anti-PD-1 Immunotherapy Treatment Response**

Hongye Jiang , Gang Ning , Yensheng Wang , and Weibiao Lv 

Research Article (15 pages), Article ID 5576683, Volume 2021 (2021)

**Transcriptome-Wide Gene Expression in a Murine Model of Ventilator-Induced Lung Injury**

Zhao Li , Guoshao Zhu, Chen Zhou, Hui Wang, Le Yu, Yunxin Xu, Li Xu , and Qingxiu Wang 

Research Article (23 pages), Article ID 5535890, Volume 2021 (2021)

**Identified GNGT1 and NMU as Combined Diagnosis Biomarker of Non-Small-Cell Lung Cancer Utilizing Bioinformatics and Logistic Regression**

Jia-Jia Zhang , Jiang Hong , Yu-Shui Ma , Yi Shi , Dan-Dan Zhang , Xiao-Li Yang , Cheng-You Jia , Yu-Zhen Yin , Geng-Xi Jiang , Da Fu , and Fei Yu 

Research Article (14 pages), Article ID 6696198, Volume 2021 (2021)

## Research Article

# The Relationship between Body Mass Index, Obesity, and LINE-1 Methylation: A Cross-Sectional Study on Women from Southern Italy

Andrea Maugeri , Martina Barchitta , Roberta Magnano San Lio , Giuliana Favara ,  
Claudia La Mastra, Maria Clara La Rosa, and Antonella Agodi 

*Department of Medical and Surgical Sciences and Advanced Technologies “GF Ingrassia”, University of Catania, Catania 95123, Italy*

Correspondence should be addressed to Antonella Agodi; [agodia@unict.it](mailto:agodia@unict.it)

Received 12 March 2021; Revised 18 May 2021; Accepted 10 November 2021; Published 3 December 2021

Academic Editor: Wen-Jun Tu

Copyright © 2021 Andrea Maugeri et al. This is an open access article distributed under the Creative Commons Attribution License, which permits unrestricted use, distribution, and reproduction in any medium, provided the original work is properly cited.

Uncovering the relationship between body mass index (BMI) and DNA methylation could be useful to understand molecular mechanisms underpinning the effects of obesity. Here, we presented a cross-sectional study, aiming to evaluate the association of BMI and obesity with long interspersed nuclear elements (LINE-1) methylation, among 488 women from Catania, Italy. LINE-1 methylation was assessed in leukocyte DNA by pyrosequencing. We found a negative association between BMI and LINE-1 methylation level in both the unadjusted and adjusted linear regression models. Accordingly, obese women exhibited lower LINE-1 methylation level than their normal weight counterpart. This association was confirmed after adjusting for the effect of age, educational level, employment status, marital status, parity, menopause, and smoking status. Our findings were in line with previous evidence and encouraged further research to investigate the potential role of DNA methylation markers in the management of obesity.

## 1. Introduction

Overweight and obesity are delineated by an excessive accumulation of body fat, which results in a body mass index (BMI) greater than or equal to  $25 \text{ kg/m}^2$  and  $30 \text{ kg/m}^2$ , respectively [1]. According to the most recent estimates by the World Health Organization (WHO), nearly 2 billion adults were overweight in 2016, out of which approximately 650 million were obese [2]. In line with these estimates, more than one adult in ten (~13%) were obese in 2016, with a prevalence that tripled in the last four decades [2]. The reasons behind this increment is probably attributable—at least in part—to the increased intake of energy-dense foods and to the increasingly sedentary nature of human life [2]. Overweight and obesity also account for an important burden for public health [3], because raised BMI is often associated with an increased risk of cardiovascular diseases, diabetes, musculoskeletal disorders, and some cancers [4]. It is also

noteworthy that raised BMI could have adverse consequences on women of childbearing age and especially during pregnancy. For instance, excessive weight gain prior and during pregnancy was associated with adverse outcome in both mothers and their children [5–11]. Moreover, children born from overweight or obese women were not only at higher risk of being born large for gestational age [7, 9, 12, 13] and preterm [14] but also to develop metabolic disorders later in life [15–17].

In this complex scenario, it would be interesting to uncover molecular mechanisms associated with raised BMI and obesity. Among them, epigenetic mechanisms surely attracted the attention of many researchers, due to their potential role in development of obesity from the early stages of life [18]. For instance, previous studies already suggested the involvement of DNA methylation, aberrant miRNA expression, histone modification, and nucleosome release in obesity and associated comorbidities [19–21].

Specifically, DNA methylation is one of the best characterized epigenetic mechanisms, and previous studies investigated its association with cardiovascular diseases, obesity, diabetes, and cancer [22–24]. DNA methylation is generally regulated by different DNA methyltransferases (DNMTs), which are involved in several physiological and molecular processes, such as genomic imprinting, X-chromosome inactivation, gene expression, maintenance of chromosome integrity, and DNA-protein interactions [25]. Several studies used the methylation of long interspersed nuclear elements (LINE-1) sequences as a proxy of global DNA methylation level. Although there is still no consensus on the validity of measuring LINE-1 methylation as a surrogate marker, aberrant methylation of these sequences might influence both chromosomal stability and gene expression [26, 27]. Previous research suggested the potential relationship between obesity and LINE-1 methylation, but further investigation is still needed. Thus, the current cross-sectional study is aimed at assessing the association of BMI and obesity with LINE-1 methylation level among women from Catania, Italy.

## 2. Materials and Methods

**2.1. Study Design.** The population of the present cross-sectional study consisted of women from 15 to 85 years, who underwent routine physical examination at three clinical laboratories in Catania (Italy) from 2010 to 2017. Overall, the study was conducted on nonpregnant women without previous or current diagnosis of cancer, diabetes, cardiovascular, neurodegenerative, and autoimmune diseases. The study protocol was in accordance with the Declaration of Helsinki and approved by the ethics committees “Catania” and “Catania 2” with the following protocol numbers: 52/2010/VE, 16/2015/CECT2, and 227/2011/BE. All women who met inclusion criteria were invited to participate, after being informed of all aspects of the research protocol. Those who agreed to participate in the study had to sign a written informed consent. At recruitment, height and weight were measured to the nearest 1 cm and 1 kg, respectively, using a medical digital scale with meter. BMI was calculated as the ratio between weight (kg) and squared height (m<sup>2</sup>), and participants were categorized into underweight, normal weight, overweight, and obesity according to the WHO criteria [28]. At the same time, women provided a blood sample for DNA extraction and LINE-1 methylation assessment. Women with incomplete information on anthropometric measures and those who did not provide a blood sample were excluded from the current analysis.

**2.2. LINE-1 Methylation Analysis.** DNA extraction and the assessment of LINE-1 methylation were performed using standardized protocols [29]. In brief, DNA was extracted from leukocytes using the QIAamp DNA Mini Kit (Qiagen, Milan, Italy). Next, bisulphite conversion of 40 ng of the extracted DNA was performed using the EpiTect Bisulfite Kit (Qiagen, Milan, Italy). Specifically, the assessment of methylation levels was performed on three CpG sites within the LINE-1 sequence (GenBank Accession No. X58075). To

do that, the LINE-1 sequence was amplified by Hot start PCR on the Eppendorf Mastercycler (Eppendorf, Milan, Italy). The PCR reaction was conducted in a final volume of 25  $\mu$ l, containing 1.5  $\mu$ l of bisulfite-converted DNA, 12.5  $\mu$ l of PyroMark PCR Master Mix 2x, 2.5  $\mu$ l of Coral Load Concentrate 10x, and 2  $\mu$ l of primers (0.2  $\mu$ M for each). The sequences of forward and reverse-biotinylated primer were 5'-TTTTGAGTTAGGTGTGGGATATA-3' and 5'-biotin AAAATCAAAAATTC CTTTC-3', respectively [29]. The PCR conditions were the following: 1 cycle at 95°C for 15 min, 40 cycles at 94°C for 30 s, 50°C for 30 s, 72°C for 30 s, and a final extension at 72°C for 10 min. Finally, the PCR products were sequenced by pyrosequencing on the PyroMark Q24 instrument (Qiagen, Milan, Italy), using 0.3 mM of the sequencing primer 5'-AGTTAGGTG TGGGATATAGT-3'. For each CpG site, methylation level was calculated as the percentage of methylated cytosines over all cytosines. All the protocols were performed according to the manufacturers' instructions, and each sample was analysed in triplicate. All the assays included a positive (100% methylated DNA) and a negative (0% methylated DNA) control, while failed assays were repeated. Intraobserver coefficient of variability between replicates was 2.2% (SD = 1.0%), as previously reported. For each sample, LINE-1 methylation level was calculated as the mean of methylation level of the three CpG sites [30].

**2.3. Covariates.** At the recruitment, information on socio-demographic and behavioral factors were collected through the administration of structured questionnaires. Specifically, educational level was classified as low (primary school diploma or none), medium (secondary school diploma), or high (bachelor's degree or higher). Women were also classified, according to their employment status, as employed (including both part-time and full-time employment) or unemployed (including housewives and retired). For each woman, we also collected information about family structure and specifically asking if women lived alone or in couple and if they had at least a child. Regarding smoking status, women were classified as current, former, and never smokers. Instead, dietary data were obtained using a semiquantitative Food Frequency Questionnaires (FFQ), from which we estimated total daily energy intake [31].

**2.4. Statistical Analysis.** Statistical analyses were performed on the STATA software (version SE 16.0, StataCorp, College Station, USA). Prior to analysis, quantitative variables were tested for normality using the Kolmogorov-Smirnov test. Descriptive statistics were used to summarize categorical variables (using frequency and percentage) and quantitative variables (using median and interquartile range (IQR)). All variables were compared across BMI categories using the Chi-squared test for categorical variables and the Kruskal-Wallis test for quantitative variables. The association of BMI with LINE-1 methylation was examined by simple linear regression and further adjusting for age, educational level, employment status, marital status, parity, menopause, and smoking status. Similarly, the association of BMI categories with LINE-1 methylation was examined using normal

weight as the reference group in unadjusted and adjusted linear regression models. Results were reported as  $\beta$  coefficients and their standard error (SE). All the analyses were two-sided and performed with a significance level of 0.05.

### 3. Results

**3.1. Population Characteristics.** Figure 1 describes the selection of participants according to inclusion and exclusion criteria. In brief, 494 out of 844 participating women provided a blood sample for the assessment of LINE-1 methylation. Among them, 6 women were excluded because of incomplete information on anthropometric measures. Thus, the study population consisted of 488 women, aged 15-85 years, with a complete assessment of anthropometric measures and LINE-1 methylation of leukocyte DNA. No differences between included and excluded women were evident. Regarding their education, 35.2% had a primary school diploma, 47.1% obtained a secondary school diploma, and 17.6% earned a degree. Overall, 44.1% of women were part-time or full-time employed, while 50.4% lived in couple. Approximately 70% had at least a child, while only 9.3% were menopausal. With respect to smoking status, most women never smoked (57.3%), a low proportion of them were former smokers (11.7%), and about one-third were current smokers (31.0%). The median total energy intake was 1935 kcal, and 17.4% used dietary supplements.

**3.2. Comparisons across BMI Categories.** According to their BMI (median of 23.3 kg/m<sup>2</sup>), women were classified as underweight (6.4%), normal weight (57.6%), overweight (23.6%), or obese (12.5%). Table 1 compares the abovementioned characteristics across these BMI categories. Interestingly, the median age and hence also the proportion of menopausal women increased from the underweight to the obese category ( $p < 0.001$  and  $p = 0.023$ ). In line with increasing age, also the proportion of women who lived in couple and those who had at least a child increased ( $p < 0.001$  and  $p = 0.004$ ). Regarding social factors, the proportion of women with low educational level and those who were unemployed increased from the underweight to the obese category ( $p$  values  $< 0.001$ ). With respect to behavioral information, the proportion of current smokers decreased from the underweight to the obese category ( $p < 0.001$ ), while no differences were evident for total energy intake and use of dietary supplements.

**3.3. The Relationship between BMI and LINE-1 Methylation.** We first tested the relationship between BMI and LINE-1 methylation. As showed in the scatter plot reported in Figure 2, we noted a negative association so that the percentage of LINE-1 methylation decreased by 0.125 for each unit increase of BMI (SE = 0.057;  $p = 0.029$ ). Accordingly, as depicted in the violin plot reported in Figure 3, we observed that LINE-1 methylation tended to decrease from the underweight to the obese category ( $p = 0.048$ ). Indeed, median LINE-1 methylation level was 69.7 (IQR = 10.0) in underweight, 68.7 (10.0) in normal weight, 67.3 (10.7) in overweight, and 65.0 (IQR = 9.5) in obese women.

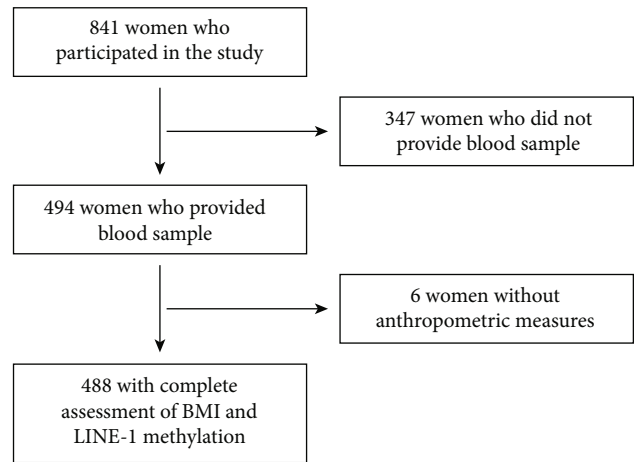


FIGURE 1: Flow chart of population selection.

**3.4. The Association of Obesity with LINE-1 Methylation.** Finally, we tested the association of BMI and its categories with LINE-1 methylation level. To do that, we first adjusted the negative relationship between BMI and LINE-1 methylation for the potential effect of covariates (Table 2). Notably, the percentage of LINE-1 methylation significantly decreased by 0.145 for each unit increase of BMI (SE = 0.058;  $p = 0.013$ ). Moreover, we evaluated the association between specific BMI categories and LINE-1 methylation, using normal weight women as the reference group. In the unadjusted model, obese women exhibited lower LINE-1 methylation level than their normal weight counterpart ( $\beta = -1.971$ ; SE = 0.876;  $p = 0.025$ ), while no significant differences were evident for underweight or overweight women. Interestingly, the negative association between obesity and LINE-1 methylation remained significant ( $\beta = -2.050$ ; SE = 0.868;  $p = 0.019$ ) after adjusting for age, educational level, employment and marital status, parity, menopause, and smoking habits.

### 4. Discussion

Our study demonstrated a negative relationship between BMI and LINE-1 methylation, which resulted in lower methylation level among obese women if compared with their normal weight counterpart. These findings were partially in line with the evidence summarized by a comprehensive review published by Samblas and colleagues in 2019 [18]. Indeed, several investigations have already suggested the relationship of weight gain and obesity traits with DNA methylation. Yet, these studies were heterogeneous in terms of study design, DNA source, methylation marker under investigation, and outcome of interest [18]. This produced a lot of findings, which, however, were not easy to interpret because in many cases they were often inconclusive or controversial. Indeed, obesity was associated with DNA methylation both positively and negatively, depending on the genes or DNA sequences under study [18].

To the best of our knowledge, few studies investigated the association between obesity and LINE-1 methylation.

TABLE 1: Characteristics of the study population across categories of the body mass index.

Characteristics	Underweight ( $n = 31$ )	Normal weight ( $n = 281$ )	Overweight ( $n = 115$ )	Obese ( $n = 61$ )	$p$ value
Age, years	30 (11)	39 (18)	46 (22)	44 (21)	<0.001
Educational level					
Low	19.3%	30.4%	46.2%	53.9%	
Medium	49.1%	46.9%	44.0%	34.8%	<0.001
High	31.6%	22.7%	9.9%	11.2%	
Unemployed	45.6%	51.3%	59.9%	74.2%	<0.001
Living in couple	18.6%	46.1%	68.3%	75.6%	<0.001
Having children	36.8%	70.5%	80.9%	78.9%	0.004
Menopause	0.0%	15.2%	21.8%	15.8%	0.023
Smoking status					
Never smokers	47.7%	54.0%	60.4%	61.8%	
Former smokers	7.0%	7.9%	15.9%	13.5%	<0.001
Current smokers	45.6%	38.1%	23.6%	24.7%	
Total energy intake, kcal	2014 (705)	1923 (650)	1935 (708)	1950 (778)	0.335
Users of supplements	11.6%	15.7%	16.3%	15.6%	0.905

Results are reported as median (IQR) or percentage (%) and compared using the Kruskal-Wallis or the Chi-squared tests.

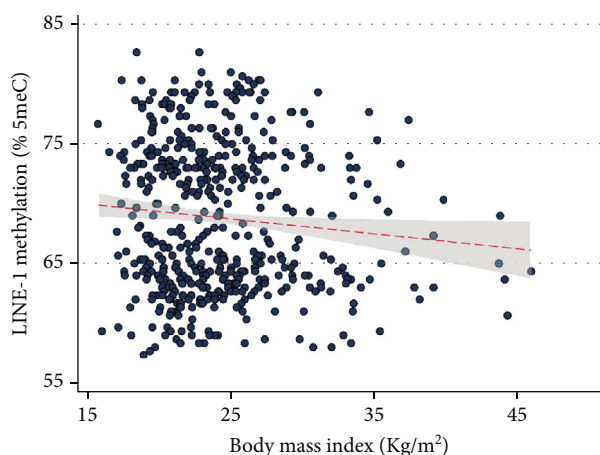


FIGURE 2: Scatter plot of the relationship between body mass index and LINE-1 methylation. The red line represents the linear regression line with its 95% confidence interval.

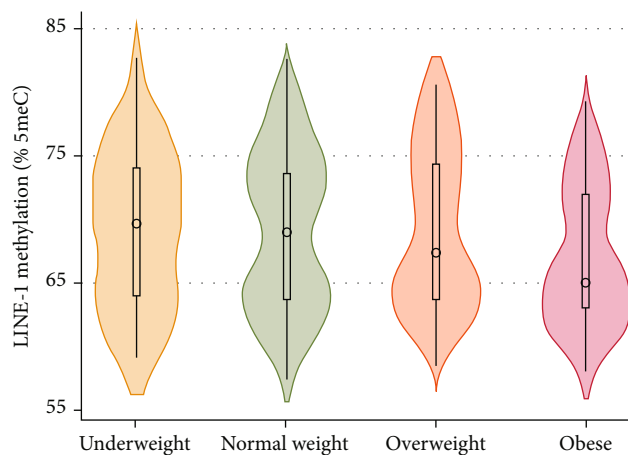


FIGURE 3: Violin plot showing the distribution of LINE-1 methylation level across categories of body mass index.

Among them, the cross-sectional study by Carraro and colleagues showed a positive association of waist circumference and BMI with methylation level in blood samples from 40 health professionals aged 20–59 years [32]. By contrast, a longitudinal analysis of the Bogota School Children Cohort demonstrated a negative association between adiposity measures and LINE-1 methylation in blood samples from children aged 5–12 years [33]. A negative association was also observed in our study, which for the first time evaluated the relationship between BMI, obesity, and LINE-1 methylation in a large population of women without previous or current diagnosis of severe diseases.

These controversies might be at least partially explained by the fact that several demographic, behavioral,

and physiological factors could affect DNA methylation [18]. In the context of LINE-1 sequences, for example, it has already been demonstrated how nutrients, foods, and dietary patterns might influence methylation level. Specifically, the intake of nutrients involved in one-carbon metabolism, the consumption of fruits and vegetables, and the adherence to healthy dietary patterns appeared to be associated with higher LINE-1 methylation level [29]. In line with these findings, there was also evidence that weight loss interventions might significantly increase LINE-1 methylation level in blood samples [34, 35]. Moreover, it has been proposed that LINE-1 methylation level prior to the intervention might significantly predict the amount of weight loss [35]. Despite these interesting

TABLE 2: Linear regression analyses between BMI, its categories, and LINE-1 methylation level.

Model <sup>a</sup>	BMI	$\beta$ coefficient	Standard error	<i>p</i> value
Unadjusted	Continuous	-0.125	0.057	0.029
	Categories			
	Underweight	0.194	1.173	0.868
	Normal weight		Ref.	
	Overweight	0.170	0.687	0.803
	Obese	-1.971	0.876	0.025
Adjusted	Continuous	-0.145	0.058	0.013
	Categories			
	Underweight	-0.015	1.161	0.990
	Normal weight		Ref.	
	Overweight	-0.108	0.687	0.875
	Obese	-2.050	0.868	0.019

Results are reported as  $\beta$  coefficients, standard errors, and *p* values obtained through the linear regression analyses. The normal weight category was used as the reference group (Ref.) where indicated. The adjusted models included age, educational level, employment status, marital status, parity, menopause, and smoking status.

suggestions, however, there were also studies that produced inconclusive or opposite results [36, 37]. This was the case of the study by Martin-Nunez and colleagues, which instead showed a reduction in LINE-1 methylation level after an intervention promoting the adherence to the Mediterranean diet [36].

Although our findings confirm the relationship between obesity and LINE-1 methylation, their clinical utility for predicting obesity risk and response to weight loss programs is not immediate. In fact, the observational and cross-sectional nature of our study did not allow to establish a cause-effect relation. Specifically, further prospective studies should be encouraged to assess if LINE-1 methylation is a molecular mechanism underpinning obesity development or a consequence of this condition. Moreover, additional experimental research is necessary to confirm if LINE-1 methylation could be useful to predict weight loss in obese patients.

From a physiological point of view, several obesity-related factors were associated with aberrant DNA methylation. However, most of them were investigated only in vitro since they were challenging to be isolated in humans. Indeed, obese subjects often exhibited nutritional and physiological factors simultaneously, masking and/or confounding their independent effect on DNA methylation [18]. Despite these difficulties, it appeared clear that chronic inflammation [38, 39], oxidative stress [40], and insulin resistance [41] might play a key role in DNA methylation changes associated with obesity.

Our study had some limitations that should be considered when interpreting our findings. Firstly, the cross-sectional nature of our analysis did not allow to understand the causal relationship between obesity and LINE-1 methylation. Secondly, we used information on BMI and its classification, even if other anthropometric measures and adiposity indexes should have been considered addi-

tionally. For example, further studies should evaluate the association of LINE-1 methylation with several measures of fat deposition and abdominal obesity commonly used in epidemiological research [1, 18]. Thirdly, although our analyses were adjusted for several variables, other factors that could potentially affect DNA methylation and obesity (e.g., diet and physical activity) [42] should have been considered.

## 5. Conclusions

Our study demonstrated how increased BMI was associated with lower LINE-1 methylation level, especially in obese women. These findings—adding to the current knowledge on the relationship between obesity and DNA methylation—sustained the hypothesis that measuring obesity-related DNA methylation markers could be helpful to understand the molecular effects of inadequate weight gain. Moreover, it could be also useful for identifying people at higher risk of obesity or those who respond well to weight loss programs. However, at present, these are just interesting perspectives that merit further investigation through longitudinal and well-structured studies.

## Data Availability

The data used to support the findings of this study are available from the corresponding author upon request.

## Conflicts of Interest

The authors declare that there is no conflict of interest regarding the publication of this paper.

## Acknowledgments

We are grateful to Giuseppa Giusino, Anna Elisa Marchese, and Aurora Scalisi, from the involved clinical laboratories, for their contribution in recruiting patients and for their help in blood sampling. We would also like to thank all women who gave their consent to participate in the study. This work was supported by the Department of Medical and Surgical Sciences and Advanced Technologies “GF Ingrassia”, University of Catania (Piano Triennale di Sviluppo delle Attività di Ricerca Scientifica del Dipartimento–2016–2018). Andrea Maugeri was granted by the University of Catania (Research Fellowship—Biomarcatori molecolari in sanità pubblica: un approccio epidemiologico per la sorveglianza e la prevenzione delle malattie trasmissibili e non trasmissibili).

## References

- [1] P. González-Muniesa, M. A. Martínez-González, F. B. Hu et al., “Obesity,” *Nature Reviews Disease Primers*, vol. 3, no. 1, p. 17034, 2017.
- [2] *Obesity and overweight* <https://www.who.int/en/news-room/fact-sheets/detail/obesity-and-overweight>.
- [3] M. Kroes, G. Osei-Assibey, R. Baker-Searle, and J. Huang, “Impact of weight change on quality of life in adults with overweight/obesity in the United States: a systematic review,” *Current Medical Research and Opinion*, vol. 32, no. 3, pp. 485–508, 2016.
- [4] E. P. Williams, M. Mesidor, K. Winters, P. M. Dubbert, and S. B. Wyatt, “Overweight and obesity: prevalence, consequences, and causes of a growing public health problem,” *Current Obesity Reports*, vol. 4, no. 3, pp. 363–370, 2015.
- [5] M. Cedergren, “Effects of gestational weight gain and body mass index on obstetric outcome in Sweden,” *International Journal of Gynaecology and Obstetrics*, vol. 93, no. 3, pp. 269–274, 2006.
- [6] M. W. Gillman, “Gestational weight gain: now and the future,” *Circulation*, vol. 125, no. 11, pp. 1339–1340, 2012.
- [7] R. Lucia Bergmann, K. E. Bergmann, E. Haschke-Becher et al., “Does maternal docosahexaenoic acid supplementation during pregnancy and lactation lower BMI in late infancy?,” *Journal of Perinatal Medicine*, vol. 35, no. 4, pp. 295–300, 2007.
- [8] J. C. Johnston, D. A. McNeil, M. Best, and C. MacLeod, “A growth status measurement pilot in four Calgary area schools: perceptions of grade 5 students and their parents,” *The Journal of School Nursing*, vol. 27, no. 1, pp. 61–69, 2011.
- [9] E. A. Nohr, M. Vaeth, J. L. Baker, T. I. Sørensen, J. Olsen, and K. M. Rasmussen, “Pregnancy outcomes related to gestational weight gain in women defined by their body mass index, parity, height, and smoking status,” *The American Journal of Clinical Nutrition*, vol. 90, no. 5, pp. 1288–1294, 2009.
- [10] B. L. Rooney, C. W. Schauburger, and M. A. Mathiason, “Impact of perinatal weight change on long-term obesity and obesity-related illnesses,” *Obstetrics and Gynecology*, vol. 106, no. 6, pp. 1349–1356, 2005.
- [11] B. L. Rooney and C. W. Schauburger, “Excess pregnancy weight gain and long-term obesity: one decade later,” *Obstetrics and Gynecology*, vol. 100, no. 2, pp. 245–252, 2002.
- [12] S. J. Herring, M. Z. Rose, H. Skouteris, and E. Oken, “Optimizing weight gain in pregnancy to prevent obesity in women and children,” *Diabetes, Obesity & Metabolism*, vol. 14, no. 3, pp. 195–203, 2012.
- [13] A. A. Mamun, M. Kinarivala, M. J. O’Callaghan, G. M. Williams, J. M. Najman, and L. K. Callaway, “Associations of excess weight gain during pregnancy with long-term maternal overweight and obesity: evidence from 21 y postpartum follow-up,” *The American Journal of Clinical Nutrition*, vol. 91, no. 5, pp. 1336–1341, 2010.
- [14] Z. H. E. N. HAN, O. L. H. A. LUTSIV, S. O. H. A. I. L. MULLA et al., “Low gestational weight gain and the risk of preterm birth and low birthweight: a systematic review and meta-analyses,” *Acta Obstetrica et Gynecologica Scandinavica*, vol. 90, no. 9, pp. 935–954, 2011.
- [15] S. N. Hinkle, A. J. Sharma, D. W. Swan, L. A. Schieve, U. Ramakrishnan, and A. D. Stein, “Excess gestational weight gain is associated with child adiposity among mothers with normal and overweight prepregnancy weight status,” *The Journal of Nutrition*, vol. 142, no. 10, pp. 1851–1858, 2012.
- [16] L. Poston, “Gestational weight gain: influences on the long-term health of the child,” *Current Opinion in Clinical Nutrition and Metabolic Care*, vol. 15, no. 3, pp. 252–257, 2012.
- [17] S. B. Sridhar, J. Darbinian, S. F. Ehrlich et al., “Maternal gestational weight gain and offspring risk for childhood overweight or obesity,” *American Journal of Obstetrics and Gynecology*, vol. 211, no. 3, pp. 259.e1–259.e8, 2014.
- [18] M. Samblas, F. I. Milagro, and A. Martínez, “DNA methylation markers in obesity, metabolic syndrome, and weight loss,” *Epigenetics*, vol. 14, no. 5, pp. 421–444, 2019.
- [19] M. Oses, J. Margareto Sanchez, M. P. Portillo, C. M. Aguilera, and I. Labayen, “Circulating miRNAs as biomarkers of obesity and obesity-associated comorbidities in children and adolescents: a systematic review,” *Nutrients*, vol. 11, no. 12, p. 2890, 2019.
- [20] A. Ortiz-Dosal, P. Rodil-García, and L. A. Salazar-Olivo, “Circulating microRNAs in human obesity: a systematic review,” *Biomarkers*, vol. 24, no. 6, pp. 499–509, 2019.
- [21] P. E. Macchia, I. C. Nettore, F. Franchini, L. Santana-Viera, and P. Ungaro, “Epigenetic regulation of adipogenesis by histone-modifying enzymes,” *Epigenomics*, vol. 13, no. 3, pp. 235–251, 2021.
- [22] Y. Bergman and H. Cedar, “DNA methylation dynamics in health and disease,” *Nature Structural & Molecular Biology*, vol. 20, no. 3, pp. 274–281, 2013.
- [23] O. Rennert and T. L. Lee, “Epigenetics dynamics in development and disease,” *The International Journal of Biochemistry & Cell Biology*, vol. 67, p. 44, 2015.
- [24] C. M. Reynolds, C. Gray, M. Li, S. A. Segovia, and M. H. Vickers, “Early life nutrition and energy balance disorders in offspring in later life,” *Nutrients*, vol. 7, no. 9, pp. 8090–8111, 2015.
- [25] M. H. Jiang, J. Fei, M. S. Lan et al., “Hypermethylation of hepatic Gck promoter in ageing rats contributes to diabetogenic potential,” *Diabetologia*, vol. 51, no. 8, pp. 1525–1533, 2008.
- [26] W. A. Schulz, “L1 retrotransposons in human cancers,” *Journal of Biomedicine & Biotechnology*, vol. 2006, no. 1, 2006.
- [27] R. K. Slotkin and R. Martienssen, “Transposable elements and the epigenetic regulation of the genome,” *Nature Reviews. Genetics*, vol. 8, no. 4, pp. 272–285, 2007.
- [28] “Physical status: the use and interpretation of anthropometry. Report of a WHO Expert Committee,” *World Health Organization Technical Report Series*, vol. 854, pp. 1–452, 1995.

- [29] M. Barchitta, A. Maugeri, R. Magnano San Lio et al., "Dietary patterns are associated with leukocyte LINE-1 methylation in women: a cross-sectional study in southern Italy," *Nutrients*, vol. 11, no. 8, p. 1843, 2019.
- [30] M. Barchitta, A. Maugeri, A. Quattrocchi et al., "Mediterranean diet and particulate matter exposure are associated with LINE-1 methylation: results from a cross-sectional study in women," *Frontiers in Genetics*, vol. 9, p. 514, 2018.
- [31] A. Maugeri, M. Barchitta, V. Fiore et al., "Determinants of adherence to the Mediterranean diet: findings from a cross-sectional study in women from Southern Italy," *International Journal of Environmental Research and Public Health*, vol. 16, no. 16, p. 2963, 2019.
- [32] J. C. Carraro, M. L. Mansego, F. I. Milagro et al., "LINE-1 and inflammatory gene methylation levels are early biomarkers of metabolic changes: association with adiposity," *Biomarkers*, vol. 21, no. 7, pp. 625–632, 2016.
- [33] W. Perng, M. Mora-Plazas, C. Marín, L. S. Rozek, A. Baylin, and E. Villamor, "A prospective study of LINE-1 DNA methylation and development of adiposity in school-age children," *PLoS One*, vol. 8, no. 4, article e62587, 2013.
- [34] L. Delgado-Cruzata, W. Zhang, J. A. McDonald et al., "Dietary modifications, weight loss, and changes in metabolic markers affect global DNA methylation in Hispanic, African American, and Afro-Caribbean breast cancer survivors," *The Journal of Nutrition*, vol. 145, no. 4, pp. 783–790, 2015.
- [35] M. Garcia-Lacarte, F. I. Milagro, M. A. Zulet, J. A. Martinez, and M. L. Mansego, "LINE-1 methylation levels, a biomarker of weight loss in obese subjects, are influenced by dietary antioxidant capacity," *Redox Report*, vol. 21, no. 2, pp. 67–74, 2016.
- [36] G. M. Martín-Núñez, R. Cabrera-Mulero, E. Rubio-Martín et al., "Methylation levels of the SCD1 gene promoter and LINE-1 repeat region are associated with weight change: an intervention study," *Molecular Nutrition & Food Research*, vol. 58, no. 7, pp. 1528–1536, 2014.
- [37] C. Duggan, L. Xiao, M. B. Terry, and A. McTiernan, "No effect of weight loss on LINE-1 methylation levels in peripheral blood leukocytes from postmenopausal overweight women," *Obesity (Silver Spring)*, vol. 22, no. 9, pp. 2091–2096, 2014.
- [38] F. M. Davis and K. A. Gallagher, "Epigenetic mechanisms in monocytes/macrophages regulate inflammation in cardiometabolic and vascular disease," *Arteriosclerosis, Thrombosis, and Vascular Biology*, vol. 39, no. 4, pp. 623–634, 2019.
- [39] X. Wang, Q. Cao, L. Yu, H. Shi, and B. Xue, "Epigenetic regulation of macrophage polarization and inflammation by DNA methylation in obesity," *JCI Insight*, vol. 1, no. 19, article e87748, 2016.
- [40] S. Yara, J. C. Lavoie, and E. Levy, "Oxidative stress and DNA methylation regulation in the metabolic syndrome," *Epigenomics*, vol. 7, no. 2, pp. 283–300, 2015.
- [41] A. Arpón, F. I. Milagro, O. Ramos-Lopez et al., "Epigenome-wide association study in peripheral white blood cells involving insulin resistance," *Scientific Reports*, vol. 9, no. 1, p. 2445, 2019.
- [42] S. Voisin, N. Eynon, X. Yan, and D. J. Bishop, "Exercise training and DNA methylation in humans," *Acta Physiologica (Oxford, England)*, vol. 213, no. 1, pp. 39–59, 2015.

## Research Article

# Identification of an m6A-Related Signature as Biomarker for Hepatocellular Carcinoma Prognosis and Correlates with Sorafenib and Anti-PD-1 Immunotherapy Treatment Response

Hongye Jiang <sup>1</sup>, Gang Ning <sup>2</sup>, Yensheng Wang <sup>3</sup>, and Weibiao Lv <sup>1</sup>

<sup>1</sup>Department of Clinical Laboratory, Shunde Hospital, Southern Medical University (The First People's Hospital of Shunde), Foshan, Guangdong Province, China

<sup>2</sup>Department of Gastroenterology and Hepatology, Guangzhou Digestive Diseases Center, Guangzhou First People's Hospital, South China University of Technology, Guangzhou, Guangdong Province, China

<sup>3</sup>Department of Medicine, Chang-Gung Memorial Hospital, Linkou, Taiwan, China

Correspondence should be addressed to Weibiao Lv; [weibiao2004@163.com](mailto:weibiao2004@163.com)

Received 17 February 2021; Accepted 26 May 2021; Published 11 June 2021

Academic Editor: Andrea Maugeri

Copyright © 2021 Hongye Jiang et al. This is an open access article distributed under the Creative Commons Attribution License, which permits unrestricted use, distribution, and reproduction in any medium, provided the original work is properly cited.

**Background.** N6-methyladenosine (m6A) modification plays an essential role in diverse key biological processes and may take part in the development and progression of hepatocellular carcinoma (HCC). Here, we systematically analyzed the expression profiles and prognostic values of 13 widely reported m6A modification-related genes in HCC. **Methods.** The mRNA expression of 13 m6A modification-related genes and clinical parameters of HCC patients were downloaded from TCGA, ICGC, GSE109211, and GSE78220. Univariate and LASSO analyses were used to develop risk signature. Time-dependent ROC was performed to assess the predictive accuracy and sensitivity of risk signature. **Results.** FTO, YTHDC1, YTHDC2, ALKBH5, KIAA1429, HNRNPC, METTL3, RBM15, YTHDF2, YTHDF1, and WTAP were significantly overexpressed in HCC patients. YTHDF1, HNRNPC, RBM15, METTL3, and YTHDF2 were independent prognostic factors for OS and DFS in HCC patients. Next, a risk signature was also developed and validated with five m6A modification-related genes in TCGA and ICGC HCC cohort. It could effectively stratify HCC patients into high-risk patients with shorter OS and DFS and low-risk patients with longer OS and DFS and showed good predictive efficiency in predicting OS and DFS. Moreover, significantly higher proportions of macrophages M0 cells, neutrophils, and Tregs were found to be enriched in HCC patients with high risk scores, while significantly higher proportions of memory CD4 T cells, gamma delta T cells, and naive B cells were found to be enriched in HCC patients with low scores. Finally, significantly lower risk scores were found at sorafenib treatment responders and anti-PD-1 immunotherapy responders compared to that in nonresponders, and anti-PD-1 immunotherapy-treated patients with lower risk scores had better OS than patients with higher risk scores. **Conclusion.** A risk signature developed with the expression of 5 m6A-related genes could improve the prediction of prognosis of HCC and correlated with sorafenib treatment and anti-PD-1 immunotherapy response.

## 1. Introduction

Hepatocellular carcinoma (HCC) is a common type of cancer and represents the leading cause of cancer-related death worldwide. HCC is still a serious burden to public health [1]. There were about 841,000 patients developed HCC, and 782,000 patients died from HCC alone in 2018 because of late diagnosis and limited treatment

options [1, 2]. Moreover, the incidence of HCC is increasing rapidly with 50% recurrence rate after surgical treatment [3, 4]. It is well recognized that development and progression of HCC is the result of multistep process, where interactions between genetics and epigenetics have played important roles [5–8]. Understanding the pathogenesis of HCC is the key to discover new diagnostic biomarkers and therapeutic targets.

RNA modification, discovered in the 1970s, has recently been recognized as a third layer of epigenetics that could modify a plethora of native cellular RNAs [9–11]. N6-methyladenosine (m6A) modification is the most abundant form of internal mRNA methylation among the kinds of RNA modifications in eukaryotes [12]. m6A modifications in mammalian cells are dynamic and reversible and are commonly regulated by binding proteins (“readers”), methyltransferases (“writers”), and demethylases (“erasers”) [13]. Among m6A modification-related genes, 13 genes, including *ZC3H13*, *WTAP*, *KIAA1429*, *METTL3*, *METTL14*, *RBM15*, *YTHDC1*, *YTHDC2*, *YTHDF1*, *YTHDF2*, *HNRNPC*, *ALKBH5*, and *FTO*, are the most prominent [14–16]. These m6A modification-related genes are primarily involved in modulation of alternative mRNA splicing, precession of pre-miRNA, stability of mRNA, and enhancement of translation efficiency of mRNA [13]. Not only do these 13 m6A modification-related genes play essential roles in many important biological processes, such as development of embryonic and neural cells, differentiation of stem cell, and stress responses [17–19], they also take part in the development, progression, and radio resistance of various kinds of cancers [20–23]. For example, overexpression of *YTHDF1* is found to be related with poorer survival of HCC patients, and *KIAA1429* and *METTL3* are found to regulate migration and invasion of HCC, indicating an important role of m6A modification-related genes playing in HCC [24–26].

Recently, Zhou et al. explored the expression pattern and prognostic values of m6A modification-related genes of HCC patients, but they mainly focused on the role of *METTL3* and *YTHDF1* [27]. In the present study, we comprehensively analyzed the expression pattern and prognosis of the thirteen widely reported m6A modification-related genes in TCGA HCC cohort. Besides, we also developed and validated a risk signature with the expression of 5 selected m6A modification-related genes and analyzed its prognostic value for HCC patients and its relation with tumor-infiltrating immune cells in TCGA and ICGC HCC cohort. Moreover, the prediction values of risk signature in sorafenib treatment and anti-PD-1 immunotherapy response were also evaluated.

## 2. Materials and Methods

**2.1. Ethics Statement.** All the data analyzed in the present study were received from TCGA, ICGC, and GEO dataset, and written consents were already obtained before our study.

**2.2. Data Collection.** mRNA expression of TCGA HCC cohorts, which included 374 HCC cases and 50 normal controls, was got from GDC Data Portal (<https://cancergenome.nih.gov/>). Meanwhile, corresponding clinical-pathological data, including gender, age, histologic grade, tumor T stage, N stage, M stage (M), TNM stage, overall survival (OS) time, and disease-free survival (DFS) time, were also downloaded. It was of note that 9 of 374 HCC patients were excluded because of absence of corresponding clinical-pathological data, and basic characteristics of 365 HCC patients were summarized in Table 1. In addition, a total of 232 HCC patients with available OS information and mRNA expres-

sion were got from the ICGC portal (<https://dcc.icgc.org/projects/LIRI-JP>). The mRNA expression of 67 sorafenib-treated HCC patients of GSE109211 was downloaded from the GEO database (<https://www.ncbi.nlm.nih.gov/geo/>), and there were 21 sorafenib treatment responders and 46 nonresponders in GSE109211. Moreover, the mRNA expression of 27 melanoma patients with anti-PD-1 checkpoint inhibition therapy of GSE78220 was also downloaded from the GEO database. Four patients achieved complete response, 10 patients achieved partial response, and 13 patients achieved no response.

**2.3. Development and Validation of Risk Signature.** First, univariate analysis was carried out to select the genes related with survival. Then LASSO algorithm was used for selecting the most prognostic-related genes [28]. A risk signature was developed based on the coefficients weighted by LASSO analysis. With this signature, we calculated a risk score for HCC patients and divided HCC patients into high-risk group and low-risk group based on the median risk score.

**2.4. CIBERSORT.** CIBERSORT (<https://cibersort.stanford.edu>) is an online tool designed for estimating the abundances of 22 kinds of tumor-infiltrating immune cells with transcriptomic data [29], and we used it to calculate the tumor-infiltrating immune cells of HCC patients basing on the mRNA expression profiles of TCGA HCC cohort and ICGC HCC cohort, respectively.

**2.5. Data Analysis Flow Chart.** To make the study to be better understood, a workflow of the study was depicted and was shown at Figure 1.

**2.6. Statistical Analysis.** The R software (version 3.5.1) was used for statistical analysis. Wilcox test was performed to compare difference of m6A modification-related genes between HCC and healthy controls. Correlation of the 13 m6A modification-related genes with each other was compared by Spearman correlation analysis. One-way ANOVA was carried out to compare difference of m6A modification-related genes among different histologic grades and TNM stages. Chi-square analysis was carried out to analyze distribution of clinical-pathologic parameters between high-risk HCC patients and low-risk HCC patients. Univariate and multivariate Cox regression analyses were carried out to analyze the prognostic value of m6A modification-related genes and risk signature. Kaplan-Meier analysis with log-rank test was carried out to analyze difference of OS or DFS between patients of different clusters or with risk scores. Time-dependent ROC was carried out to analyze the predictive accuracy and sensitivity of risk signature. Additional statistical analyses were performed with STAMP [30].  $P < 0.05$  was considered as statistically significant.

## 3. Results

**3.1. Expression of m6A Modification-Related Genes of HCC Patients and Their Associations with Clinical-Pathologic Parameters.** First, the mRNA expression of 13 m6A modification-related genes was downloaded from TCGA

TABLE 1: Basic characteristics of 365 HCC patients from TCGA.

Variables	HCC patients (N = 365)
Gender (male/female)	246 (67%)/119 (33%)
Age (years, ≤60/>60)	173 (47%)/192 (53%)
Histologic grade (G1+G2/G3+G4/NA)	230 (63%)/130 (36%)/5 (1%)
T stage (T1+T2/T3+T4/NA)	271 (74%)/91 (25%)/3 (1%)
N stage (N0/N1/NA)	248 (68%)/4 (1%)/113 (31%)
M stage (M0/N1/NA)	263 (72%)/3 (1%)/99 (27%)
TNM stage (stage I+II/stage III+IV/NA)	254 (70%)/87 (24%)/24 (6%)

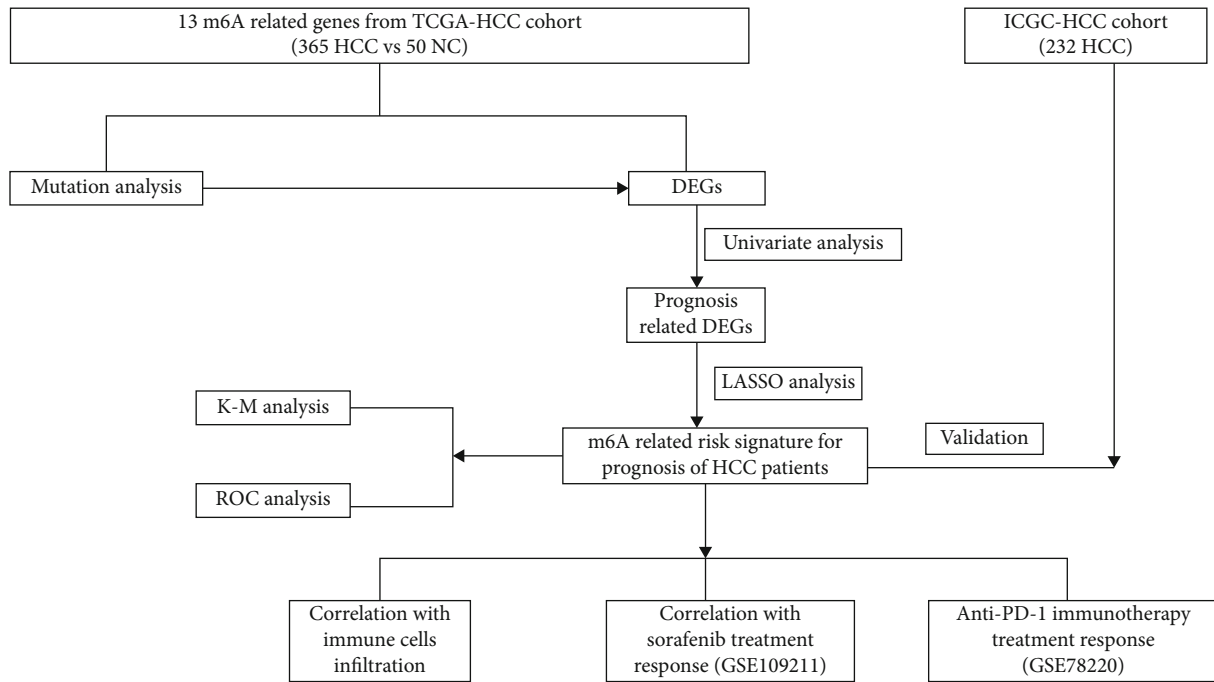


FIGURE 1: The workflow chart of the present study.

and compared between HCC patients and normal controls. As shown at Figures 2(a) and 2(b), significantly higher expression of *FTO*, *YTHDC1*, *YTHDC2*, *ALKBH5*, *KIAA1429*, *HNRNPC*, *METTL3*, *RBM15*, *YTHDF2*, *YTHDF1*, and *WTAP* was found in the tissues of HCC patients compared to normal tissues (all  $P < 0.001$ ). Interestingly, we also found that the expression of most of the 13 m6A modification-related genes seemed to be lower than those of other 32 kinds of tumors. Besides, most of the 13 m6A modification-related genes were positively correlated with each other (Figure 2(c)). Moreover, genetic changes, such as missense mutation, truncating mutation, amplification, deep deletion, diploid, and gain, were observed in about 80% of the HCC patients (Figure 2(d)). Specifically, each HCC patient might have one or more kinds of genetic changes. The genetic rates of *WTAP*, *KIAA1429*, *RBM15*, *METTL3*, *METTL14*, *ALKBH5*, *YTHDC1*, *YTHDC2*, *HNRNPC*, *YTHDF1*, *YTHDF2*, *FTO*, and *ZC3H13* were 7%, 4%, 17%, 40%, 5%, 5%, 7%, 8%, 18%, 11%, 9%, 13%, and

17%, respectively, suggesting that higher expression of m6A modification-related genes might be the result of genetic changes in related genes. Taken together, these results indicated that m6A modification-related genes played important roles in HCC.

**3.2. Prognostic Value of m6A Modification-Related Genes in HCC Cases.** Next, we further analyzed prognostic values of m6A modification-related genes. Univariate analysis showed that higher expression of *YTHDF1*, *WTAP*, *HNRNPC*, *RBM15*, *METTL3*, *KIAA1429*, *YTHDC1*, and *YTHDF2* and lower expression of *ZC3H13* were statistically related to poorer OS of HCC patients (all  $P < 0.05$ , supplementary figure 1A); multivariate analysis showed that the expression of *YTHDF1*, *WTAP*, *HNRNPC*, *RBM15*, *METTL3*, *KIAA1429*, and *YTHDF2* still remained significantly related with OS after adjusting for gender, age, histologic grade, T stage, N stage, M stage, and TNM stage (all  $P < 0.05$ , supplementary figure 1B-1J). Then, the prognostic values of

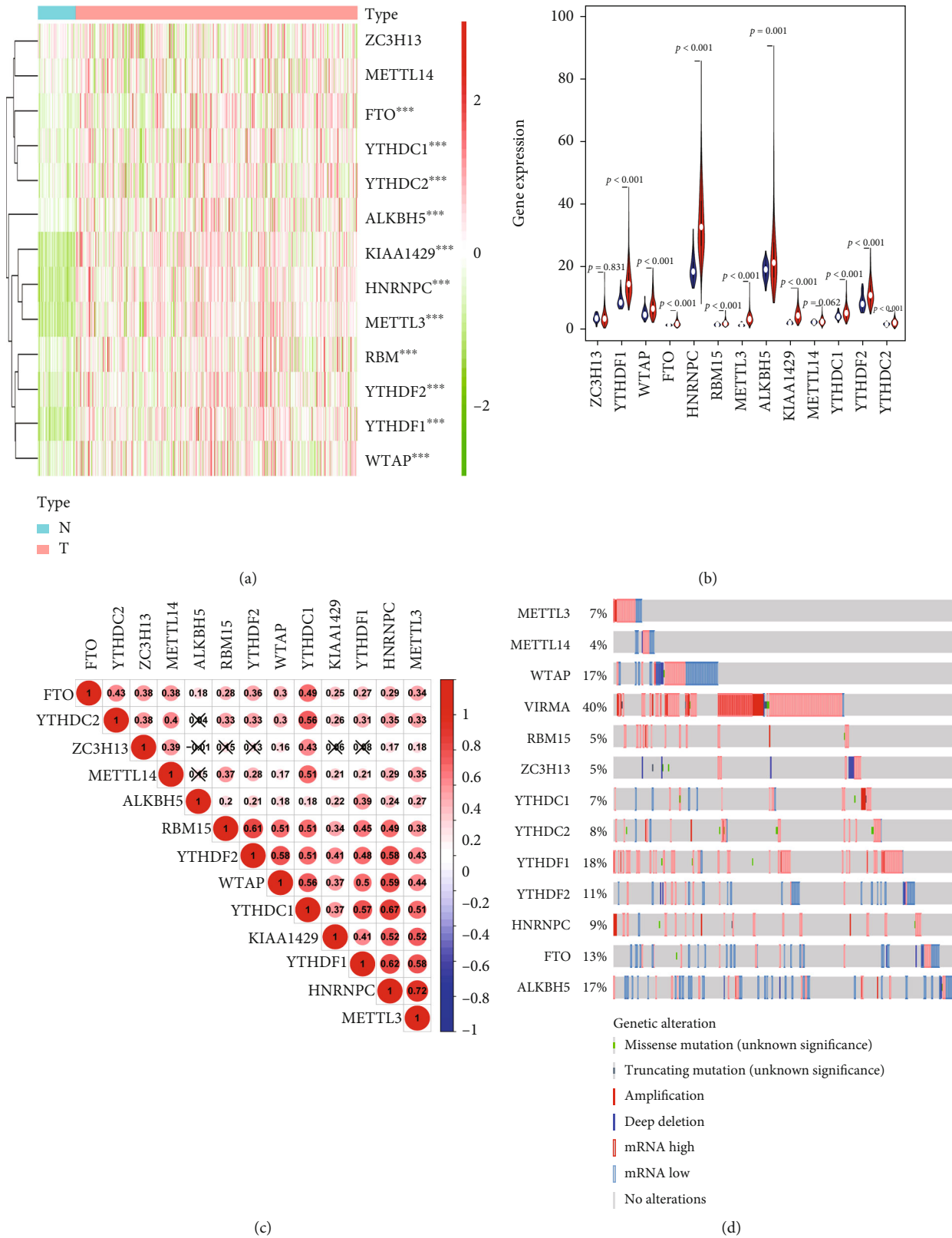


FIGURE 2: Expression of 13 m6A modification-related genes in HCC and their associations with clinical-pathologic parameters. (a) Heatmap of log2 transformed expression of 13 m6A modification-related genes between HCC patients and normal controls. (b) Violin plot of expression of 13 m6A modification-related genes between HCC patients and normal controls. (c) Correlation of the 13 m6A modification-related genes with each other. (d) Genetic changes of the 13 m6A modification-related genes. \* $P < 0.05$ , \*\* $P < 0.01$ , and \*\*\* $P < 0.001$ .

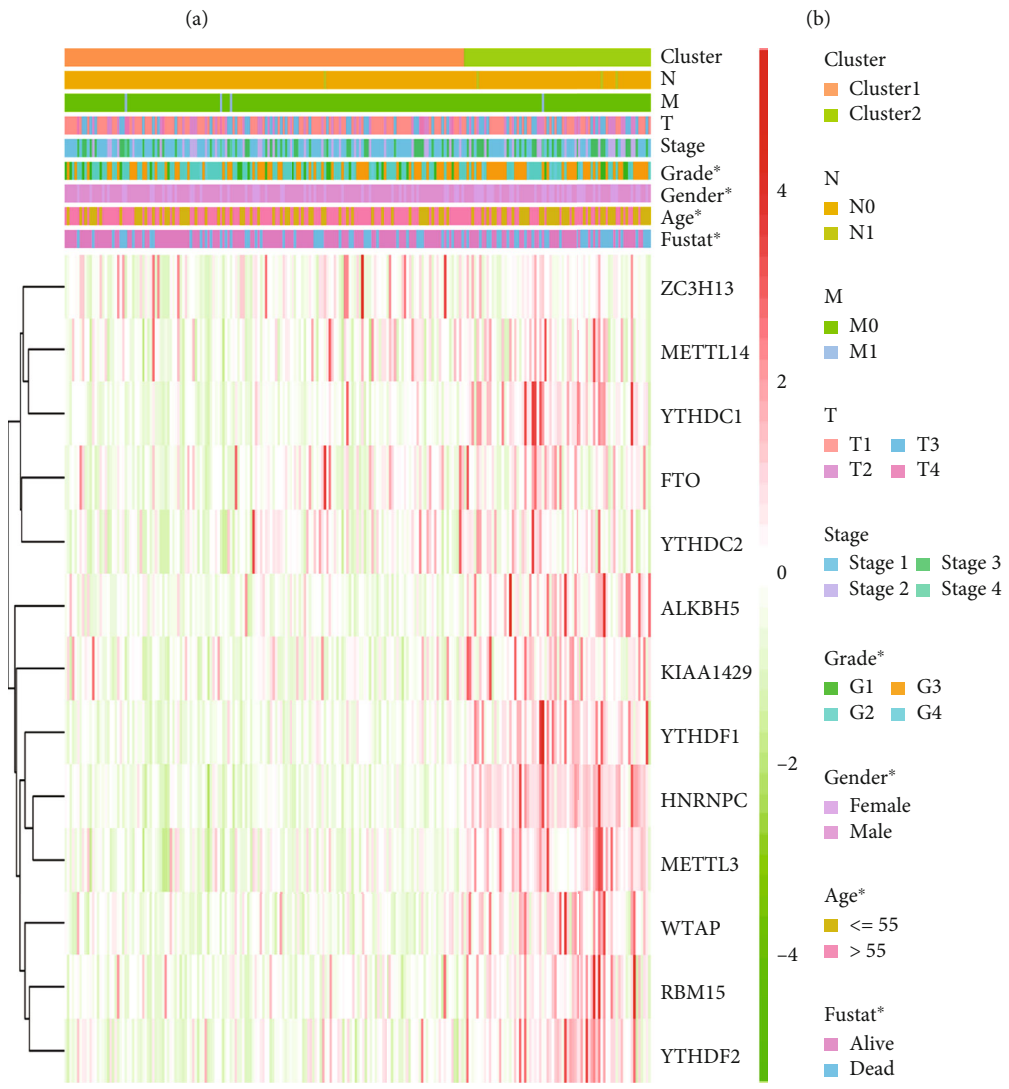
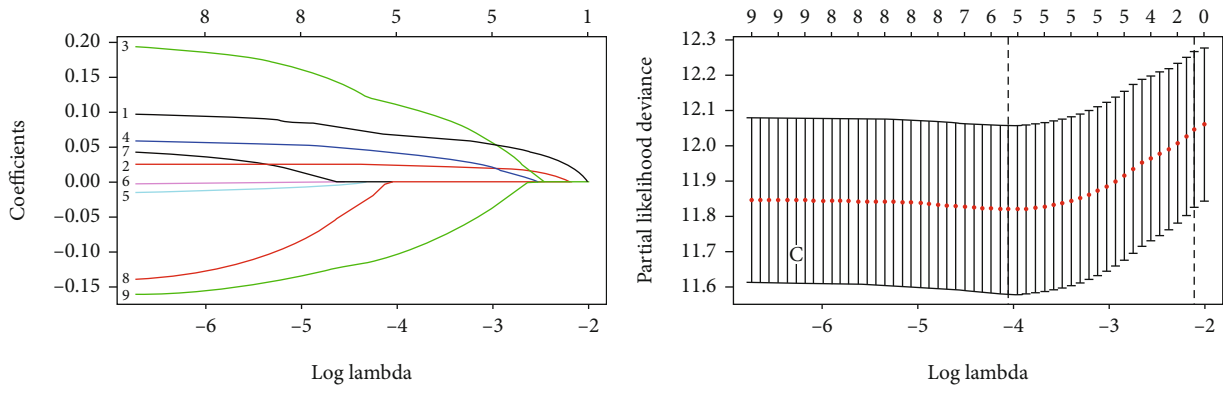


FIGURE 3: Continued.

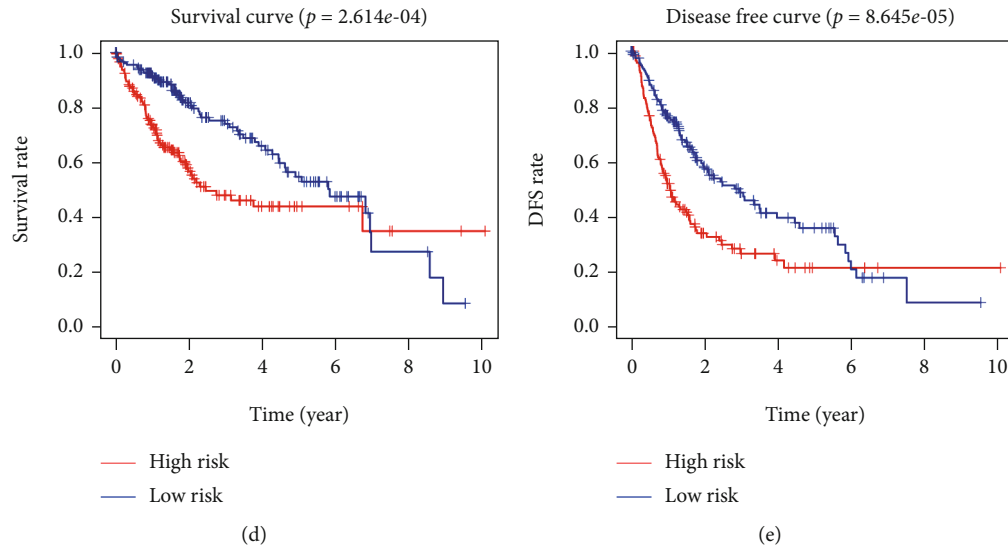


FIGURE 3: Construction of risk signature with 5 m6A modification-related genes and its association with clinical parameters. (a, b) 5 m6A modification-related genes identified by LASSO analysis. (c) Heatmap of the association of risk score with clinical-pathologic parameters. (d) Kaplan-Meier analysis of OS of patients of high-risk subgroup and low-risk subgroup. (e) Kaplan-Meier analysis of DFS of patients of high-risk subgroup and low-risk subgroup. T: tumor stage; N: lymph node stage; M: metastasis stage; stage: TNM stage; \* $P < 0.05$ , \*\* $P < 0.01$ , and \*\*\* $P < 0.001$ .

m6A modification-related genes for recurrence of HCC patients were also analyzed. Univariate analysis indicated that overexpression of *YTHDF1*, *WTAP*, *HNRNPC*, *RBM15*, *METTL3*, *YTHDC1*, and *YTHDF2* was statistically related with shorter DFS (all  $P < 0.05$ , supplementary figure 2A); multivariate analysis showed that the expression of *YTHDF1*, *HNRNPC*, *RBM15*, *METTL3*, and *YTHDF2* was still statistically related with DFS after adjusting for gender, age, histologic grade, T stage, N stage, M stage, and TNM stage (all  $P < 0.05$ , supplementary figure 2B-2H). These results strongly confirmed the important roles played by m6A modification-related genes in HCC.

**3.3. Development of Risk Signature with 5 m6A Modification-Related Genes and Its Association with Clinical-Pathologic Parameters.** To better explore the prognostic value of m6A modification-related genes, a risk signature was developed. Based on the results of univariate analysis (Figure 3(a)), *ZC3H13*, *YTHDF1*, *WTAP*, *HNRNPC*, *RBM15*, *METTL3*, *KIAA1429*, *YTHDC1*, and *YTHDF2* were associated with OS and were considered as prognostic-related genes. Then, LASSO analysis was used to further screen the prognostic-related genes. In the end, 5 genes, including *YTHDF2*, *YTHDF1*, *METTL3*, *KIAA1429*, and *ZC3H13*, were used to develop the risk signature (Figures 3(a) and 3(b)). The risk score was then constructed based on the coefficients weighted by LASSO analysis and calculated as follows: risk score =  $(0.07 * YTHDF2) + (0.02 * YTHDF1) + (0.11 * METTL3) + (0.04 * KIAA1429) - (0.1 * ZC3H13)$ . We calculated the risk score for every HCC case and assigned them into high-risk group and low-risk group on the basis of the median risk score. The expression of *YTHDF2*, *YTHDF1*, *METTL3*, and *KIAA1429* tended to be higher in patients with high risk

score; the expression of *ZC3H13* seemed to be higher in patients with low risk score (Figure 3(c)). Distribution of histologic grade, T stage, and TNM stage was significantly different between high-risk subgroup and low-risk subgroup (all  $P < 0.05$ , Figure 3(c)). High-risk subgroup contained more patients with advanced histologic grade, T stage, and TNM stage compared to patients of the low-risk subgroup. Lastly, patients in the high-risk subgroup had poorer OS (median OS time: 2.46 vs. 5.79 years, HR = 1.98, 95% CI: 1.39-2.83, and  $P < 0.001$ ; Figure 3(d)) and shorter DFS (median DFS: 1.07 vs. 2.97 years, HR = 3.83, 95% CI: 2.56-5.90, and  $P < 0.001$ ; Figure 3(e)) than those of patients of the low-risk subgroup, which were consistent with the previous results.

**3.4. Prognostic Value of Risk Signature for OS and DFS of HCC Cases.** The risk signature was found to be associated with clinical-pathologic parameters. We next performed univariate and multivariate analyses to analyze its prognostic value. Based on the univariate analysis, T stage, M stage, TNM stage, and risk signature were statistically related with OS of HCC patients (all  $P < 0.05$ , Figure 4(a)). The risk signature still remained statistically related with OS after adjusting for T stage, M stage, and TNM stage by multivariate analysis. In multivariate analysis, after adjusting for TNM stage, the risk signature was still significantly related with OS ( $P < 0.01$ , Figure 4(b)). Similarly, univariate analysis also showed that T stage, TNM stage, and risk signature were statistically related with DFS of HCC patients. In univariate analysis, T stage, TNM stage, and the risk signature were also significantly associated with DFS in HCC patients (all  $P < 0.001$ , Figure 4(c)). By incorporating these factors into

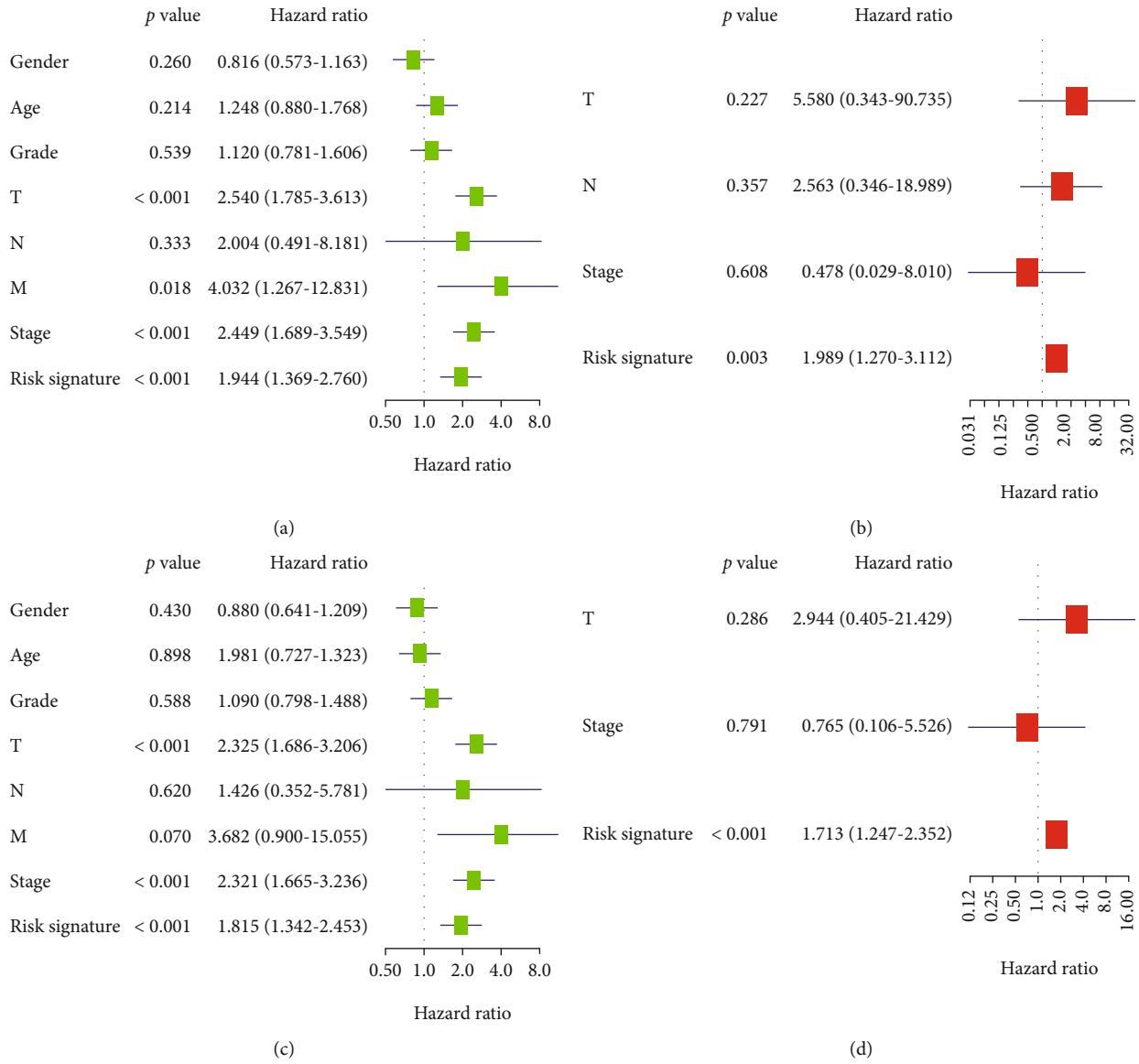


FIGURE 4: Prognostic value of risk signature for OS and DFS of HCC patients. (a) Univariate analysis of risk signature with OS of HCC patients. (b) Multivariate analysis of risk signature with OS of HCC patients. (c) Univariate analysis of risk signature with DFS of HCC patients. (d) Multivariate analysis of risk signature with DFS of HCC patients. Gender: male vs. female; age: >60 vs. ≤60; grade: G3+G4 vs. G1+G2; T: T1 vs. T0; N: N1 vs. N0; M: M1 vs. M0; TNM stage: stage III+IV vs. stage I+II.

multivariate analysis, the result suggested that only the risk signature was statistically related with DFS ( $P < 0.001$ , Figure 4(d)). To conclude, these results indicated that the risk signature was an independent prognostic factor for OS and DFS of HCC patients.

Next, we used time-dependent ROC curve analysis to analyze the predictive value of risk signature for HCC patients. As were shown at Figure 5, the AUC of risk signature for predicting 1-, 3-, and 5-year OS was 0.765, 0.73, and 0.678, respectively, which exhibited better predictive efficiency compared to TNM stage, *YTHDF2*, *YTHDF1*, *METTL3*, *KIAA1429*, and *ZC3H13* (Figures 5(a), 5(c), and 5(e)). Likewise, the AUC of risk signature for predicting 1-, 3-, and 5-year DFS was 0.695, 0.643, and 0.68, respectively, which also

showed better predictive accuracy than TNM stage, *YTHDF2*, *YTHDF1*, *METTL3*, *KIAA1429*, and *ZC3H13* (Figures 5(b), 5(d), and 5(f)).

**3.5. Validation of Risk Signature.** To independently test the applicability of the signature, 232 HCC patients with available OS information from the ICGC portal (<https://dcc.icgc.org/projects/LIRI-JP>) were further used to examine the applicability of the signature. Risk score for every patient was computed. Similarly, the signature could effectively stratify high-risk HCC patients with poorer OS and low-risk patients with better OS (HR = 2.309, 95% CI: 1.302-4.369, and  $P = 0.006$ ; Figure 6(a)). Moreover, the AUC of risk signature for predicting 1-, 3-, and 5-year OS was 0.7, 0.74, and

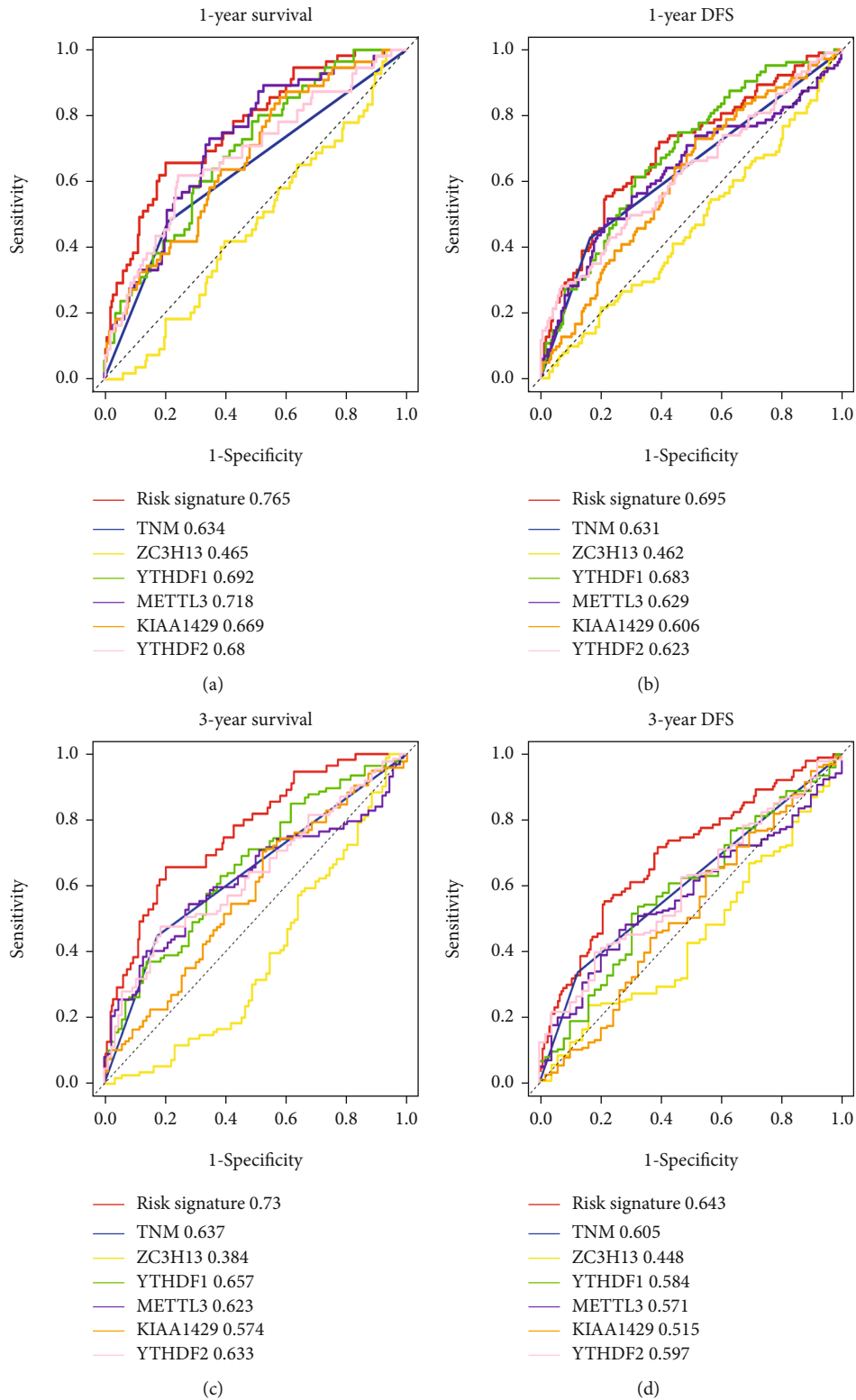


FIGURE 5: Continued.

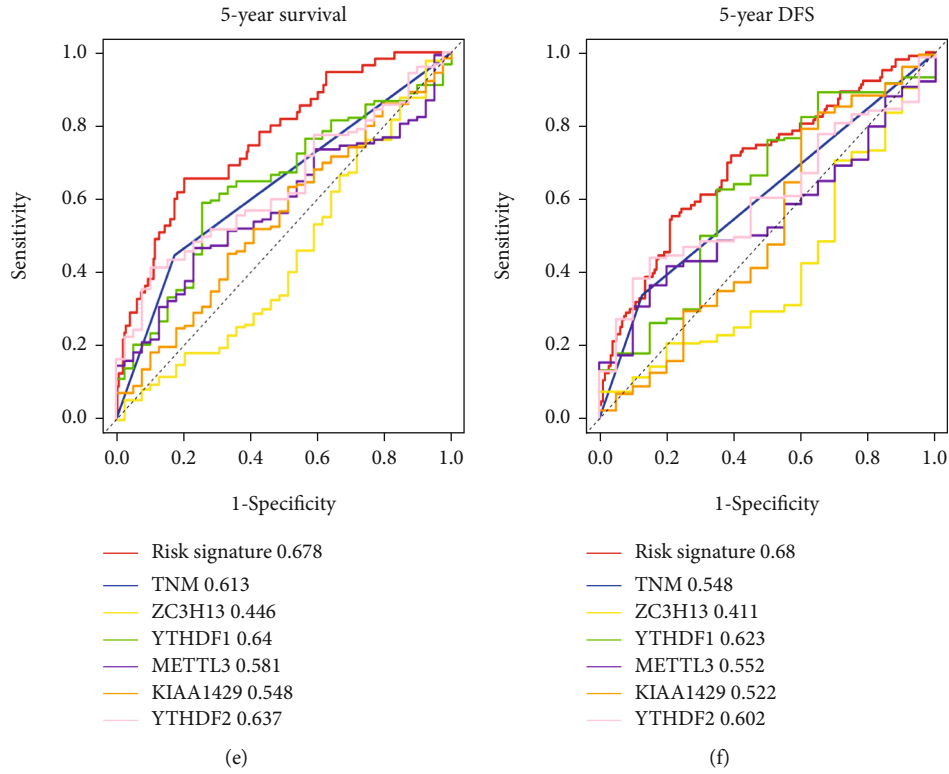


FIGURE 5: Predictive value of risk signature, TNM stage, *YTHDF2*, *YTHDF1*, *METTL3*, *KIAA1429*, and *ZC3H13*. Time-dependent ROC analysis was used to evaluate the predictive value in predicting (a) 1-year, (c) 3-year, and (e) 5-year OS and predicting (b) 1-year, (d) 3-year, and (f) 5-year DFS in HCC patients.

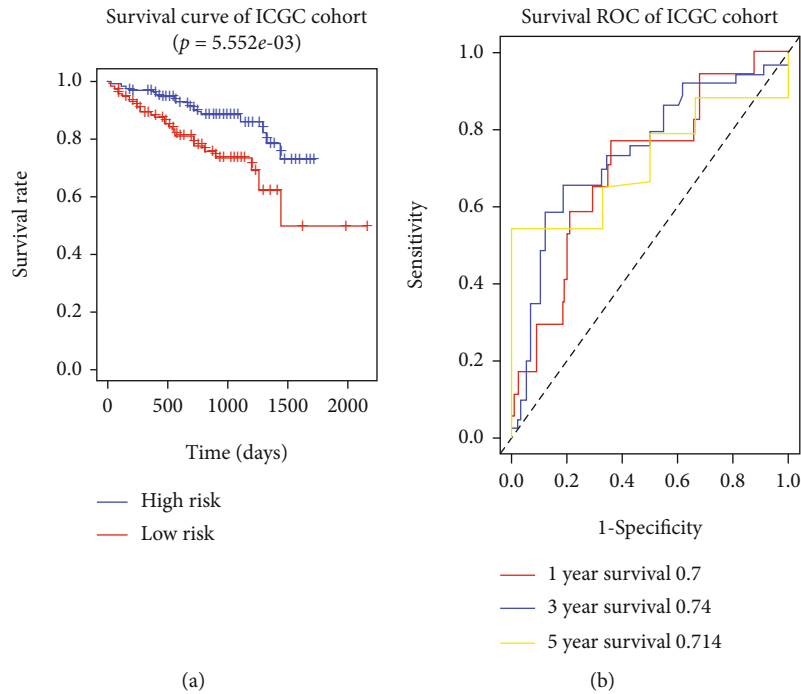
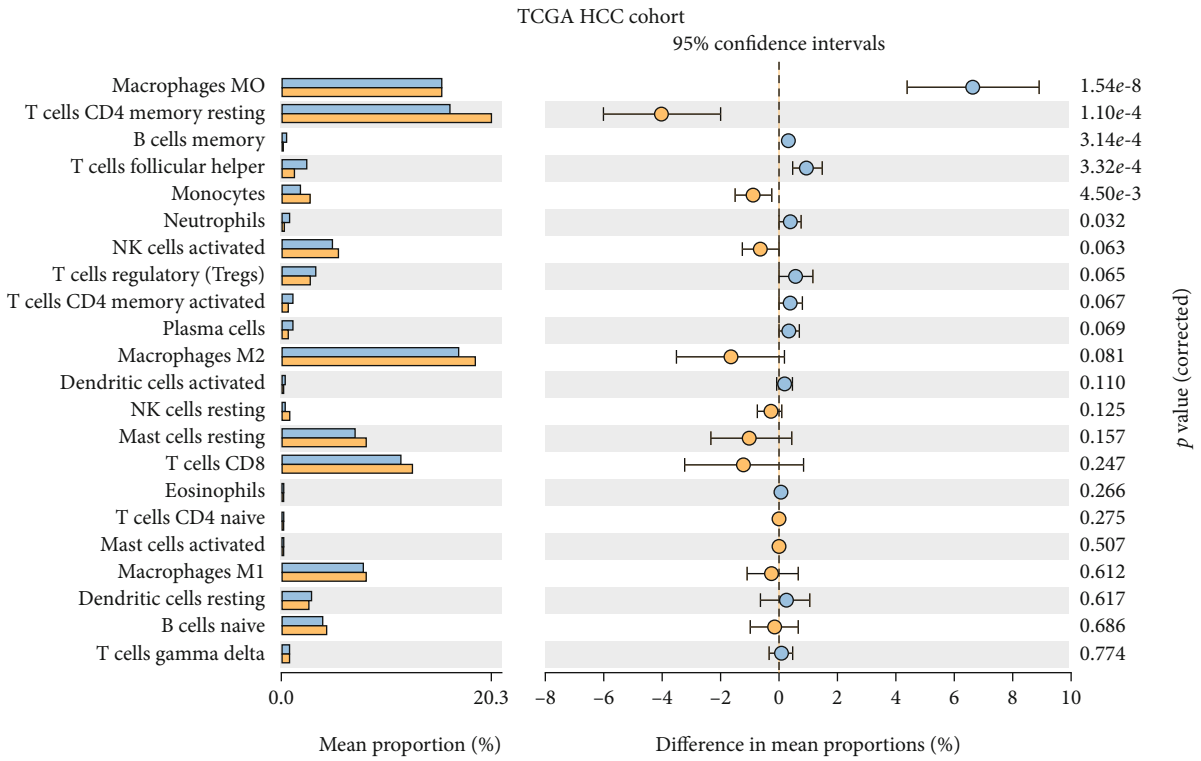
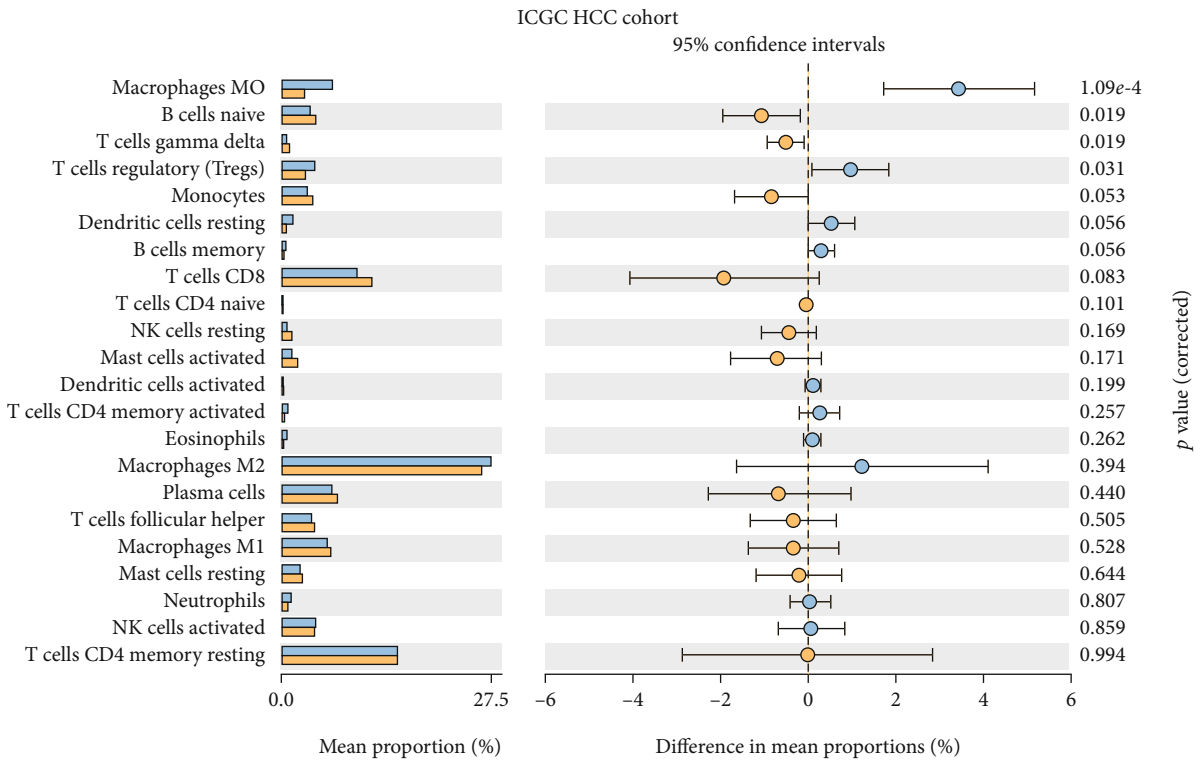


FIGURE 6: External validation of the applicability of the signature in ICGC HCC cohort. (a) Kaplan-Meier analysis of OS of patients of high-risk subgroup and low-risk subgroup in ICGC cohort. (b) AUC of risk signature in predicting 1-year, 3-year, and 5-year OS in HCC patients.



(a)



(b)

FIGURE 7: Correlation of risk signature with tumor-infiltrating immune cells in TCGA and ICGC HCC cohort. Difference of 22 kinds of infiltrating immune cells between patients with different risk scores of (a) TCGA HCC cohort. Difference of 22 kinds of infiltrating immune cells between patients with different risk scores of (b) ICGC HCC cohort.

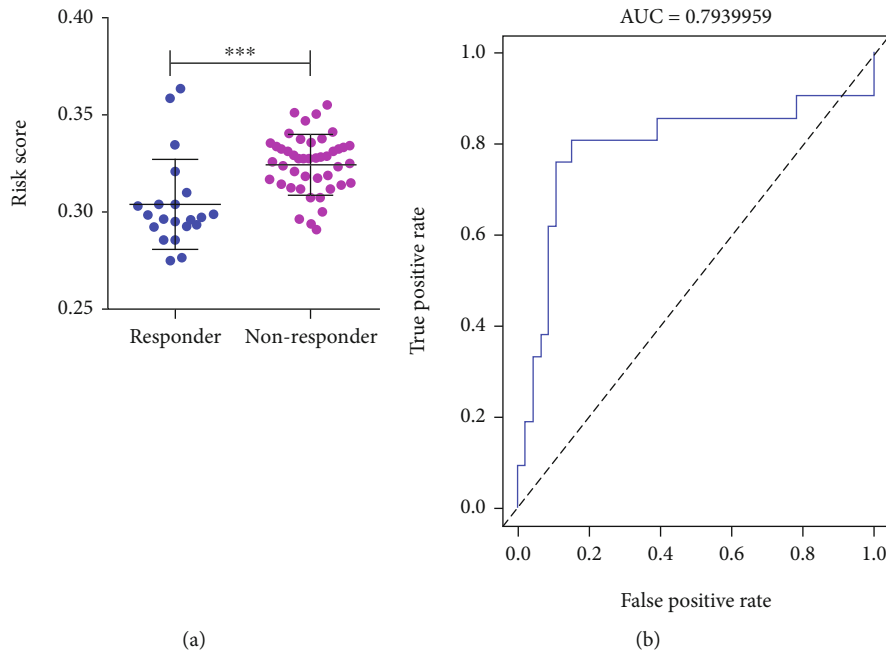


FIGURE 8: Association of risk signature with sorafenib treatment response of GSE109211 cohort. (a) Difference of risk score between sorafenib treatment responders and nonresponders. (b) AUC of risk signature in predicting in sorafenib treatment response.

0.714 (Figure 6(b)), respectively, which convincingly suggested the good discrimination and prediction of our signature.

**3.6. Correlation of Risk Signature with Tumor-Infiltrating Immune Cells in TCGA and ICGC HCC Cohort.** CIBERSOR was used to calculate 22 kinds of infiltrating immune cells in patients with different risk scores. In TCGA HCC cohort, significantly higher proportions of macrophages M0 cells, memory B cells, follicular helper T cells, and neutrophils were found to be enriched in HCC patients with high risk score, while significantly higher proportions of resting memory CD4 T cells and monocytes were found to be enriched in HCC patients with low risk score (all  $P < 0.05$ , Figure 7(a)). In ICGC HCC cohort, significantly higher proportions of macrophages M0 cells and Treg cells were found to be enriched in HCC patients with high risk score, while significantly higher proportions of naive B cells and gamma delta T cells were found to be enriched in HCC patients with low risk score (all  $P < 0.05$ , Figure 7(b)). These results suggested that the risk signature was significantly associated with tumor-infiltrating immune cells, and different kinds of infiltrating immune cells in patients with different risk scores might contribute to their different prognosis.

**3.7. Risk Signature as Indicator in Sorafenib Treatment Response for HCC Patients.** To investigate the association between risk signature and sorafenib treatment response, we calculated risk score for each HCC patients treated with sorafenib of GSE109211, which contained 21 sorafenib treatment responders and 46 nonresponders. Significantly lower risk scores were found at sorafenib treatment responders compared to those in nonresponders ( $P < 0.001$ ,

Figure 8(a)). Moreover, the AUC for predicting sorafenib treatment response was 0.794 (Figure 8(b)). Taken together, the risk signature might be served as an indicator for sorafenib treatment response in HCC patients.

**3.8. Correlation of Risk Signature with Anti-PD-1 Immunotherapy.** As a major breakthrough in cancer therapy, immunotherapies represented by immunological checkpoint blockade (PD-1/L1 and CTLA-4) proved promising clinical efficacy, and previous study proved that combination treatment with anti-PD-1 antibodies and sorafenib exhibited a more potent antitumor effect, but only a small number of patients could achieve durable responses [31, 32], so in the present study, we also explored whether the risk signature could predict patients' response to immune checkpoint blockade therapy in an anti-PD-1 cohort of GSE78220. Encouragingly, patients with lower risk score had better OS than patients with higher risk score (HR = 3.81, 95% CI: 1.13-11.08, and  $P = 0.03$ ; Figure 9(a)). Besides, despite there was no statistical difference, lower risk score was found at patients with complete immunotherapeutic response compared to that in patients with partial response and patients with no response, and lower risk score was also found in alive patients treated with anti-PD-1 than that in patients of death, which might due to the limitation number of patients in the cohort (Figures 9(b) and 9(c)). Moreover, the AUC of the risk signature for predicting 1 year-, 1.5-year, and 2-year OS of patients with anti-PD-1 immunotherapies was 0.669, 0.725, and 0.639 (Figure 9(d)). In a word, the above results strongly indicated that risk signature was significantly correlated with response to anti-PD-1 immunotherapy, which might be used as a new biomarker for predicting the response to anti-PD-1/L1 immunotherapy.

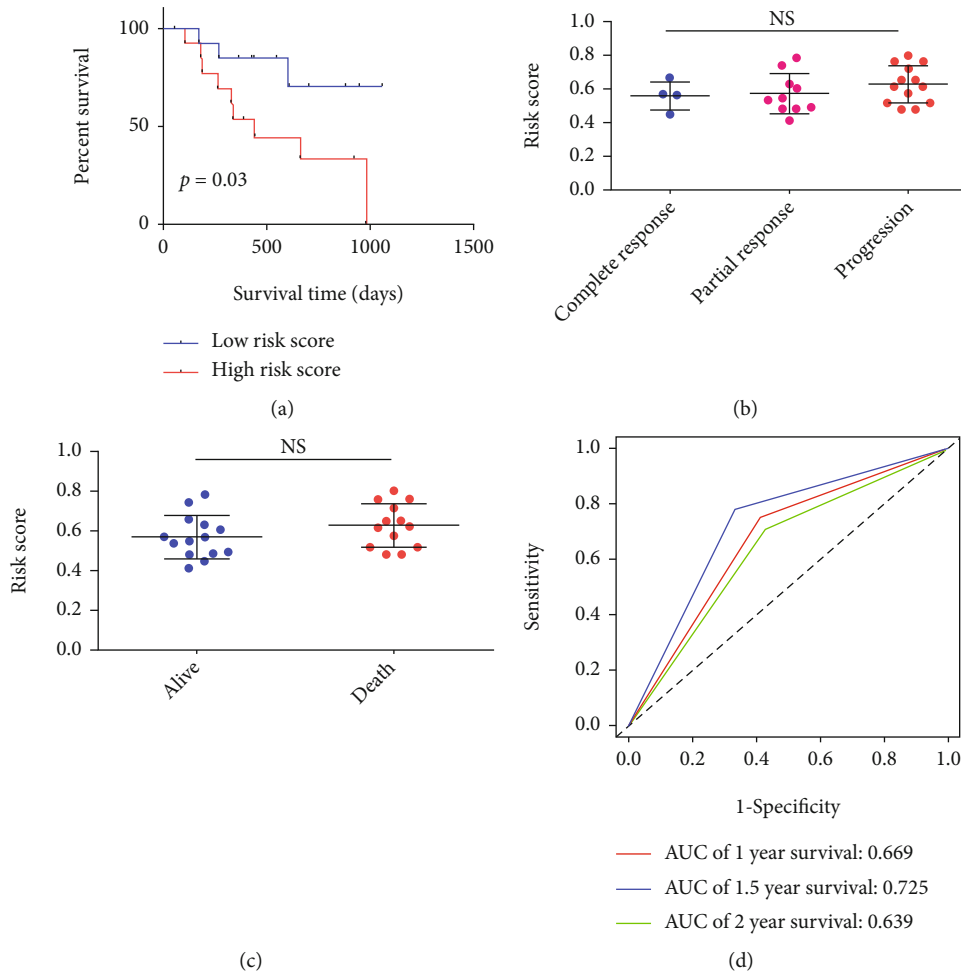


FIGURE 9: Association of risk signature with anti-PD-1 immunotherapy treatment response of GSE78220 cohort. (a) Kaplan-Meier analysis of OS of anti-PD-1 immunotherapy-treated patients with different risk scores. (b) Difference of risk score among complete anti-PD-1 immunotherapy response, partial anti-PD-1 immunotherapy response, and no anti-PD-1 immunotherapy response. (c) Difference of risk score between alive patient with anti-PD-1 immunotherapy and dead patients with anti-PD-1 immunotherapy. (d) AUC of risk signature in predicting 1-year, 1.5-year, and 2-year OS in patients with anti-PD-1 immunotherapy response.

#### 4. Discussion

m6A modifications are mainly controlled by methyltransferases and binding proteins and [13]. Studies have reported the conservative role and mechanism of m6A modification-related genes in regulating RNA modification, but only a few literatures have studied the role of m6A modification-related genes in HCC patients. Zhao et al. found that *YTHDF1* was significantly upregulated in HCC and positively correlated with pathology stage [24]. Cheng et al. also reported that the expression of *KIAA1429* was higher in HCC and HCC cell lines, and *KIAA1429* could regulate the progression of HCC by regulating ID2 m6A modification [26]. Chen et al. discovered that *METTL3* was significantly upregulated in HCC. Knockdown of *METTL3* was also found to suppress the tumorigenicity and progression of HCC through *YTHDF2*-dependent posttranscriptional silencing of *SOCS2* [25]. Moreover, Yang et al. found that *YTHDF2* was significantly related to malignancy of HCC, and miR-145 could inhibit the tumorigenicity of HCC by decreasing

*YTHDF2* [33]. Collectively, these results indicated that m6A modification-related genes promoted the tumorigenesis of HCC.

Whether expressions of m6A modification-related genes could be considered as prognostic biomarker is one of the trending research topics in m6A modification research [20]. Upregulation of *YTHDF1* and *METTL3* expression was found to be related to poorer OS of HCC patients [24, 25, 27]. Similarly, in our study, *THDF1*, *HNRNPC*, *RBM15*, *METTL3*, and *YTHDF2* were independent prognostic factors for OS and DFS in HCC patients. Next, a risk signature based on the expression of five genes could differentiate HCC patients into high-risk patients with poorer OS and DFS and low-risk patients with better OS and DFS. Interestingly, this risk signature together showed better predictive efficiency in predicting OS and DFS than TNM stage or any single gene estimation alone. Therefore, this risk signature might be an advantageous method for individualized therapeutic strategies in HCC patients. In addition, we also found that the risk signature was significantly associated with

tumor-infiltrating immune cells, which might influence prognosis of patients with different risk scores. Significantly higher proportions of macrophages M0 cells, neutrophils, and Treg cells were found to be enriched in HCC patients with high risk scores. Previous studies showed that macrophages could be recruited to tumor tissues and become proangiogenic cells, which were significantly associated with microvessel density and poor OS and DFS of HCC [34, 35]; Zhou et al. also found that tumor-associated neutrophils could promote the progression of HCC and resistance to sorafenib by recruiting macrophages and Treg cells [36]. These results might partly explain the reason for poorer OS and DFS in HCC patients with high risk score. Moreover, significantly higher proportions of memory CD4 T cells, gamma delta T cells, and naive B cells were found to be enriched in HCC patients with low risk score, suggesting higher proportions of infiltrated T cells and B cells. Garnelo et al. found that the degree of infiltrated T cells and B cells of tumor tissues significantly related with the improved prognosis of HCC patients [37], which might also partly explain the reason for longer OS and DFS in HCC patients with low risk score.

As an oral multikinase inhibitor, sorafenib is one of the standard care therapies for advanced stage HCC patients approved by FDA. It can prolong the survival time of HCC patients by inhibiting cell proliferation and angiogenesis and promoting cell apoptosis through inhibiting a variety of intracellular and cell surface kinases (such as c-raf, BRAF, and RET), vascular endothelial growth factor receptor (VEGFR), and platelet-derived growth factor receptor (PDGFR) [38, 39]. However, some studies have also found that HCC rapidly became sorafenib-resistant, and only about 30% of the patients could benefit from sorafenib treatment, which might greatly limit the wide clinical application of sorafenib [40, 41]. Besides, as a major breakthrough in cancer therapy, immunotherapies represented by immunological checkpoint blockade (PD-1/L1 and CTLA-4) proved promising clinical efficacy, and previous study proved that the combination treatment with anti-PD-1 antibodies and sorafenib exhibited a more potent antitumor effect, but only a small number of patients could achieve durable responses [31, 32], so identifying the HCC patients suitable for sorafenib treatment or anti-PD-1 immunotherapy or their combination therapy might be urgent and clinically significant. Encouragingly, in the present study, we found the m6A-related risk signature was significantly correlated with response to sorafenib treatment and anti-PD-1 immunotherapy. Significantly lower risk scores were found at sorafenib treatment responders or anti-PD-1 immunotherapy responders, and anti-PD-1 immunotherapy-treated patients with lower risk score had better OS than patients with higher risk score, which strongly indicated that the risk signature might be used as a new biomarker for predicting the response to sorafenib treatment and anti-PD-1 immunotherapy and even the combination of them. But independent prospective studies with a larger sample size were still needed to confirm our findings.

Though the risk signature exhibited good performance for the prognosis of HCC, several limitations should be addressed. First of all, although the prognostic value of the

risk signature has been validated in external cohort, independent cohorts consist of more HCC patients were required to further verify the model. Secondly, we did not explore the potential biological functions and pathways of risk signature. The experiment in vitro and in vivo should be carried out to uncover the relevant mechanisms. Finally, previously, Huang et al. suggested that the significant expression of m6A modification-related genes was found in circulating tumor cells (CTCs) [42]. Further studies were needed to examine whether these m6A modification-related genes could be detected in peripheral blood in HCC patients and whether the risk signature in blood could still have good prognostic value.

In conclusion, *THDF1*, *HNRNPC*, *RBM15*, *METTL3*, and *YTHDF2* were independent prognostic factors for OS and DFS in HCC patients. A risk signature developed with the expression of *YTHDF2*, *YTHDF1*, *METTL3*, *KIAA1429*, and *ZC3H1* could improve the prediction of prognosis and correlate with sorafenib treatment and anti-PD-1 immunotherapy response.

## Abbreviations

HCC:	Hepatocellular carcinoma
m6A:	N6-methyladenosine
OS:	Overall survival
DFS:	Disease-free survival
LASSO:	Least absolute shrinkage and selection operator
GSC:	Glioblastoma stem cell
VEGFR:	Vascular endothelial growth factor receptor
PDGFR:	Platelet-derived growth factor receptor
CTCs:	Circulating tumor cells.

## Data Availability

The data of the study are available from the corresponding web page link, including GDC Data portal (<https://cancergenome.nih.gov/>), ICGC portal (<https://dcc.icgc.org/projects/LIRI-JP>), and GEO database (<https://www.ncbi.nlm.nih.gov/geo/>).

## Ethical Approval

All the data analyzed in the present study were got from TCGA, ICGC and GEO.

## Consent

Informed consents had already been obtained from the patients before the present study.

## Disclosure

The manuscript has been presented as preprint (<https://www.researchsquare.com/article/rs-130710/v1>), but it has not been published in any magazines.

## Conflicts of Interest

The authors declare that the research was conducted in the absence of any commercial or financial relationships that could be construed as a potential conflict of interest.

## Authors' Contributions

Hongye Jiang and Gang Ning analyzed the data and wrote the paper; Yensheng Wang downloaded the data and wrote the R codes to process the data. Weibiao Lv got the idea of this study and designed the experiment. Weibiao Lv discussed with all of the authors and provided the suggestions about the experiments. All authors read and approved the final manuscript. Hongye Jiang and Gang Ning contributed equally to this work.

## Acknowledgments

This study was supported by China Postdoctoral Science Foundation (No. 2020M682626), Guangdong Basic and Applied Basic Research Foundation (No. 2021A1515011117), and Regional Joint Youth Fund Project of Guangdong Province (No. 2020A1515110976).

## Supplementary Materials

Supplementary figure 1: association of m6A modification-related genes with OS of HCC patients. Univariate analysis of mRNA expression of m6A modification-related genes with OS of HCC patients (A). Multivariate analysis of mRNA expression of m6A modification-related genes with OS of HCC patients (B-J). Gender: male vs. female; age: >60 vs. ≤60; grade: G3+G4 vs. G1+G2; T: T1 vs. T0; N: N1 vs. N0; M: M1 vs. M0; TNM stage: stage III+IV vs. stage I+II. Supplementary figure 2: relationship of m6A modification-related genes with DFS of HCC patients. Univariate analysis of mRNA expression of m6A modification-related genes with DFS of HCC patients (A). Multivariate analysis of mRNA expression of m6A modification-related genes with DFS of HCC patients (B-H). Gender: male vs. female; age: >60 vs. ≤60; grade: G3+G4 vs. G1+G2; T: T1 vs. T0; N: N1 vs. N0; M: M1 vs. M0; TNM stage: stage III+IV vs. stage I+II. (Supplementary Materials)

## References

- [1] F. Bray, J. Ferlay, I. Soerjomataram, R. L. Siegel, L. A. Torre, and A. Jemal, "Global cancer statistics 2018: GLOBOCAN estimates of incidence and mortality worldwide for 36 cancers in 185 countries," *CA: a Cancer Journal for Clinicians*, vol. 68, no. 6, pp. 394–424, 2018.
- [2] S. F. Altekruse, S. J. Henley, J. E. Cucinelli, and K. A. McGlynn, "Changing hepatocellular carcinoma incidence and liver cancer mortality rates in the United States," *The American Journal of Gastroenterology*, vol. 109, no. 4, pp. 542–553, 2014.
- [3] T. Clark, S. Maximin, J. Meier, S. Pokharel, and P. Bhargava, "Hepatocellular carcinoma: review of epidemiology, screening, imaging diagnosis, response assessment, and treatment," *Current Problems in Diagnostic Radiology*, vol. 44, no. 6, pp. 479–486, 2015.
- [4] P. Tabrizian, G. Jibara, B. Shrager, M. Schwartz, and S. Roayaie, "Recurrence of hepatocellular cancer after resection: patterns, treatments, and prognosis," *Annals of Surgery*, vol. 261, no. 5, pp. 947–955, 2015.
- [5] A. Arzumanyan, H. M. Reis, and M. A. Feitelson, "Pathogenic mechanisms in HBV- and HCV-associated hepatocellular carcinoma," *Nature Reviews. Cancer*, vol. 13, no. 2, pp. 123–135, 2013.
- [6] V. Vedham and M. Verma, "Cancer-associated infectious agents and epigenetic regulation," *Methods in Molecular Biology*, vol. 1238, pp. 333–354, 2015.
- [7] L. Ma, M. S. Chua, O. Andrisani, and S. So, "Epigenetics in hepatocellular carcinoma: an update and future therapy perspectives," *World Journal of Gastroenterology*, vol. 20, no. 2, pp. 333–345, 2014.
- [8] Z. Herceg and A. Paliwal, "Epigenetic mechanisms in hepatocellular carcinoma: how environmental factors influence the epigenome," *Mutation Research*, vol. 727, no. 3, pp. 55–61, 2011.
- [9] Y. Fu, D. Dominissini, G. Rechavi, and C. He, "Gene expression regulation mediated through reversible m(6)A RNA methylation," *Nature Reviews. Genetics*, vol. 15, no. 5, pp. 293–306, 2014.
- [10] I. A. Roundtree, M. E. Evans, T. Pan, and C. He, "Dynamic RNA modifications in gene expression regulation," *Cell*, vol. 169, no. 7, pp. 1187–1200, 2017.
- [11] X. Wang, Z. Lu, A. Gomez et al., "N6-methyladenosine-dependent regulation of messenger RNA stability," *Nature*, vol. 505, no. 7481, pp. 117–120, 2014.
- [12] N. Liu and T. Pan, "N6-methyladenosine-encoded epitranscriptomics," *Nature Structural & Molecular Biology*, vol. 23, no. 2, pp. 98–102, 2016.
- [13] Y. Yang, P. J. Hsu, Y. S. Chen, and Y. G. Yang, "Dynamic transcriptomic m(6)A decoration: writers, erasers, readers and functions in RNA metabolism," *Cell Research*, vol. 28, no. 6, pp. 616–624, 2018.
- [14] S. Wang, C. Sun, J. Li et al., "Roles of RNA methylation by means of N(6)-methyladenosine (m(6)A) in human cancers," *Cancer Letters*, vol. 408, pp. 112–120, 2017.
- [15] C. T. Kwok, A. D. Marshall, J. E. Rasko, and J. J. Wong, "Genetic alterations of m(6)A regulators predict poorer survival in acute myeloid leukemia," *Journal of Hematology & Oncology*, vol. 10, no. 1, p. 39, 2017.
- [16] R. C. Chai, F. Wu, Q. X. Wang et al., "m(6)A RNA methylation regulators contribute to malignant progression and have clinical prognostic impact in gliomas," *Aging*, vol. 11, no. 4, pp. 1204–1225, 2019.
- [17] M. Mendel, K. M. Chen, D. Homolka et al., "Methylation of structured RNA by the m(6)A writer METTL16 is essential for mouse embryonic development," *Molecular Cell*, vol. 71, no. 6, pp. 986–1000.e11, 2018.
- [18] M. Engel, C. Eggert, P. M. Kaplick et al., "The Role of m<sup>6</sup>A/mRNA Methylation in Stress Response Regulation," *Neuron*, vol. 99, no. 2, pp. 389–403.e9, 2018.
- [19] K. Du, L. Zhang, T. Lee, and T. Sun, "m(6)A RNA methylation controls neural development and is involved in human diseases," *Molecular Neurobiology*, vol. 56, no. 3, pp. 1596–1606, 2019.
- [20] Y. Pan, P. Ma, Y. Liu, W. Li, and Y. Shu, "Multiple functions of m(6)A RNA methylation in cancer," *Journal of Hematology & Oncology*, vol. 11, no. 1, p. 48, 2018.

- [21] D. Dai, H. Wang, L. Zhu, H. Jin, and X. Wang, "N6-methyladenosine links RNA metabolism to cancer progression," *Cell Death & Disease*, vol. 9, no. 2, p. 124, 2018.
- [22] C. X. Wang, G. S. Cui, X. Liu et al., "METTL3-mediated m6A modification is required for cerebellar development," *PLoS Biology*, vol. 16, no. 6, article e2004880, 2018.
- [23] A. Visvanathan, V. Patil, A. Arora et al., "Essential role of METTL3-mediated m(6)A modification in glioma stem-like cells maintenance and radioresistance," *Oncogene*, vol. 37, no. 4, pp. 522–533, 2018.
- [24] X. Zhao, Y. Chen, Q. Mao et al., "Overexpression of YTHDF1 is associated with poor prognosis in patients with hepatocellular carcinoma," *Cancer Biomarkers: Section A of Disease Markers*, vol. 21, no. 4, pp. 859–868, 2018.
- [25] M. Chen, L. Wei, C. T. Law et al., "RNA N6-methyladenosine methyltransferase-like 3 promotes liver cancer progression through YTHDF2-dependent posttranscriptional silencing of SOCS2," *Hepatology*, vol. 67, no. 6, pp. 2254–2270, 2018.
- [26] X. Cheng, M. Li, X. Rao et al., "KIAA1429 regulates the migration and invasion of hepatocellular carcinoma by altering m6A modification of ID2 mRNA," *OncoTargets and Therapy*, vol. - Volume 12, pp. 3421–3428, 2019.
- [27] Y. Zhou, Z. Yin, B. Hou et al., "Expression profiles and prognostic significance of RNA N6-methyladenosine-related genes in patients with hepatocellular carcinoma: evidence from independent datasets," *Cancer Management and Research*, vol. - Volume 11, pp. 3921–3931, 2019.
- [28] J. Gao, P. W. Kwan, and D. Shi, "Sparse kernel learning with LASSO and Bayesian inference algorithm," *Neural Networks*, vol. 23, no. 2, pp. 257–264, 2010.
- [29] A. M. Newman, C. L. Liu, M. R. Green et al., "Robust enumeration of cell subsets from tissue expression profiles," *Nature Methods*, vol. 12, no. 5, pp. 453–457, 2015.
- [30] D. H. Parks, G. W. Tyson, P. Hugenholtz, and R. G. Beiko, "STAMP: statistical analysis of taxonomic and functional profiles," *Bioinformatics*, vol. 30, no. 21, pp. 3123–3124, 2014.
- [31] S. L. Topalian, F. S. Hodi, J. R. Brahmer et al., "Safety, activity, and immune correlates of anti-PD-1 antibody in cancer," *The New England Journal of Medicine*, vol. 366, no. 26, pp. 2443–2454, 2012.
- [32] H. Deng, A. Kan, N. Lyu et al., "Dual vascular endothelial growth factor receptor and fibroblast growth factor receptor inhibition elicits antitumor immunity and enhances programmed cell death-1 checkpoint blockade in hepatocellular carcinoma," *Liver Cancer*, vol. 9, no. 3, pp. 338–357, 2020.
- [33] Z. Yang, J. Li, G. Feng et al., "MicroRNA-145 modulates N(6)-methyladenosine levels by targeting the 3'-untranslated mRNA region of the N(6)-methyladenosine binding YTH domain family 2 protein," *The Journal of Biological Chemistry*, vol. 292, no. 9, pp. 3614–3623, 2017.
- [34] T. Matsubara, T. Kanto, S. Kuroda et al., "TIE2-expressing monocytes as a diagnostic marker for hepatocellular carcinoma correlates with angiogenesis," *Hepatology*, vol. 57, no. 4, pp. 1416–1425, 2013.
- [35] Y. F. He, C. Q. Wang, Y. Yu et al., "Tie2-expressing monocytes are associated with identification and prognoses of hepatitis B virus related hepatocellular carcinoma after resection," *PLoS One*, vol. 10, no. 11, article e0143657, 2015.
- [36] S. L. Zhou, Z. J. Zhou, Z. Q. Hu et al., "Tumor-associated neutrophils recruit macrophages and T-regulatory cells to promote progression of hepatocellular carcinoma and resistance to sorafenib," *Gastroenterology*, vol. 150, no. 7, pp. 1646–1658.e17, 2016.
- [37] M. Garnelo, A. Tan, Z. Her et al., "Interaction between tumour-infiltrating B cells and T cells controls the progression of hepatocellular carcinoma," *Gut*, vol. 66, no. 2, pp. 342–351, 2017.
- [38] J. M. Llovet, S. Ricci, V. Mazzaferro et al., "Sorafenib in advanced hepatocellular carcinoma," *The New England Journal of Medicine*, vol. 359, no. 4, pp. 378–390, 2008.
- [39] S. M. Wilhelm, L. Adnane, P. Newell, A. Villanueva, J. M. Llovet, and M. Lynch, "Preclinical overview of sorafenib, a multi-kinase inhibitor that targets both Raf and VEGF and PDGF receptor tyrosine kinase signaling," *Molecular Cancer Therapeutics*, vol. 7, no. 10, pp. 3129–3140, 2008.
- [40] A. L. Cheng, Y. K. Kang, Z. Chen et al., "Efficacy and safety of sorafenib in patients in the Asia-Pacific region with advanced hepatocellular carcinoma: a phase III randomised, double-blind, placebo-controlled trial," *The Lancet Oncology*, vol. 10, no. 1, pp. 25–34, 2009.
- [41] H. K. Sanoff, Y. Chang, J. L. Lund, B. H. O'Neil, and S. B. Dusetzina, "Sorafenib effectiveness in advanced hepatocellular carcinoma," *The Oncologist*, vol. 21, no. 9, pp. 1113–1120, 2016.
- [42] W. Huang, C. B. Qi, S. W. Lv et al., "Determination of DNA and RNA methylation in circulating tumor cells by mass spectrometry," *Analytical Chemistry*, vol. 88, no. 2, pp. 1378–1384, 2016.

## Research Article

# Transcriptome-Wide Gene Expression in a Murine Model of Ventilator-Induced Lung Injury

Zhao Li <sup>1</sup>, Guoshao Zhu,<sup>2</sup> Chen Zhou,<sup>1</sup> Hui Wang,<sup>1</sup> Le Yu,<sup>1</sup> Yunxin Xu,<sup>1</sup> Li Xu <sup>3</sup>,  
and Qingxiu Wang <sup>1</sup>

<sup>1</sup>Department of Anesthesiology, East Hospital, Tongji University School of Medicine, Shanghai 200120, China

<sup>2</sup>Department of Anesthesiology, Quanzhou First Hospital Affiliated to Fujian Medical University, Quanzhou 362000, China

<sup>3</sup>Department of Anesthesiology, The First People's Hospital of Changde, Changde 415000, China

Correspondence should be addressed to Li Xu; [lilyxulixuli@163.com](mailto:lilyxulixuli@163.com) and Qingxiu Wang; [qxw1123@126.com](mailto:qxw1123@126.com)

Received 1 February 2021; Revised 1 March 2021; Accepted 5 March 2021; Published 8 April 2021

Academic Editor: Andrea Maugeri

Copyright © 2021 Zhao Li et al. This is an open access article distributed under the Creative Commons Attribution License, which permits unrestricted use, distribution, and reproduction in any medium, provided the original work is properly cited.

**Background.** Mechanical ventilation could lead to ventilator-induced lung injury (VILI), but its underlying pathogenesis remains largely unknown. In this study, we aimed to determine the genes which were highly correlated with VILI as well as their expressions and interactions by analyzing the differentially expressed genes (DEGs) between the VILI samples and controls. **Methods.** GSE11434 was downloaded from the gene expression omnibus (GEO) database, and DEGs were identified with GEO2R. Gene Ontology (GO) and Kyoto Encyclopedia of Genes and Genomes (KEGG) pathway enrichment analyses were conducted using DAVID. Next, we used the STRING tool to construct protein-protein interaction (PPI) network of the DEGs. Then, the hub genes and related modules were identified with the Cytoscape plugins: cytoHubba and MCODE. qRT-PCR was further used to validate the results in the GSE11434 dataset. We also applied gene set enrichment analysis (GSEA) to discern the gene sets that had a significant difference between the VILI group and the control. Hub genes were also subjected to analyses by CyTargetLinker and NetworkAnalyst to predict associated miRNAs and transcription factors (TFs). Besides, we used CIBERSORT to detect the contributions of different types of immune cells in lung tissues of mice in the VILI group. By using DrugBank, small molecular compounds that could potentially interact with hub genes were identified. **Results.** A total of 141 DEGs between the VILI group and the control were identified in GSE11434. Then, seven hub genes were identified and were validated by using qRT-PCR. Those seven hub genes were largely enriched in TLR and JAK-STAT signaling pathways. GSEA showed that VILI-associated genes were also enriched in NOD, antigen presentation, and chemokine pathways. We predicted the miRNAs and TFs associated with hub genes and constructed miRNA-TF-gene regulatory network. An analysis with CIBERSORT showed that the proportion of M0 macrophages and activated mast cells was higher in the VILI group than in the control. Small molecules, like nadroparin and siltuximab, could act as potential drugs for VILI. **Conclusion.** In sum, a number of hub genes associated with VILI were identified and could provide novel insights into the pathogenesis of VILI and potential targets for its treatment.

## 1. Introduction

Mechanical ventilation is widely used in surgery and intensive care and offers a substantial advantage in managing patients' breathing during general anesthesia. It is also regarded as one of the most important means to treat patients who are undergoing respiratory failure as well as acute or chronic lung injury [1]. However, mechanical ventilation is a double-edged sword during respiratory support in some

cases [2]. For example, improper use of mechanical ventilation may aggravate the original pathological damage or lead to direct lung injury, known as ventilator-induced lung injury (VILI) [3]. Patients with no original acute lung injury may develop acute lung injury after being subjected to mechanical ventilation for more than 48 hours [4]. Nearly half of the patients who had received mechanical ventilation for more than two weeks got pulmonary complications associated with mechanical ventilation. For this reason, it is of

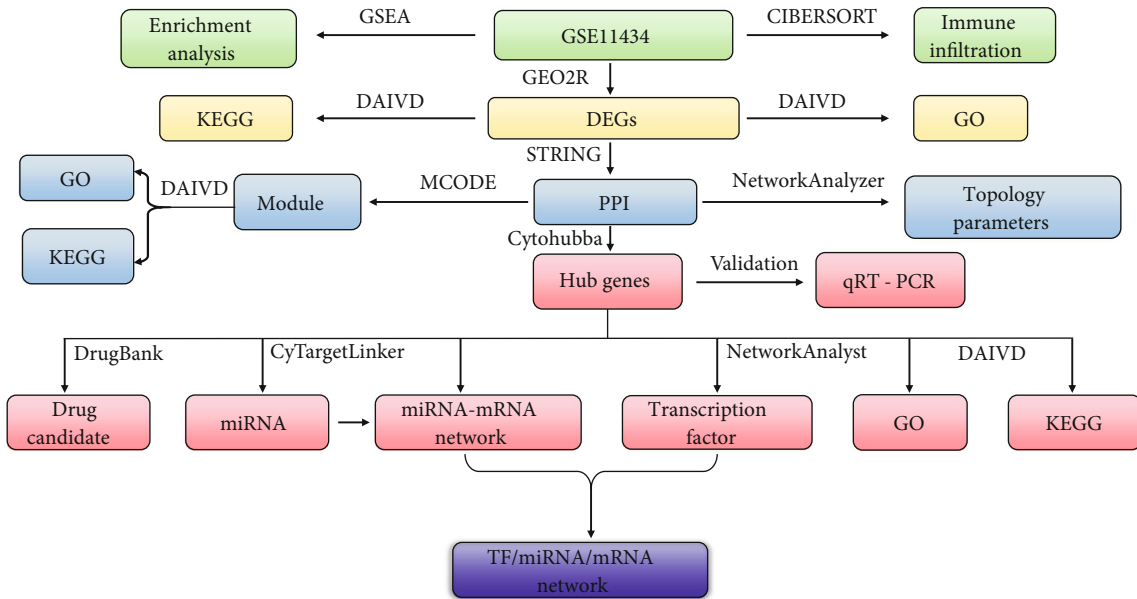


FIGURE 1: Flow chart of investigations in this study.

great pertinence to elucidate the pathogenesis of VILI and take protective or therapeutic measures against it. A lot of efforts have been made to reduce VILI occurrences during perioperative anesthesia and in critical care units.

At present, the primary measure taken for VILI prevention is the lung protective ventilation approach in which a small tidal volume is used, but its efficacy is highly limited [5]. The pathogenesis of VILI is still unclear, and effective interventions have yet to be investigated [6]. Therefore, it is vital to identify the involved key genes to better understand the molecular mechanism of VILI pathogenesis for an early, effective intervention.

As a powerful analytic tool, bioinformatics analysis has gradually been used in predicting the molecular mechanisms of VILI pathogenesis. For instance, Tamás et al. conducted the gene expression analysis in a mouse overventilation model and validated upregulated expressions of five genes (Areg, Akap12, Nur77, Cyr61, and Il11) [7]. Similarly, Ma et al. analyzed genes affected by VILI and validated the expression levels of randomly selected genes [8]. Despite those reports, the VILI-correlated hub genes have not yet been identified. In this study, analyses of hub genes that could be associated with VILI were performed based on extensive gene expression data of a mouse VILI model published online, to study their potential and specific roles in VILI.

## 2. Materials and Methods

**2.1. Gene Chip Analysis and Identification of DEGs.** The procedures of analysis in this study can be seen in Figure 1. GEO is a database for storing and distributing the sequencing data [9]. In this study, we downloaded the GSE11434 dataset from GEO, based on the GPL1261 [10, 11]. GSE11434 was used to identify the hub genes associated with VILI. GSE11434 consisted of ten microarray chips and was divided into two groups: the VILI and control groups, with five samples in

each group. The criteria of  $\text{adj. } p < 0.05$  and  $|\log_2 \text{FC}| > 1$  were applied for screening DEGs.

**2.2. GO and KEGG Enrichment Analysis.** GO defines and standardizes terms for describing genes and their products, which contain three aspects [12]: cellular component (CC), molecular function (MF), and biological process (BP). CC is used to describe the area where the gene products are located in cells and could be a cellular substructure, an organelle (such as cytoplasm and nucleus), or a gene product set (such as a major histocompatibility complex). MF describes the function of gene products, such as carbohydrate binding and ATP-dependent hydrolase activity. BP specifies a more complex and advanced form of function systematically formed by a particular set of molecular process, such as mitosis and purine metabolism. DAVID (Ver. 6.8) was used to conduct the GO and KEGG enrichment analysis of DEGs [13]. The Benjamini-Hochberg corrected  $p$  value ( $p < 0.05$ ) was set as the threshold for statistically significant enrichment.

**2.3. Protein-Protein Interaction (PPI) Network Construction and Hub Gene Identification.** PPI represents the process of forming a protein complex by noncovalent bonding between proteins [14]. The gene set data were imported into the STRING database to analyze their interaction. A confidence score  $\geq 0.4$  was considered as statistically significant. A PPI network graph was retrieved based on this standard.

Cytoscape (Ver. 3.7.1) is open-sourced software for bioinformatics analysis and is commonly used to visualize the molecular interaction network [15]. NetworkAnalyzer, a Cytoscape plugin, was used to perform topological analysis. The results exported from the STRING database were imported into Cytoscape to identify the top 10 DEGs by applying five algorithms in cytoHubba, and the overlapping genes of them were considered as hub genes [16]. The

MCODE was used to screen out the statistically significant modules which were visualized by using Cytoscape [17].

**2.4. Analysis of miRNA and TFs Related to VILI.** CyTarget-Linker is a plugin for Cytoscape that can extend the biological regulatory interactive network [18] and can be used to analyze the interactive relationship between various miRNA targets. In this study, we downloaded the murine gene datasets and selected miRTarBase, MicroCosm, and TargetScan databases to predict the regulatory relationship between hub genes and miRNAs. NetworkAnalyst was used to predict the TFs that could regulate VILI-associated genes [19]. Hub genes were selected in the above cases of prediction. The miRNA-TF-hub gene network was constructed using Cytoscape.

**2.5. Gene Set Enrichment Analysis (GSEA).** GSEA uses a pre-defined gene set that can sort genes according to the degree of differential expression between samples from different groups and can subsequently validate whether the preset gene set is enriched at the top or bottom of the sorting list [20]. We downloaded the GSEA software from its official website and run it in a Java environment following instructions from a previous literature. Later, a curated KEGG gene set was downloaded from the MSigDB database, and then, an enrichment analysis was conducted according to the weighted enrichment statistic method in GSEA. The random number was set to 1000 to calculate the normalized enrichment score (NES) and false discovery rate (FDR). In GSEA, gene sets were considered significantly enriched when meeting the condition of  $NES \geq 1.0$ ,  $NOM\ p < 0.05$ , and  $FDR \leq 0.25$ .

**2.6. Immune Cell Composition Analysis.** CIBERSORT is an algorithm that could be applied to estimate cell composition in complex tissues based on standardized gene expression data [21]. In this study, we used CIBERSORT to assess the relative proportion of 22 immune cells in each lung tissue. The mRNA expression profiling data of lung tissues from the VILI and control groups were extracted. Then, these data were calibrated using the Limma package in R. Subsequently, the LM22 signature matrix was applied in 1000 arrays to predict the proportion of immune cells. The samples were screened at the significance level of  $p < 0.05$ . The histogram of the proportion of each type of immune cell, the heat map of immune cell expression, the violin plots, and the correlation chart of immune cell proportion in lung tissues were plotted accordingly.

**2.7. Identification of Potential Drugs.** DrugBank is a database that integrates detailed data of drugs and comprehensive information of the drug target [22]. The identified hub genes were analyzed in the DrugBank database to determine potential molecules associated with VILI.

**2.8. Animal Preparation and Experimental Protocol.** Ten healthy specific pathogen-free male ICR mice (20-25 g) were procured from Shanghai JSJ-Lab and were separated in two groups: the VILI group (in which mice received mechanical ventilation) and the control group (in which mice breathed

without any mechanical assistance). Mice were abstained from food 4 hours prior to anesthetization by intraperitoneal injection of 7.5% pentobarbital sodium solution (75 mg/kg). After the mice forming the VILI group were deeply anesthetized, they then received mechanical ventilation. Mice of the mechanical ventilation group were ventilated with tidal volume of 30 ml/kg, 65 breaths/min, and fraction of inspired oxygen of 0.21. Mice from the control group were allowed to breathe spontaneously. After 4 h of mechanical ventilation, the mice were euthanized, and then, lung tissues were harvested.

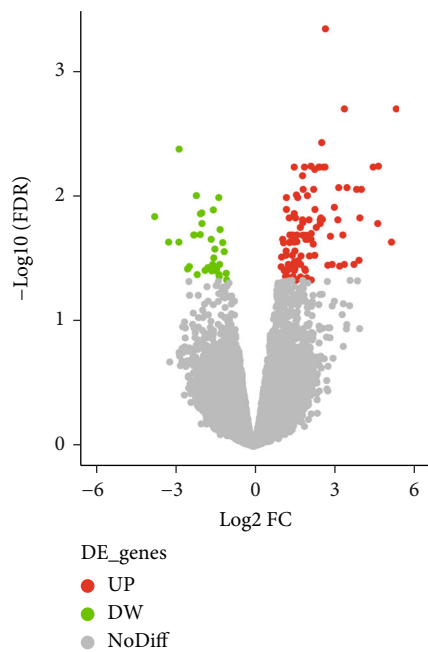
**2.9. RNA Extraction and Quantitative Real-Time Reverse Transcription PCR (qRT-PCR).** The total RNA was extracted from mice lung tissues using TRIzol reagent (Takara, Japan). cDNA synthesis was performed using the PrimeScript RT Reagent kit (Takara, Japan). qRT-PCR was operated with the SYBR Green method (Qiagen, Germany) on the QuantStudio 7 flex real-time PCR system. The cDNA was used as templates to perform qRT-PCR for 40 cycles under the following conditions: an initial denaturation at 95°C for 20 s, followed by denaturation at 95°C for 15 seconds, and annealing at 60°C for 1 minute. The primers for cDNA sequences used in qRT-PCR are listed in Supplemental Table (available here). The mRNA expression levels of target gene were normalized to that the housekeeping gene GAPDH. The  $\Delta\Delta Ct$  method was used to calculate expression fold change of target genes.

**2.10. Statistical Analysis.** The histograms of gene expression were plotted using GraphPad (Ver. 8.0). The gene expressions were expressed in the form of mean  $\pm$  standard deviation (SD). The comparison of differences between the VILI group and control was performed by independent samples *t*-test.  $p < 0.5$  was deemed as denoting statistical significance.

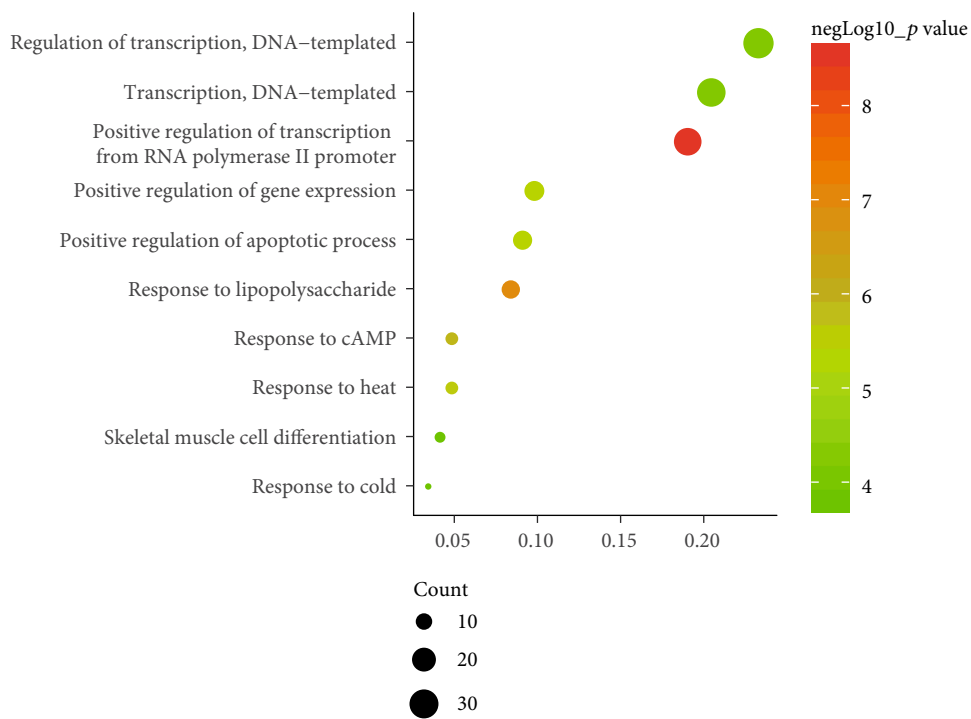
### 3. Results

**3.1. Identification and Enrichment of DEGs between the VILI and Control Groups.** To identify VILI-associated DEGs, we downloaded the GSE11434 expression profiles from GEO. A total of 141 DEGs were evaluated with GEO2R by following the criteria of  $adj. p < 0.05$  and  $|\log_2 \text{fold change}| \geq 1$ . Among them, 108 genes were upregulated and 33 were downregulated (Figure 2(a)).

To determine the specific functions of DEGs, GO annotation and KEGG pathway analyses were conducted with DAVID. In terms of BP, these DEGs were mainly involved in positive regulation of transcription from RNA polymerase II promoter as well as responses to lipopolysaccharide and cAMP (Figure 2(b)). In terms of CC, they were mostly enriched in the cytoplasm, nucleus, and nucleoplasm (Figure 2(c)). And primary enrichments in MF were mainly associated with TF activity, sequence-specific DNA binding, and protein binding (Figure 2(d)). *p* values were ranked in ascending order based on the results of pathway enrichment analysis. The top 20 enriched pathways, including MAPK, JAK-STAT, and TLR signaling, are shown in Figure 2(e).

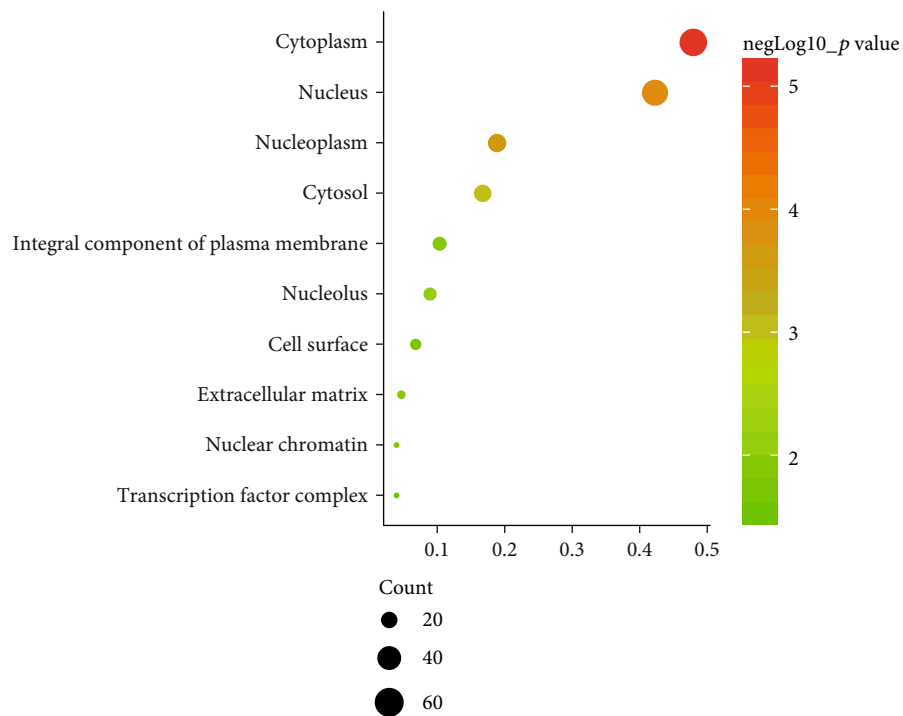


(a)

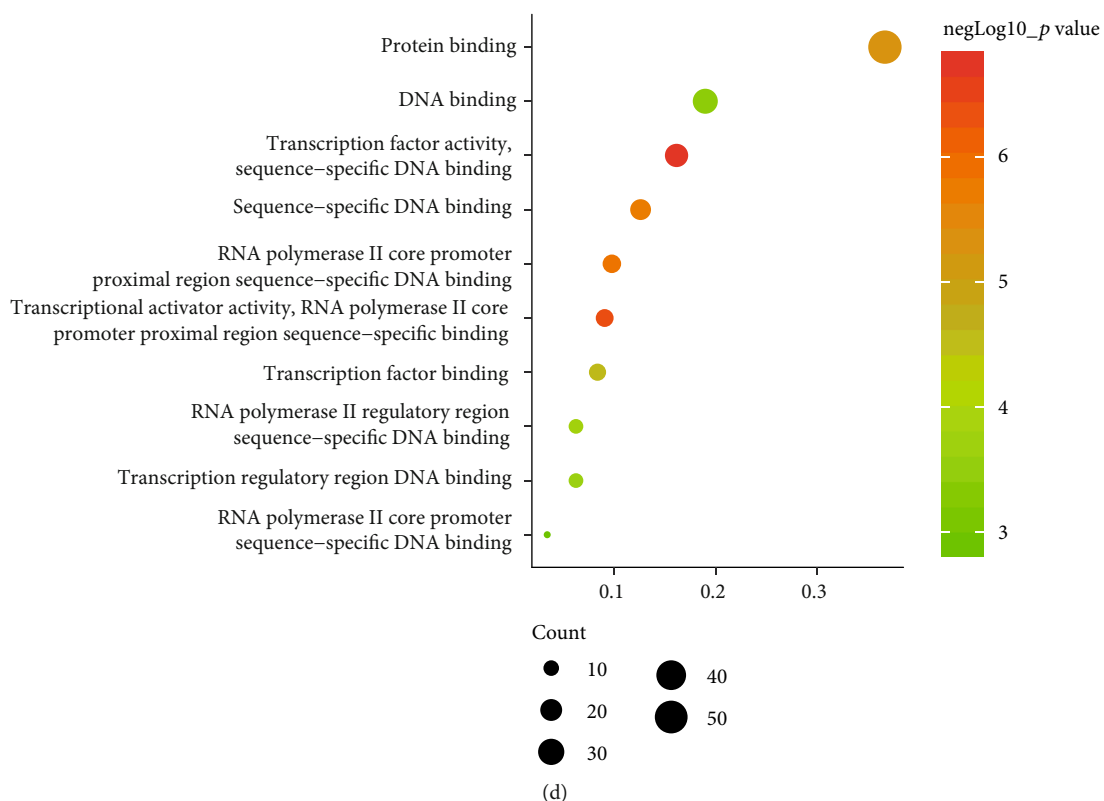


(b)

FIGURE 2: Continued.



(c)



(d)

FIGURE 2: Continued.

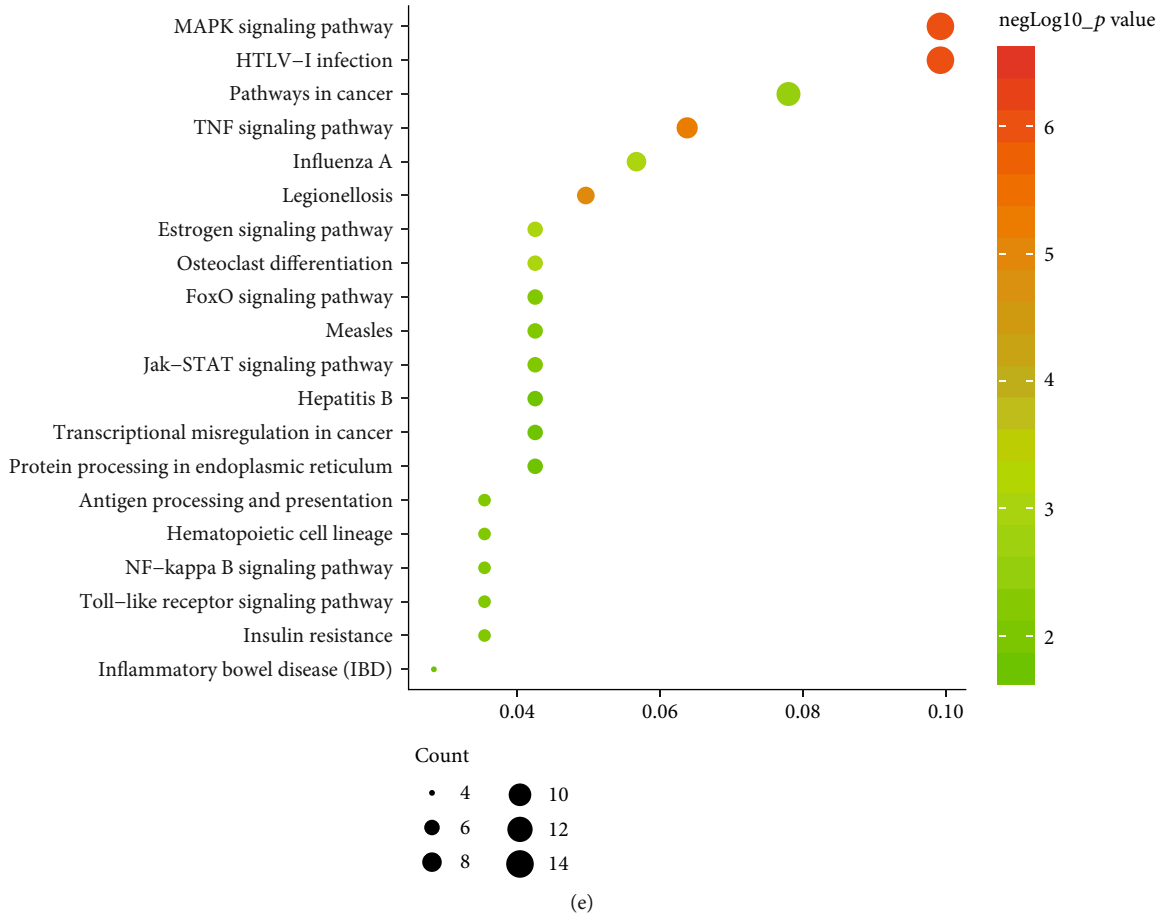


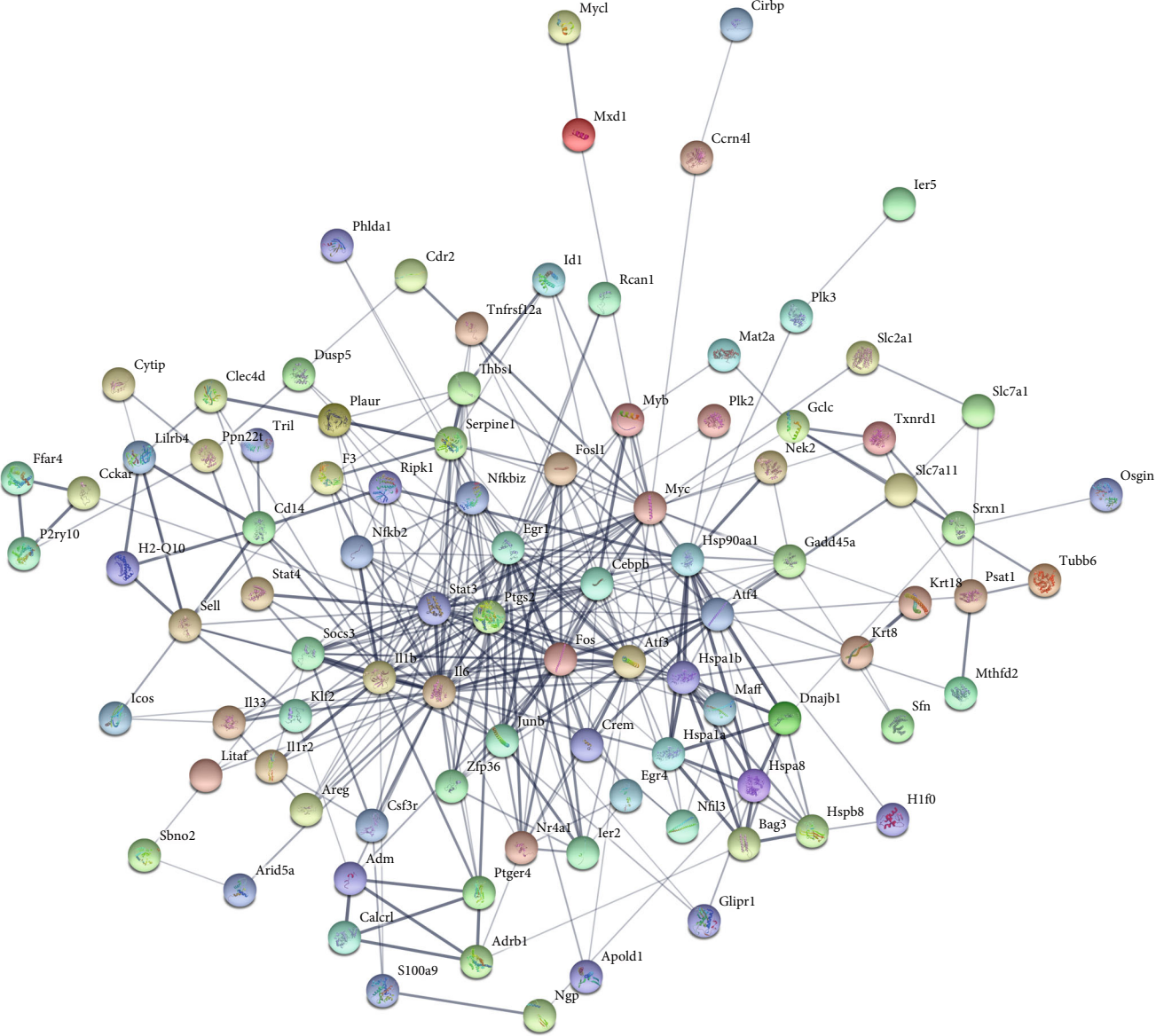
FIGURE 2: DEGs and enrichment analysis in the VILI and control groups. (a) Volcano plot of all DEGs in GSE11434. Red dots indicate upregulated genes and green dots indicate downregulated genes. (b) Top 15 terms in BP. (c) Top 15 terms in CC. (d) Top 15 terms in MF. (e) Top 15 KEGG pathway analysis.

**3.2. PPI Network and Module Analysis of DEGs.** To determine the interactive relationship between VILI-associated DEGs, an interaction network of DEG-encoded proteins was constructed. A total of 141 DEGs were mapped into the STRING database to retrieve a PPI network graph. As shown in Figure 3(a), the network included 133 nodes (target proteins) and three hundred and forty-eight edges (PPI). Topological analysis of the constructed PPI network was conducted using NetworkAnalyzer and revealed that the network topological parameters followed a power law distribution (Figures 3(b)–3(e)). The most significant module was screened out from the PPI network using MCODE, and 14 genes were identified (Figure 3(f)). We conducted functional enrichment analysis for these genes and found that they were mainly enriched in TNF and JAK-STAT signaling pathways (Tables 1 and 2).

**3.3. The Identification and Validation of Hub Genes.** To determine the VILI-associated hub genes, cytoHubba was used throughout the PPI network construction. Five algorithms (Degree, EPC, MCC, MNC, and Stress) present in cytoHubba were utilized to evaluate hub genes. The top 10 genes identified by each algorithm were intersected to obtain hub genes, which included Fos Proto-Oncogene (FOS), MYC

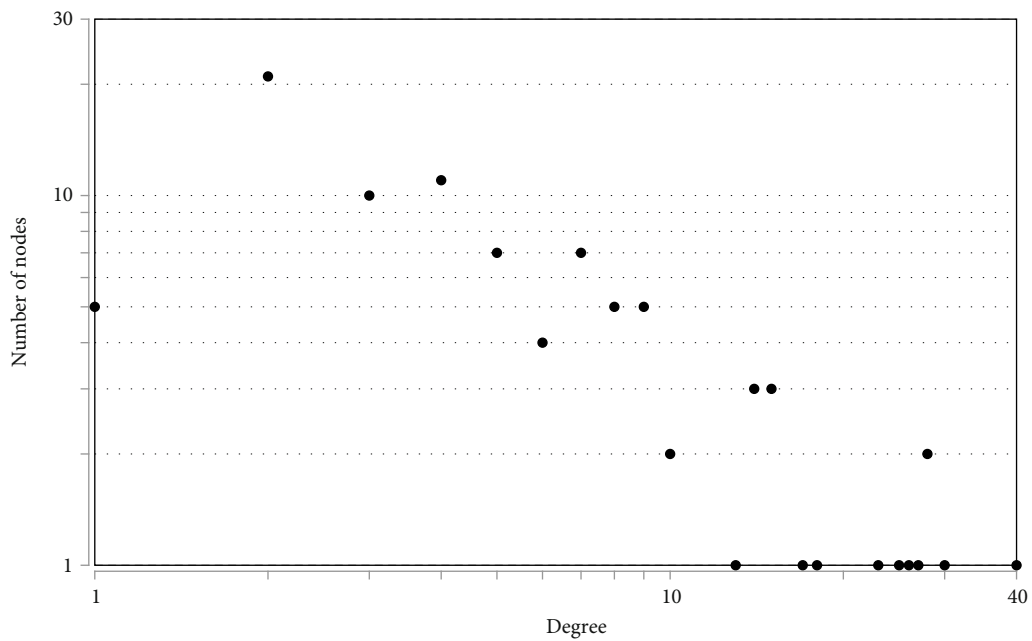
Proto-Oncogene (MYC), Signal Transducer and Activator of Transcription 3 (STAT3), Early Growth Response 1 (EGR1), Activating Transcription Factor 3 (ATF3), Interleukin-6 (IL-6), and Interleukin-1 Beta (IL-1B) (Figure 4(a)). Notably, all those hub genes were contained in the most highly connected module mentioned above. In comparison with the control, the expression levels of all seven hub genes were upregulated in the VILI group (Figure 4(b)). We found out that the functions of these hub genes were mainly about inducing inflammation and TLR signaling pathway regulation. Then, we performed qRT-PCR experiment for further validation. The results showed that the hub genes were all overexpressed in VILI tissues, which is consistent with the prediction results (Figure 4(c)). GO and KEGG enrichment analyses of hub genes were then conducted. It turned out that hub genes were largely enriched in TLR and JAK-STAT inflammatory signaling pathways (Tables 3 and 4).

**3.4. GSEA.** GSEA was performed to determine the gene sets that had significant difference between the VILI and control groups. The gene sets positively correlated with the VILI group were mainly involved in the TLR and JAK-STAT pathways, which was consistent with the results obtained in GO and KEGG enrichment analysis (Figure 5). It was revealed

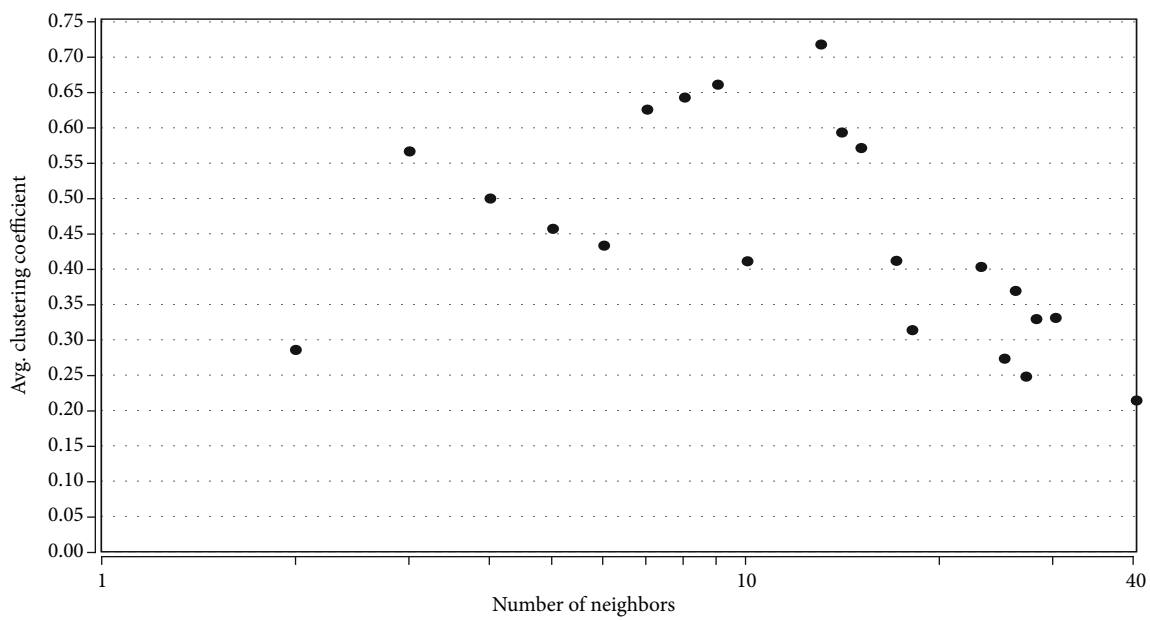


(a)

FIGURE 3: Continued.



(b)



(c)

FIGURE 3: Continued.

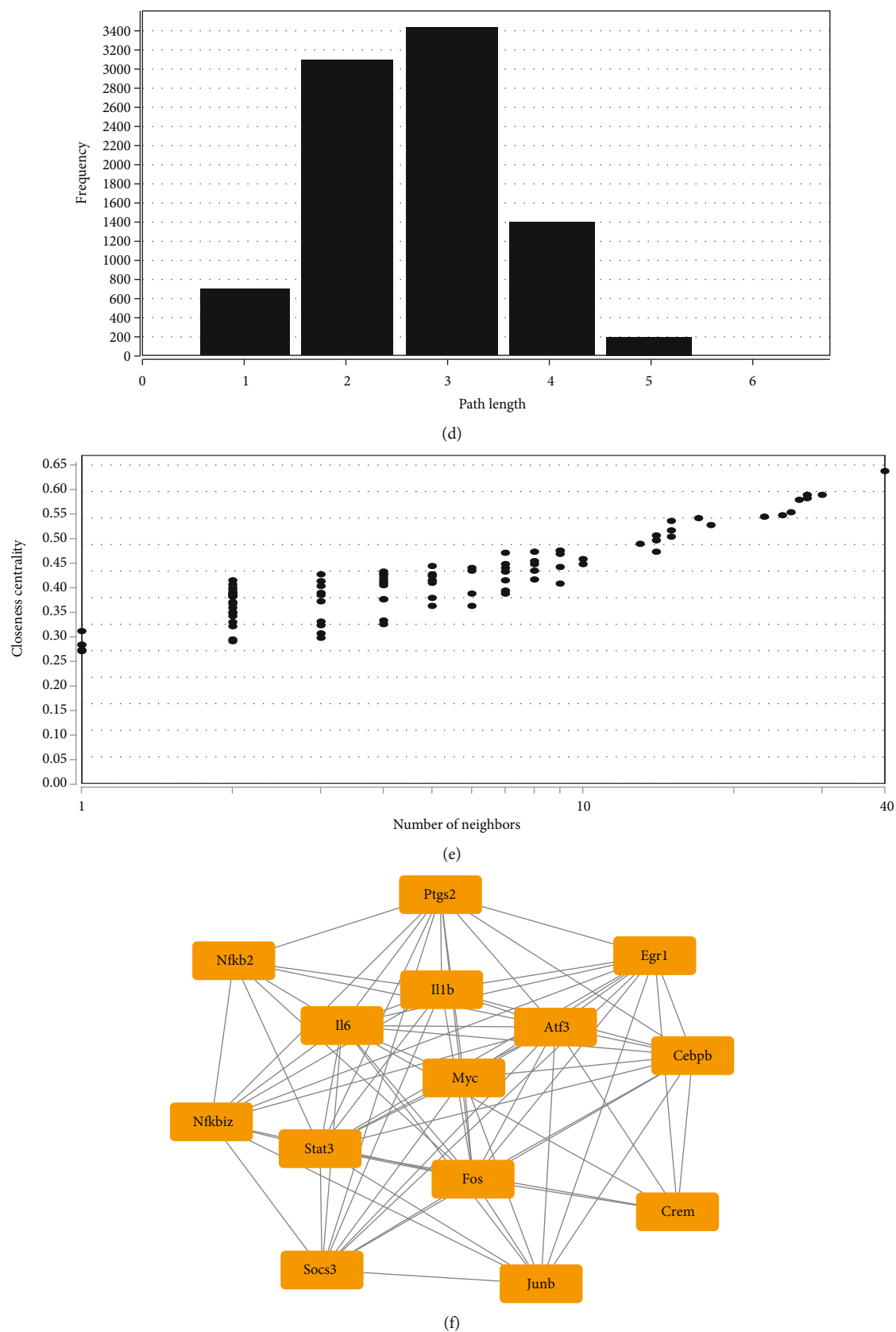


FIGURE 3: PPI network and module analysis. (a) PPI networks of DEGs. The topological parameters of PPI networks were as follows: (b) distribution of degrees, (c) clustering coefficient, (d) distribution of the shortest path, and (e) closeness centrality. (f) Most significant clustering module screened by MCODE from PPI networks.

TABLE 1: GO analysis of the most significant clustering module in PPI networks.

Category	Term	<i>p</i> value
GOTERM_BP_DIRECT	GO:0006351~transcription, DNA-templated	1.19E - 04
GOTERM_BP_DIRECT	GO:0045893~positive regulation of transcription, DNA-templated	7.52E - 04
GOTERM_BP_DIRECT	GO:0006357~regulation of transcription from RNA polymerase II promoter	7.63E - 04
GOTERM_BP_DIRECT	GO:0006954~inflammatory response	0.013427
GOTERM_BP_DIRECT	GO:0043066~negative regulation of apoptotic process	0.014684
GOTERM_BP_DIRECT	GO:0035914~skeletal muscle cell differentiation	0.024883
GOTERM_BP_DIRECT	GO:0051091~positive regulation of sequence-specific DNA binding transcription factor activity	0.048278
GOTERM_BP_DIRECT	GO:0006355~regulation of transcription, DNA-templated	0.048792
GOTERM_CC_DIRECT	GO:0005634~nucleus	3.27E - 06
GOTERM_CC_DIRECT	GO:0005654~nucleoplasm	0.039133
GOTERM_MF_DIRECT	GO:0003700~transcription factor activity, sequence-specific DNA binding	1.82E - 06
GOTERM_MF_DIRECT	GO:0003677~DNA binding	8.51E - 05
GOTERM_MF_DIRECT	GO:0000978~RNA polymerase II core promoter proximal region sequence-specific DNA binding	0.001059
GOTERM_MF_DIRECT	GO:0043565~sequence-specific DNA binding	0.002782
GOTERM_MF_DIRECT	GO:0001077~transcriptional activator activity, RNA polymerase II core promoter proximal region sequence-specific binding	0.009683
GOTERM_MF_DIRECT	GO:0000982~transcription factor activity, RNA polymerase II core promoter proximal region sequence-specific binding	0.014036
GOTERM_MF_DIRECT	GO:0046983~protein dimerization activity	0.015108

TABLE 2: KEGG analysis of the most significant clustering module in PPI networks.

Category	Term	<i>p</i> value
KEGG_PATHWAY	ssc04668:TNF signaling pathway	1.84E - 08
KEGG_PATHWAY	ssc05166:HTLV-I infection	2.59E - 06
KEGG_PATHWAY	ssc05202:transcriptional misregulation in cancer	1.31E - 04
KEGG_PATHWAY	ssc05200:pathways in cancer	4.31E - 04
KEGG_PATHWAY	ssc04380:osteoclast differentiation	0.001668
KEGG_PATHWAY	ssc04630:JAK-STAT signaling pathway	0.001932
KEGG_PATHWAY	ssc05161:hepatitis B	0.0024
KEGG_PATHWAY	ssc04917:prolactin signaling pathway	0.006385
KEGG_PATHWAY	ssc04931:insulin resistance	0.017635
KEGG_PATHWAY	ssc05169:Epstein-Barr virus infection	0.018235
KEGG_PATHWAY	ssc05152:tuberculosis	0.040023
KEGG_PATHWAY	ssc05168:herpes simplex infection	0.043435

that they were also enriched in NOD, antigen presentation, and chemokine pathways.

**3.5. miRNA-TF-Hub Gene Regulatory Network.** miRNA could function as a regulator in lung injuries. Thus, miRNAs that could interact with the screened hub genes were predicted using CyTargetLinker. And 72 miRNA-target interactions were found in TargetScan, and 207 were found in MicroCosm (Figure 6(a)). The overlap threshold was set to 2 for the analysis, and the results showed that interactions occurred between 18 miRNAs and 5 target genes. TFs play important roles in controlling gene expressions. Therefore, we predicted TFs that could regulate the hub genes using

NetworkAnalyst and these TFs were incorporated with the predicted miRNA to construct the miRNA-TF-gene regulatory network (Figure 6(b)). Overall, the regulatory network could help to clarify the roles of miRNA and TFs in the development of VILI.

**3.6. Analysis of Immune Cell Composition.** To understand the involvement of immune cells in VILI, we used CIBERSORT to detect the contributions of different types of immune cell in the lung tissues of mice in the VILI group. We evaluated immune cell composition in samples from both VILI and control groups (Figure 7(a)). Accordingly, these samples were divided into two main clusters (Figure 7(b)). The three

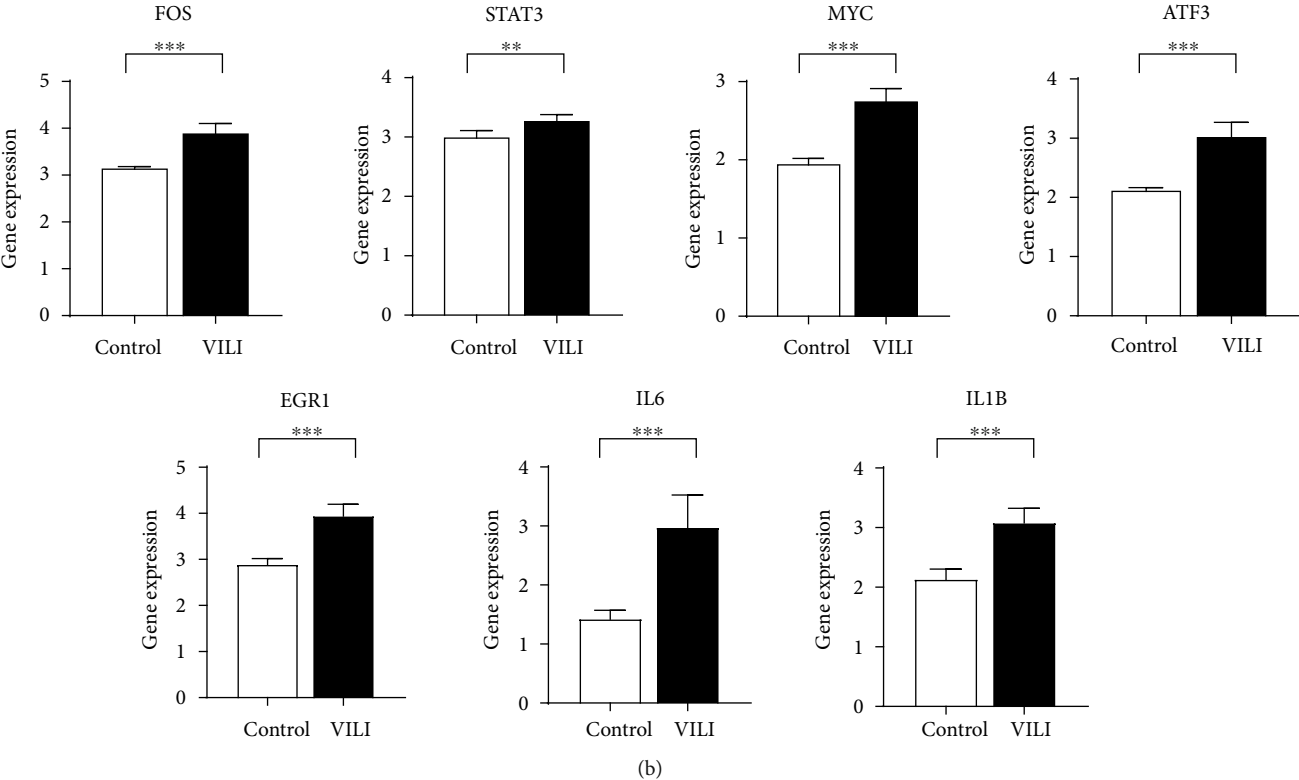
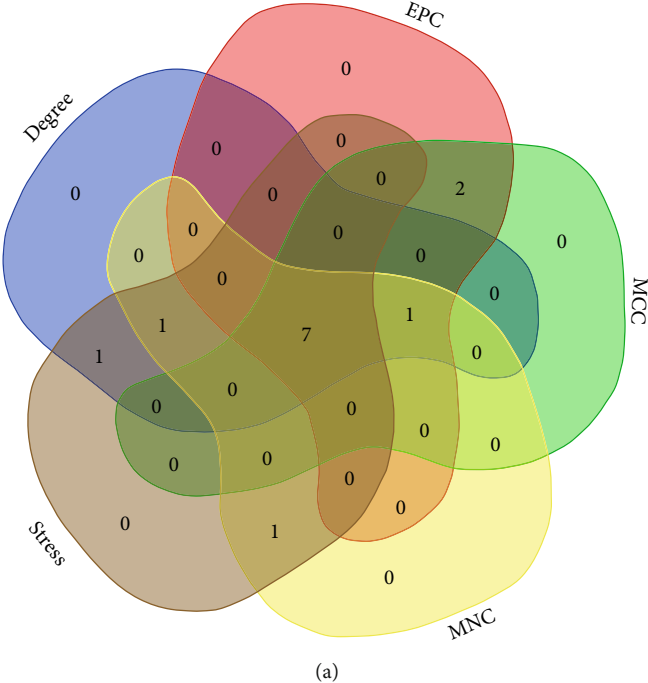
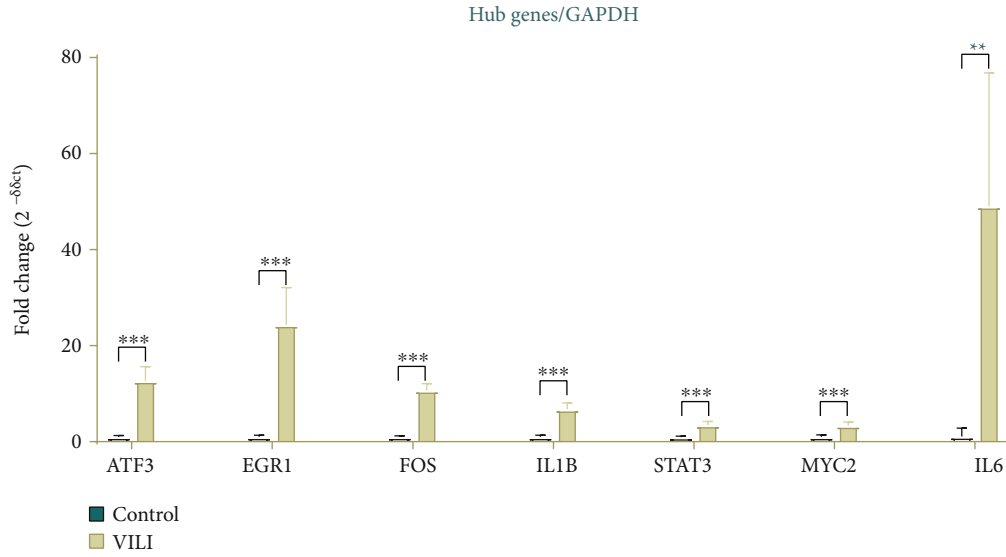


FIGURE 4: Continued.



(c)

FIGURE 4: Hub genes in the VILI group. (a) Intersecting genes selected as hub genes by using 5 algorithms in cytoHubba. (b) The expression levels of seven hub genes in the lung samples from the VILI and control groups in GSE11434 were as follows: FOS, STAT3, MYC, ATF3, EGR1, IL-6, and IL-1B. (c) qRT-PCR analysis of hub genes in lung samples of the VILI and control groups.

TABLE 3: GO enrichment analysis of hub genes.

Category	Term	<i>p</i> value
GOTERM_BP_DIRECT	GO:0035914~skeletal muscle cell differentiation	2.15E - 04
GOTERM_BP_DIRECT	GO:0045944~positive regulation of transcription from RNA polymerase II promoter	0.002266
GOTERM_BP_DIRECT	GO:0006351~transcription, DNA-templated	0.002534
GOTERM_BP_DIRECT	GO:0070102~interleukin-6-mediated signaling pathway	0.00354
GOTERM_BP_DIRECT	GO:0043066~negative regulation of apoptotic process	0.006244
GOTERM_BP_DIRECT	GO:0050679~positive regulation of epithelial cell proliferation	0.018091
GOTERM_BP_DIRECT	GO:0006355~regulation of transcription, DNA-templated	0.034263
GOTERM_BP_DIRECT	GO:0042493~response to drug	0.034428
GOTERM_BP_DIRECT	GO:0042593~glucose homeostasis	0.042752
GOTERM_CC_DIRECT	GO:0005654~nucleoplasm	0.016377
GOTERM_CC_DIRECT	GO:0005634~nucleus	0.02582
GOTERM_MF_DIRECT	GO:0005125~cytokine activity	0.001928
GOTERM_MF_DIRECT	GO:0001077~transcriptional activator activity, RNA polymerase II core promoter proximal region sequence-specific binding	0.004063
GOTERM_MF_DIRECT	GO:0000978~RNA polymerase II core promoter proximal region sequence-specific DNA binding	0.008486
GOTERM_MF_DIRECT	GO:0000982~transcription factor activity, RNA polymerase II core promoter proximal region sequence-specific binding	0.011174
GOTERM_MF_DIRECT	GO:0046983~protein dimerization activity	0.017511
GOTERM_MF_DIRECT	GO:0003700~transcription factor activity, sequence-specific DNA binding	0.022809
GOTERM_MF_DIRECT	GO:0008134~transcription factor binding	0.039418
GOTERM_MF_DIRECT	GO:0003677~DNA binding	0.042522

most relevant immune cells included eosinophils and T follicular helper cells, activated neutrophils and memory CD4 T cells, and naive CD8 T cells and B cells, all with an *R* value of 0.49 (Figure 7(c)). It was revealed that the proportion of M0 macrophages and activated mast cells was higher in the

VILI group than in the control (Figure 7(d)). The proportion of other immune cells does not show any statistically significant difference between samples from the VILI and control groups. Together, it indicated that immune cells, particularly macrophages, were involved in the early stage of VILI.

TABLE 4: KEGG enrichment analysis of hub genes.

Category	Term	<i>p</i> value
KEGG_PATHWAY	bta05161:hepatitis B	4.74E – 06
KEGG_PATHWAY	bta05166:HTLV-I infection	4.92E – 05
KEGG_PATHWAY	bta04620:toll-like receptor signaling pathway	8.79E – 05
KEGG_PATHWAY	bta05142:Chagas disease (American trypanosomiasis)	1.12E – 04
KEGG_PATHWAY	bta05162:measles	2.07E – 04
KEGG_PATHWAY	bta04630:JAK-STAT signaling pathway	2.59E – 04
KEGG_PATHWAY	bta05020:prion diseases	3.61E – 04
KEGG_PATHWAY	bta05168:herpes simplex infection	5.10E – 04
KEGG_PATHWAY	bta04623:cytosolic DNA-sensing pathway	0.001314
KEGG_PATHWAY	bta05321:inflammatory bowel disease (IBD)	0.001727
KEGG_PATHWAY	bta05133:pertussis	0.002086
KEGG_PATHWAY	bta05132:Salmonella infection	0.002419
KEGG_PATHWAY	bta05323:rheumatoid arthritis	0.003158
KEGG_PATHWAY	bta04668:TNF signaling pathway	0.004063
KEGG_PATHWAY	bta05200:pathways in cancer	0.00434
KEGG_PATHWAY	bta04380:osteoclast differentiation	0.006194
KEGG_PATHWAY	bta05164:influenza A	0.010163
KEGG_PATHWAY	bta05152:tuberculosis	0.011088
KEGG_PATHWAY	bta04060:cytokine-cytokine receptor interaction	0.015837
KEGG_PATHWAY	bta04010:MAPK signaling pathway	0.021328

**3.7. Drug Prediction for Hub Genes.** DrugBank is a database that provides detailed drug data and information about comprehensive drug targets. To predict possible drugs that may be developed for the treatment of VILI, the DrugBank database was used to identify small molecules that would potentially interact with the hub genes. As shown in Table 5, the most significant molecules included nadroparin, siltuximab, ginseng, donepezil, minocycline, and gallium nitrate.

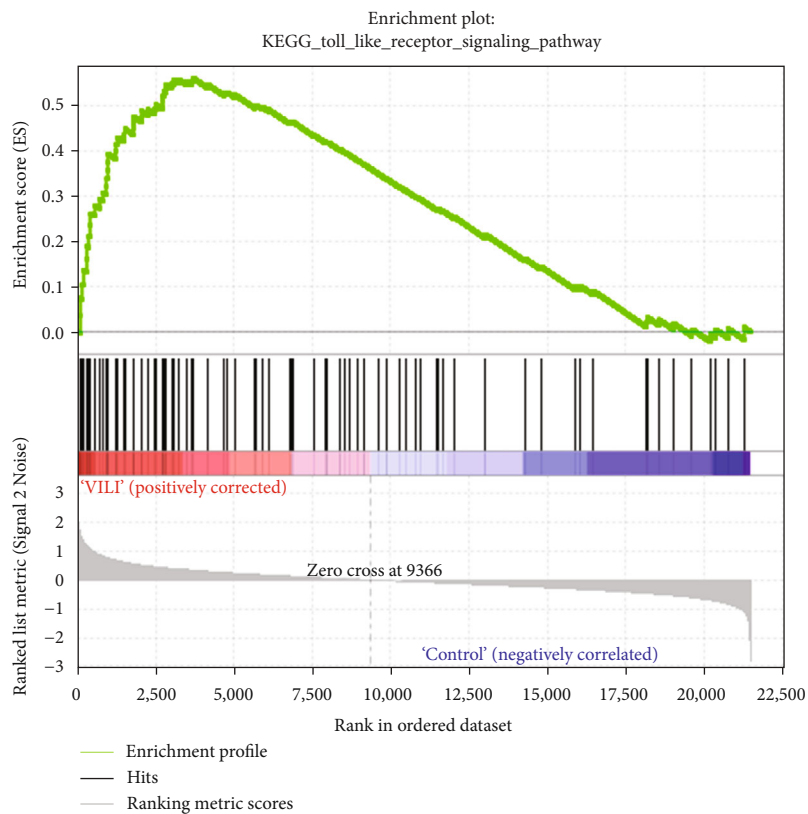
#### 4. Discussion

It has been known that mechanical ventilation could lead to VILI, though the exact pathological process of VILI is still far from clear [6]. Efforts for VILI interventions yield few positive results, and there is no specific treatment for it except preventive measures like low tidal volume ventilation. A better understanding of the underlying molecular mechanism of VILI development, therefore, may help to shed light on the VILI pathogenesis. It is noteworthy that novel tools have been widely used in several health applications. Novel bioinformatics analysis has been applied in analyzing the roles played by mRNA, lncRNA, and miRNA in the VILI development [7, 23, 24]. Xu et al. identified several critical lncRNAs which may help to get a better picture of the VILI pathogenesis [23]. Vaporidi et al. found several differentially regulated miRNAs during the pathological progress of VILI [24]. However, there have been few studies to investigate VILI-associated hub genes using bioinformatics approaches. Besides, miRNA-gene regulatory network has rarely been used in the studies of VILI.

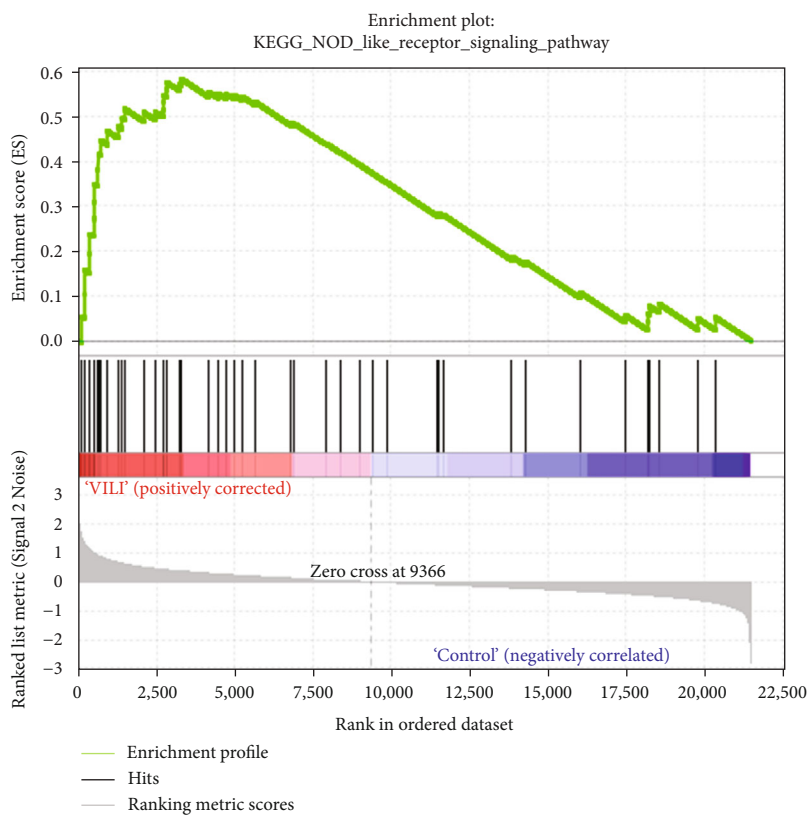
In this study, we acquired the GSE11434 dataset, containing genetic data on the tissues of mice with VILI induced by high-volume ventilation and tissues of control mice, for bioinformatics analysis. A total of 141 DEGs, including 108 upregulated and 33 downregulated genes, were identified. Then, PPI analysis and GSEA were performed to explore their biological significance as regards VILI.

Go enrichment analysis of these DEGs in this study reveals that they are largely enriched in RNA polymerase II promoter and responses to lipopolysaccharide and cAMP. And the roles played by the cAMP signaling pathway include inflammatory response and immune mediator induction [25]. Those results indicate that abnormal inflammatory responses may be involved in the pathological process of VILI.

The PPI network analysis in this study provides some insights for studying the VILI pathogenesis. We constructed a network consisting of DEG-coded proteins. The distribution of degrees, clustering coefficient, distribution of the shortest path, and closeness centrality all demonstrated high connectivity between these proteins. Our network topology analysis confirmed that the network was biologically scale-free. We further applied the MCODE plugin in the PPI network and found that a module consisting of 14 nodes could be the key regulatory network for VILI. The enrichment analysis of this module showed that those genes were largely enriched in inflammatory response, DNA binding, TNF, and JAK-STAT signaling pathways. This finding was consistent with the results in previous studies which revealed that the DNA-binding activity of NF- $\kappa$ B in VILI cases increased

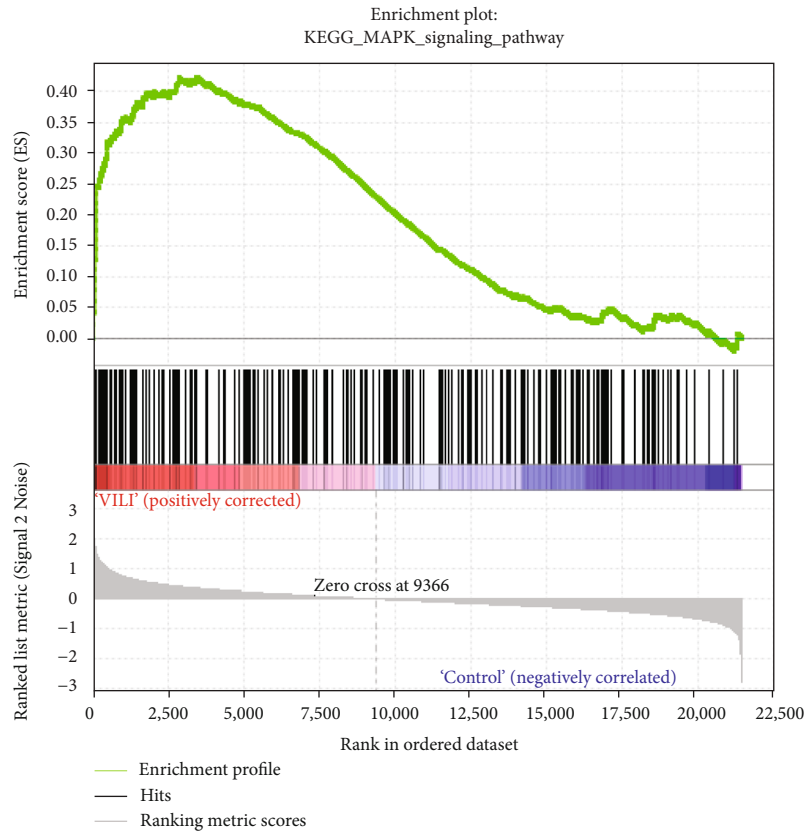


(a)

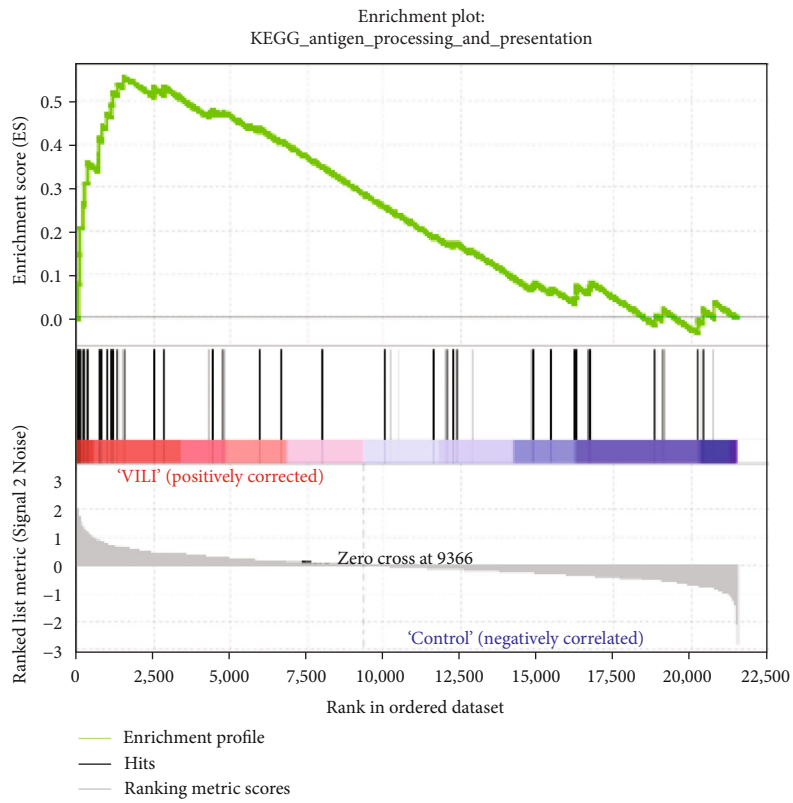


(b)

FIGURE 5: Continued.

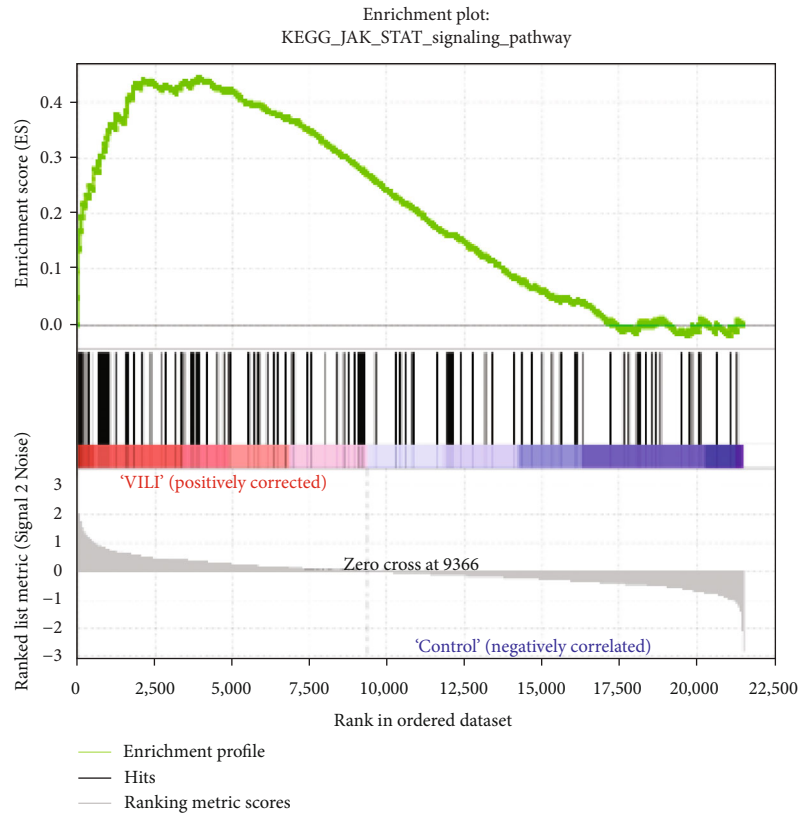


(c)

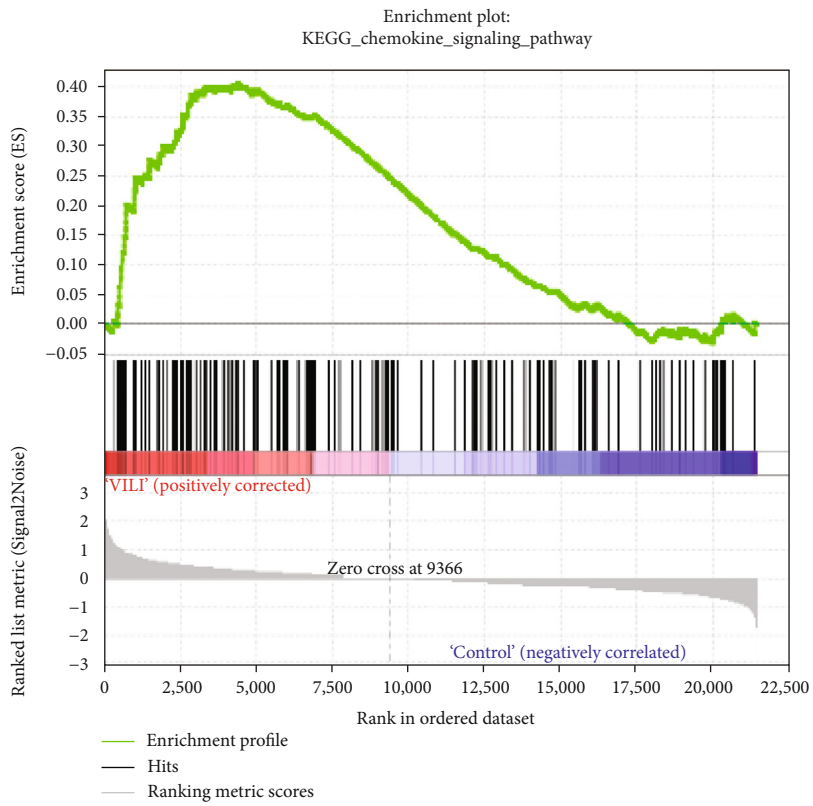


(d)

FIGURE 5: Continued.

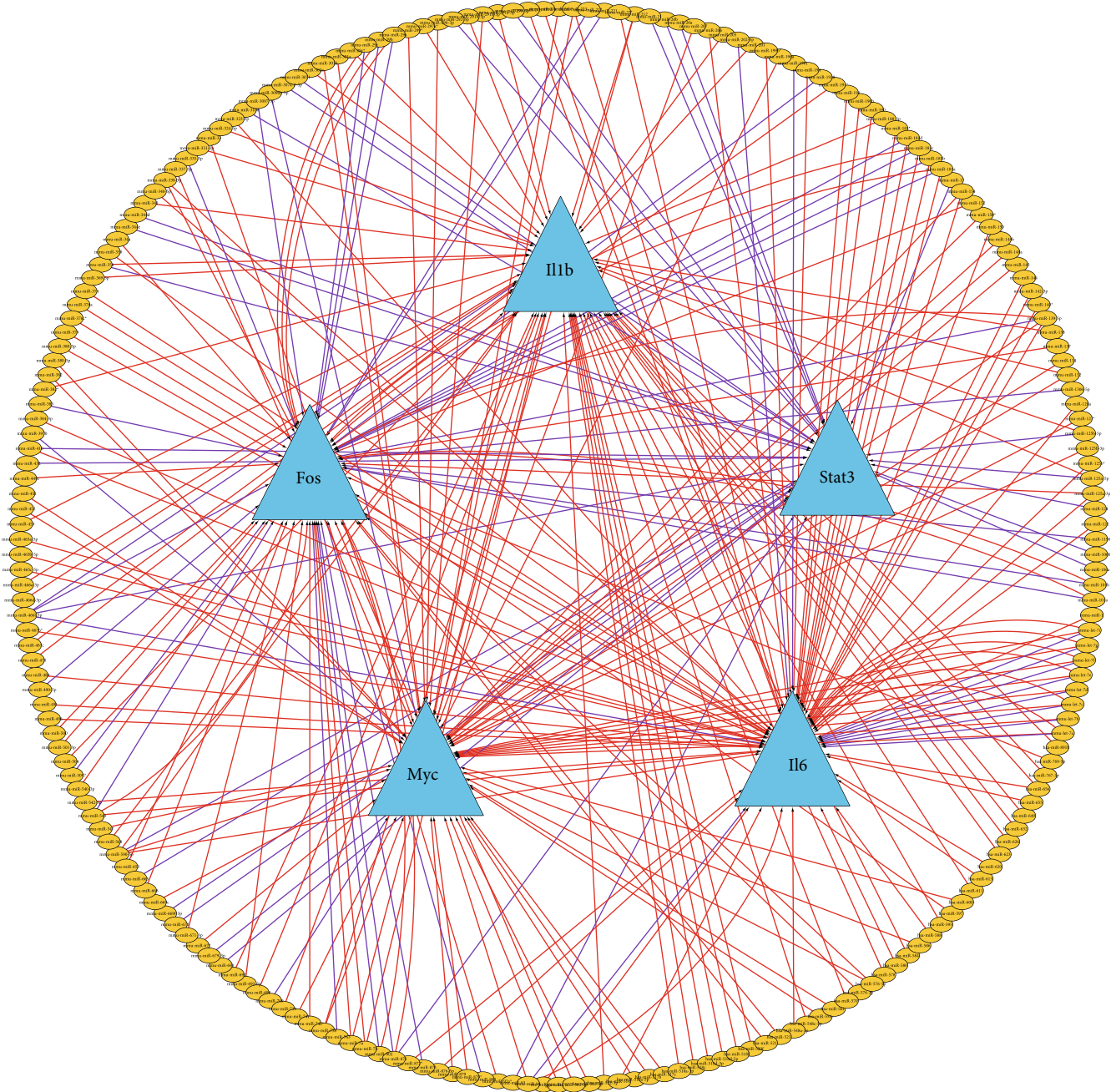


(e)



(f)

FIGURE 5: GSEA of six primary pathways in which VILI was significantly enriched.



(a)

FIGURE 6: Continued.

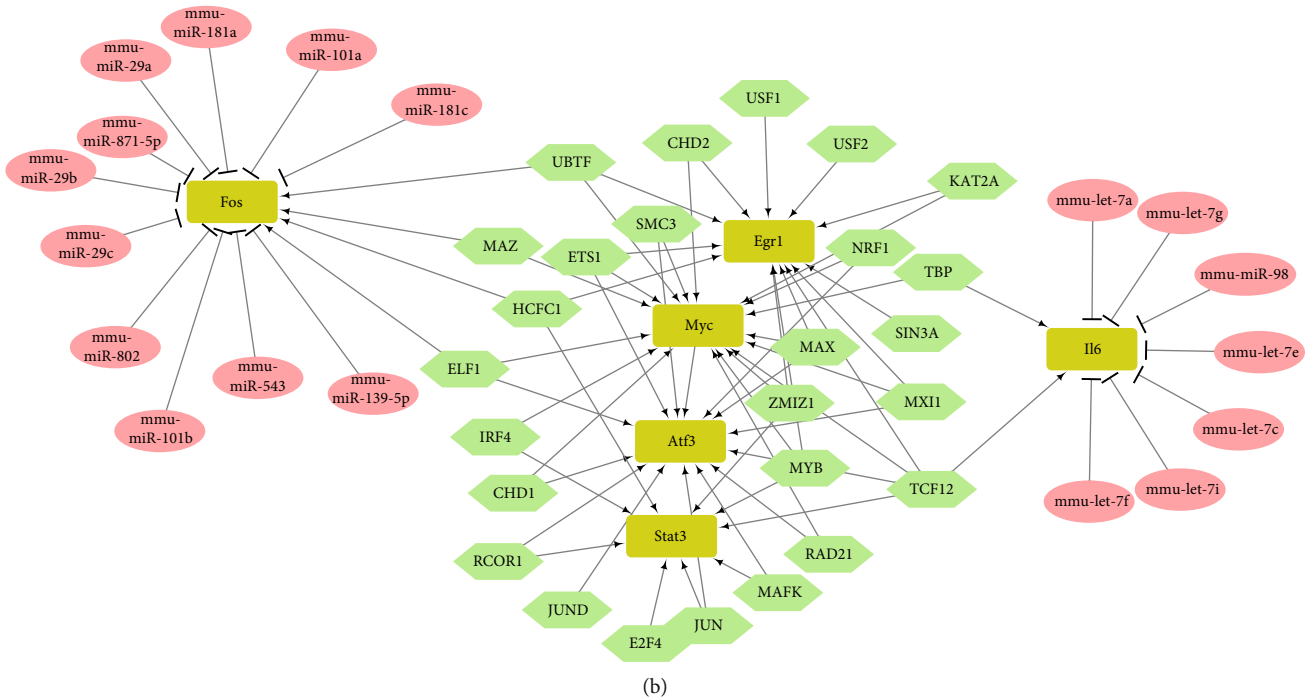


FIGURE 6: miRNA-TF-hub gene regulatory network. (a) miRNAs related to hub genes predicted by CyTargetLinker. Red edges mean predicted by MicroCosm and velvet edges mean predicted by TargetScan. (b) TFs related to the hub genes were predicted by NetworkAnalyst and then used to construct the miRNA-TF-gene network. The rectangles denote hub genes, ellipses denote miRNA, and hexagons denote TF.

[26]. TNF has been reported to be involved in early inflammatory response and stretch-induced pulmonary edema [27, 28]. Subsequently, we used the cytoHubba plugin to further screen out hub genes from the PPI network, which included FOS, STAT3, MYC, ATF3, EGR1, IL-6, and IL-1B. Strikingly, all hub genes were contained in the above-obtained module.

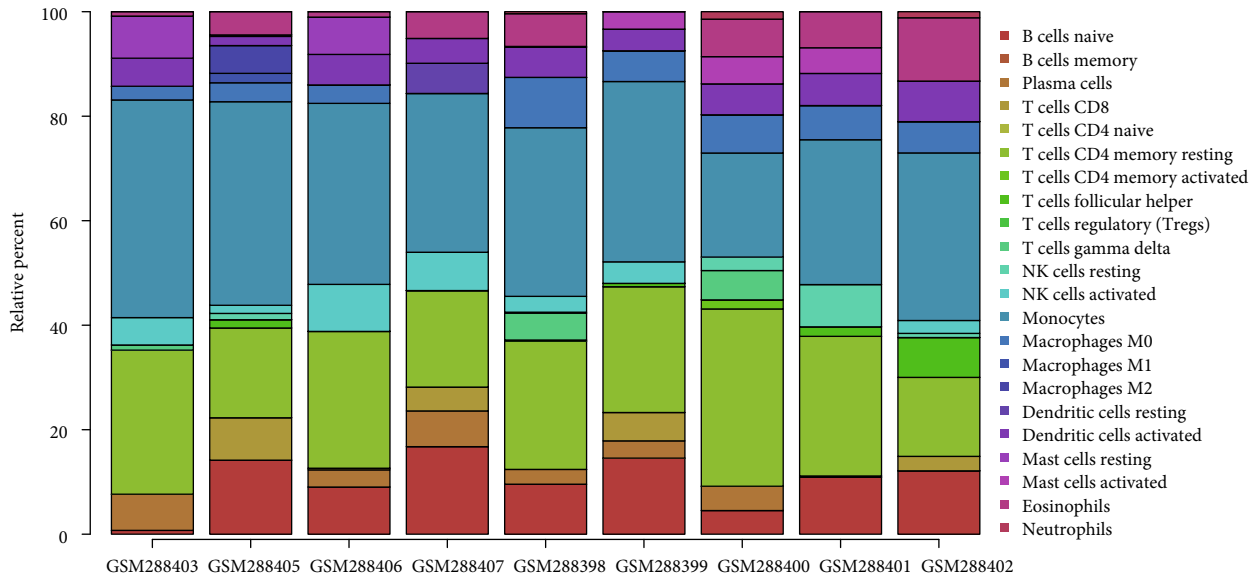
STAT3, an important member of the STAT family, is involved in the transcription activation of the JAK-STAT signaling pathway. Hoegl et al. discovered that IL-22 activates STAT3 signaling and reduces SOCS3 expression, thus alleviating lung injury in VILI cases [29]. In contrast, in our study, the expression of STAT3 is increased in the VILI group, compared with the control. This indicated that STAT3 may have dual effects on the inflammatory process. Wolfson et al. found that STAT3 upregulates HMGB1 expression, thereby exacerbating systemic inflammatory responses in VILI cases [30]. The specific roles of FOS and MYC in VILI have not been systematically studied. FOS can respond to mechanical stimuli and promote immune activation in the lung alveoli [31]. It binds with AP-1 sites to play a role in the proinflammatory signaling pathways in acute lung injuries [32]. Similar to FOS, MYC is transcribed under mechanical stimuli [33].

ATF3 is a transcription factor belonging to the CREB/ATF family. Shan et al. found that ATF3 could protect against lung injury by reducing barrier disruption and inflammatory cell recruitment [34]. Our analysis showed that the ATF3 expression in the VILI group was significantly upregulated compared with the control. Its specific pathophysiological mechanism is unclear and needs to be further

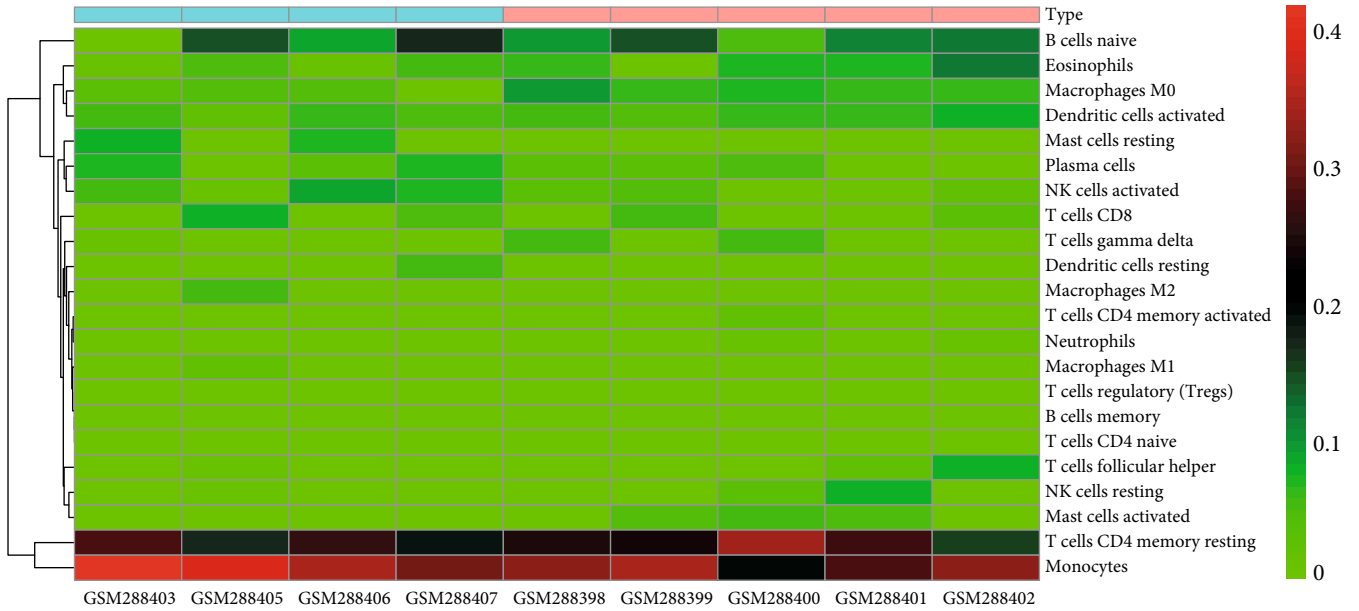
studied. EGR1 is a transcription factor in the zinc finger protein family and can be activated by various environmental signals [35]. Copland et al. found that the expression of EGR1 could increase even under low-volume mechanical ventilation, suggesting its role in the upstream regulation [36].

IL-6 is a pleiotropic cytokine that is involved in regulating leukocyte function and apoptosis and thus exhibits proinflammatory and anti-inflammatory effects [37]. Ko et al. reported that NF- $\kappa$ B-IL-6 signaling pathways contribute to the VILI development by inducing inflammation [38]. Experimental lung injury can be attenuated by an IL-1 $\beta$  antagonist [39]. This indicates that the inflammatory response may not only be a downstream reaction but also involved in the progression of lung injury. Enrichment analysis of those hub genes identified in this study showed that they were largely enriched in TLR and JAK-STAT inflammatory signaling pathways, a finding that is consistent with the results from previous studies that inflammation is an essential factor in the VILI development.

GSEA could be used to obtain relevant information when large-scale genes were at a small fold change. The GSEA in this study revealed that gene expressions in the VILI samples showed a significant correlation with TLR and JAK-STAT pathways, compared with those in the control samples. In combination with the abovementioned enrichment analysis, we speculate that TLR and JAK-STAT may play vital roles in inflammation observed in VILI cases. Moreover, the antigen presentation pathway was also where enrichment occurred. It could be inferred that the immune system might

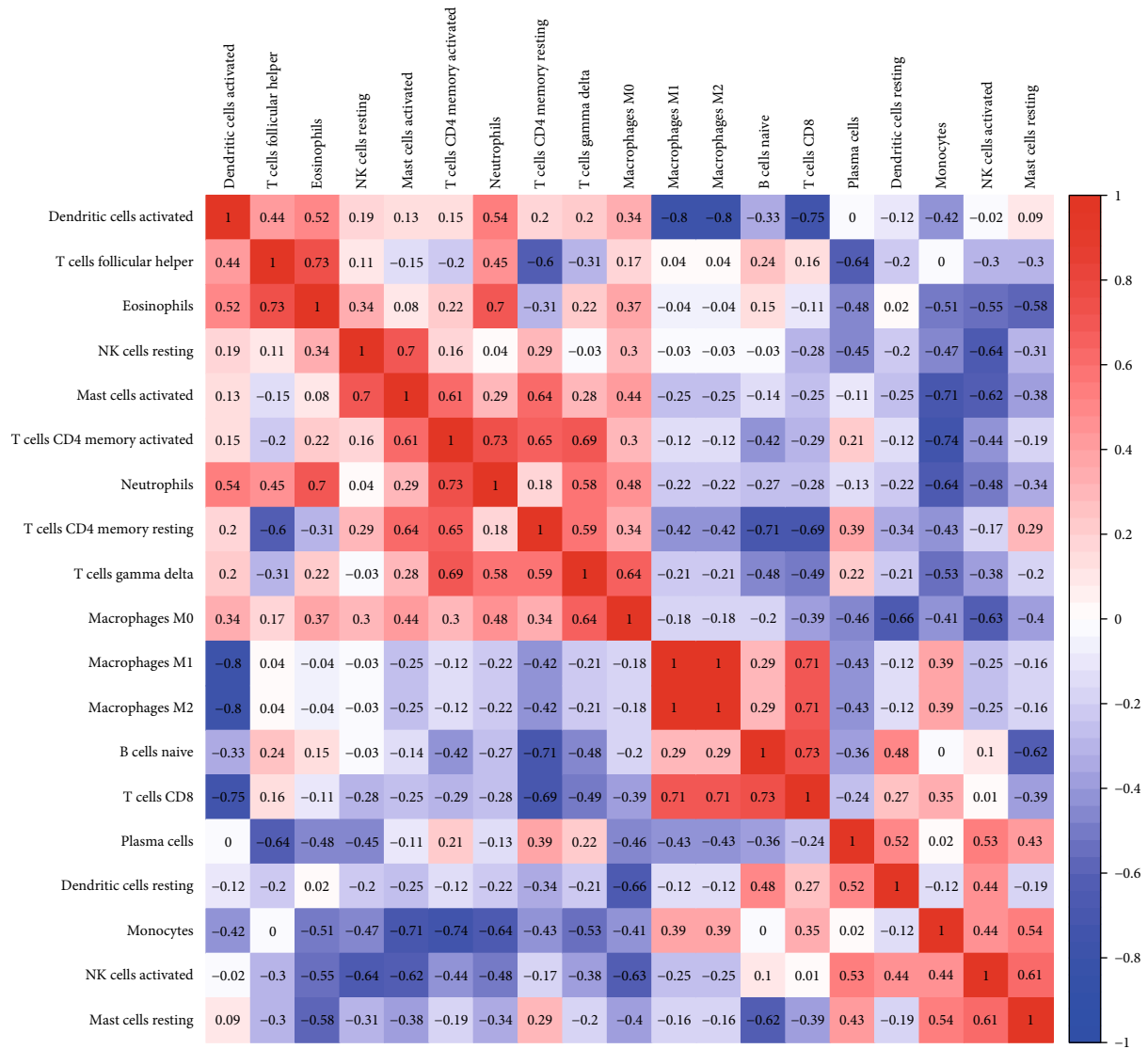


(a)



(b)

FIGURE 7: Continued.



(c)

FIGURE 7: Continued.

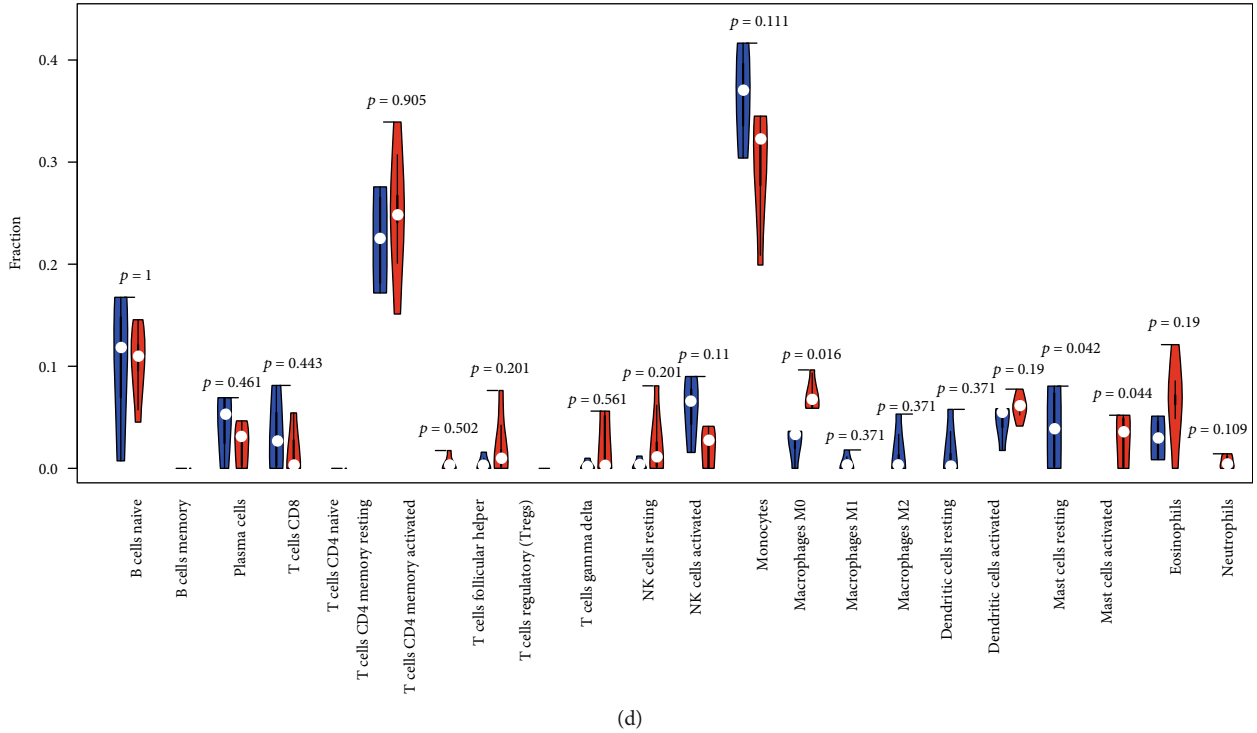


FIGURE 7: Landscape of immune cell composition in lung samples from the VILI and control groups. (a) Histogram of the immune cell composition of samples from the VILI and control groups. (b) Heat map of immune cell types in lung samples from the VILI and control groups. (c) Correlation matrix of immune cell types in lung samples of the VILI and control groups. (d) Violin plot of immune cell types in lung samples of the VILI and control groups.

TABLE 5: Potential drugs that target hub genes derived from DrugBank.

Gene	Drug	Accession number	Groups	Interaction type
FOS	Nadroparin	DB08813	Approved, investigational	Inhibitor
MYC	Nadroparin	DB08813	Approved, investigational	Inhibitor
IL-6	Siltuximab	DB09036	Approved, investigational	Antagonist
IL-6	Ginseng	DB01404	Approved, investigational, nutraceutical	Antagonist
IL-1B	Donepezil	DB00843	Approved	Inhibitor
IL-1B	Minocycline	DB01017	Approved, investigational	Modulator
IL-1B	Gallium nitrate	DB05260	Approved, investigational	Antagonist

also be involved in the VILI development. Indeed, a previous study has already raised concerns about involvement of the immune system in VILI [40].

We used CIBERSORT to analyze the immune cell composition in VILI samples and found that the proportion of M0 macrophages and activated mast cells was significantly higher in the VILI group than in the control. Macrophage is known to play a considerable role in the innate immune system. A previous study has found that mechanical ventilation may induce macrophages to switch to the M1 phenotype [41]. That indicates that macrophages could mainly remain as M0 phenotype in the early stage of VILI.

In addition, hub genes were mapped into the DrugBank database to predict small molecular drugs. It is still unclear whether these compounds can contribute therapeutic effects

on VILI, so further investigation is required as to whether these molecules can be used to treat VILI in the future.

There are still some limitations in this study. First, changes in gene mutations (such as SNPs), protein expression levels, or cellular metabolism may also play important roles in the occurrence and development of VILI. Limited by a lack of relevant data, we are currently unable to carry out such detailed analysis. Second, our study constructed a PPI network based on transcriptomics data rather than proteomics data. Proteomic analysis of VILI will be conducted in our further studies. Lastly, our study included only a small number of samples, and thus, investigations with a larger sample size shall be further conducted in our future studies.

To summarize, this study systematically analyzed the transcriptomic characteristics of lung tissues from the VILI

and control groups to identify DEGs and hub genes. These hub genes, including FOS, STAT3, MYC, ATF3, EGR1, IL-6, and IL-1B, play vital roles in the VILI pathogenesis and thus provide potential therapeutic targets for future VILI treatment.

## 5. Conclusion

In a word, we identified a series of hub genes from the DEGs between the VILI group and the control group, which may provide novel insights into the pathogenesis of VILI and gene targets for its treatment.

## Data Availability

All data generated or analyzed during this study were included in this accepted article.

## Conflicts of Interest

All of the authors declare no conflict of interest.

## Acknowledgments

This work was supported by Important Weak Subject Construction Project of Pudong Health and Family Planning Commission of Shanghai (Grant No. PWZbr2017-18) and Pu Dong Clinical Peak Discipline (PWYgf2018-05).

## Supplementary Materials

Supplemental Table: primers used in qRT-PCR. (*Supplementary Materials*)

## References

- [1] T. Pham, L. J. Brochard, and A. S. Slutsky, "Mechanical Ventilation: State of the Art," *Mayo Clinic Proceedings*, vol. 92, no. 9, pp. 1382–1400, 2017.
- [2] G. F. Nieman, J. Satalin, M. Kollisch-Singule et al., "Physiology in Medicine: Understanding dynamic alveolar physiology to minimize ventilator-induced lung injury," *Journal Applied Physiology*, vol. 122, no. 6, pp. 1516–1522, 2017.
- [3] A. J. Hoogendijk, M. T. Kuipers, T. van der Poll, M. J. Schultz, and C. W. Wieland, "Cyclin-dependent kinase inhibition reduces lung damage in a mouse model of ventilator-induced lung injury," *Shock*, vol. 38, no. 4, pp. 375–380, 2012.
- [4] O. Gajic, S. I. Dara, J. L. Mendez et al., "Ventilator-associated lung injury in patients without acute lung injury at the onset of mechanical ventilation," *Critical Care Medicine*, vol. 32, no. 9, pp. 1817–1824, 2004.
- [5] C. M. Hong, D. Q. Xu, Y. Cheng et al., "Low tidal volume and high positive end-expiratory pressure mechanical ventilation results in increased inflammation and ventilator-associated lung injury in normal lungs," *Anesthesia & Analgesia*, vol. 110, no. 6, pp. 1652–1660, 2010.
- [6] M. T. Kuipers, T. van der Poll, M. J. Schultz, and C. W. Wieland, "Bench-to-bedside review: damage-associated molecular patterns in the onset of ventilator-induced lung injury," *Critical Care*, vol. 15, no. 6, p. 235, 2011.
- [7] T. Dolinay, N. Kaminski, M. Felgendreher et al., "Gene expression profiling of target genes in ventilator-induced lung injury," *Physiological Genomics*, vol. 26, no. 1, pp. 68–75, 2006.
- [8] S.-F. Ma, D. N. Grigoryev, A. D. Taylor et al., "Bioinformatic identification of novel early stress response genes in rodent models of lung injury," *American Journal of Physiology - Lung Cellular and Molecular Physiology*, vol. 289, no. 3, pp. L468–L477, 2005.
- [9] E. Clough and T. Barrett, "The gene expression omnibus database," *Methods in Molecular Biology*, vol. 1418, p. 93, 2016.
- [10] C. Wray, Y. Mao, J. Pan, A. Chandrasena, F. Piasta, and A. James, "Claudin-4 augments alveolar epithelial barrier function and is induced in acute lung injury," *American Journal of Physiology - Lung Cellular and Molecular Physiology*, vol. 297, no. 2, pp. L219–L227, 2009.
- [11] G. Otulakowski, D. Engelberts, H. Arima et al., " $\alpha$ -Tocopherol transfer protein mediates protective hypercapnia in murine ventilator-induced lung injury," *Thorax*, vol. 72, no. 6, pp. 538–549, 2017.
- [12] M. Ashburner, C. A. Ball, J. A. Blake, D. Botstein, and J. M. Cherry, "Gene ontology: tool for the unification of biology," *Nature Genetics*, vol. 25, no. 1, pp. 25–29, 2000.
- [13] W. H. Da, B. T. Sherman, and R. A. Lempicki, "Systematic and integrative analysis of large gene lists using DAVID bioinformatics resources," *Nature Protocols*, vol. 4, no. 1, p. 44, 2009.
- [14] L. Hakes, J. W. Pinney, D. L. Robertson, and S. C. Lovell, "Protein-protein interaction networks and biology—what's the connection?," *Nature Biotechnology*, vol. 26, no. 1, pp. 69–72, 2008.
- [15] P. Shannon, A. Markiel, O. Ozier et al., "Cytoscape: a software environment for integrated models of biomolecular interaction networks," *Genome Research*, vol. 13, no. 11, pp. 2498–2504, 2003.
- [16] C. Chin, S. N. Chen, H. Wu, C. Ho, M. Ko, and C. Lin, "cytoHubba: identifying hub objects and sub-networks from complex interactome," *BMC Systems Biology*, vol. 8, no. 4, pp. 1–7, 2014.
- [17] G. D. Bader and C. W. Hogue, "An automated method for finding molecular complexes in large protein interaction networks," *BMC Bioinformatics*, vol. 4, no. 1, p. 2, 2003.
- [18] M. Kutmon, T. Kelder, P. Mandaviya, C. T. Evelo, and S. L. Coort, "CyTargetLinker: a Cytoscape app to integrate regulatory interactions in network analysis," *PLoS One*, vol. 8, no. 12, article e82160, 2013.
- [19] G. Zhou, O. Soufan, J. Ewald, R. E. W. Hancock, N. Basu, and J. Xia, "NetworkAnalyst 3.0: a visual analytics platform for comprehensive gene expression profiling and meta-analysis," *Nucleic Acids Research*, vol. 47, no. W1, pp. W234–W241, 2019.
- [20] A. Subramanian, P. Tamayo, V. K. Mootha et al., "Gene set enrichment analysis: a knowledge-based approach for interpreting genome-wide expression profiles," *Proceedings of the National Academy of Sciences of the United States of America*, vol. 102, no. 43, pp. 15545–15550, 2005.
- [21] A. M. Newman, C. L. Liu, M. R. Green et al., "Robust enumeration of cell subsets from tissue expression profiles," *Nature Methods*, vol. 12, no. 5, pp. 453–457, 2015.
- [22] D. S. Wishart, Y. D. Feunang, A. C. Guo et al., "DrugBank 5.0: a major update to the DrugBank database for 2018," *Nucleic Acids Research*, vol. 46, no. D1, pp. D1074–D1082, 2018.
- [23] B. Xu, Y. Wang, X. Li, Y. Mao, and X. Deng, "RNA-sequencing analysis of aberrantly expressed long non-coding RNAs and

- mRNAs in a mouse model of ventilator-induced lung injury,” *Molecular Medicine Reports*, vol. 18, no. 1, pp. 882–892, 2018.
- [24] V. Katerina, V. Eleni, K. Evangelos et al., “Pulmonary micro-RNA profiling in a mouse model of ventilator-induced lung injury,” *American Journal of Physiology - Lung Cellular and Molecular Physiology*, vol. 303, no. 3, p. L199, 2012.
- [25] K. A. McDonough and A. Rodriguez, “The myriad roles of cyclic AMP in microbial pathogens: from signal to sword,” *Nature Reviews Microbiology*, vol. 10, no. 1, pp. 27–38, 2012.
- [26] H. Xia, J. Wang, S. Sun et al., “Resolvin D1 alleviates ventilator-induced lung injury in mice by activating PPAR/NF- $\kappa$ B signaling pathway,” *BioMed Research International*, vol. 2019, Article ID 6254587, 9 pages, 2019.
- [27] D. N. Männel and B. Echtenacher, “TNF in the inflammatory response,” *Chemical Immunology*, vol. 74, no. 74, pp. 141–161, 2000.
- [28] M. R. Wilson, M. E. Goddard, K. P. O’Dea, S. Choudhury, and M. Takata, “Differential roles of p55 and p75 tumor necrosis factor receptors on stretch-induced pulmonary edema in mice,” *American Journal of Physiology - Lung Cellular and Molecular Physiology*, vol. 293, no. 1, pp. L60–L68, 2007.
- [29] S. Hoegl, M. Bachmann, P. Scheiermann et al., “Protective properties of inhaled IL-22 in a model of ventilator-induced lung injury,” *American Journal of Respiratory Cell and Molecular Biology*, vol. 44, no. 3, pp. 369–376, 2011.
- [30] R. K. Wolfson, B. Mapes, and J. G. N. Garcia, “Excessive mechanical stress increases HMGB1 expression in human lung microvascular endothelial cells via STAT3,” *Microvascular Research*, vol. 92, no. 3, pp. 50–55, 2014.
- [31] M. R. Gwinn and V. Vallyathan, “Respiratory burst: role in signal transduction in alveolar macrophages,” *Journal of Toxicology and Environmental Health. Part B, Critical Reviews*, vol. 9, no. 1, pp. 27–39, 2006.
- [32] I. Rahman and W. Macnee, “Role of transcription factors in inflammatory lung diseases,” *Thorax*, vol. 53, no. 7, pp. 601–612, 1998.
- [33] C. Bauters, J. M. Moalic, J. Bercovici et al., “Coronary flow as a determinant of c-myc and c-fos proto-oncogene expression in an isolated adult rat heart,” *Journal of Molecular and Cellular Cardiology*, vol. 20, no. 2, pp. 97–101, 1988.
- [34] Y. Shan, A. Akram, H. Amatullah et al., “ATF3 protects pulmonary resident cells from acute and ventilator-induced lung injury by preventing Nrf2 degradation,” *Antioxidants & Redox Signaling*, vol. 22, no. 8, pp. 651–668, 2015.
- [35] A. Gashler, “Early growth response protein 1 (Egr-1): prototype of a zinc-finger family of transcription factors,” *Progress in Nucleic Acid Research and Molecular Biology*, vol. 50, pp. 191–224, 1995.
- [36] I. B. Copland, B. P. Kavanagh, D. Engelberts, C. Mckerlie, J. Belik, and M. Post, “Early changes in lung gene expression due to high tidal volume,” *American Journal of Respiratory and Critical Care Medicine*, vol. 168, no. 9, pp. 1051–1059, 2003.
- [37] S. A. Jones, “Directing transition from innate to acquired immunity: defining a role for IL-6,” *The Journal of Immunology*, vol. 175, no. 6, pp. 3463–3468, 2005.
- [38] Y. A. Ko, M. C. Yang, H. T. Huang, C. M. Hsu, and L. W. Chen, “NF- $\kappa$ B activation in myeloid cells mediates ventilator-induced lung injury,” *Respiratory Research*, vol. 14, no. 1, p. 69, 2013.
- [39] I. O. Narimanbekov and H. J. Rozycki, “Effect of IL-1 blockade on inflammatory manifestations of acute ventilator-induced lung injury in a rabbit model,” *Experimental Lung Research*, vol. 21, no. 2, pp. 239–254, 1995.
- [40] F. F. Cruz, P. R. M. Rocco, and P. Pelosi, “Role of the extracellular matrix in the genesis of ventilator-induced lung injury,” *Medizinische Klinik Intensivmedizin Und Notfallmedizin*, vol. 113, Suppl 1, pp. 2–6, 2017.
- [41] H. Huang, H. Feng, and D. Zhuge, “M1 macrophage activated by notch signal pathway contributed to ventilator-induced lung injury in chronic obstructive pulmonary disease model,” *Journal of Surgical Research*, vol. 244, pp. 358–367, 2019.

## Research Article

# Identified GNGT1 and NMU as Combined Diagnosis Biomarker of Non-Small-Cell Lung Cancer Utilizing Bioinformatics and Logistic Regression

Jia-Jia Zhang <sup>1</sup>, Jiang Hong <sup>2</sup>, Yu-Shui Ma <sup>3,4</sup>, Yi Shi <sup>4</sup>, Dan-Dan Zhang <sup>4</sup>,  
Xiao-Li Yang <sup>4</sup>, Cheng-You Jia <sup>1</sup>, Yu-Zhen Yin <sup>1</sup>, Geng-Xi Jiang <sup>2</sup>, Da Fu <sup>4</sup>,  
and Fei Yu <sup>1</sup>

<sup>1</sup>Department of Nuclear Medicine, Shanghai Tenth People's Hospital, Tongji University School of Medicine, Shanghai 200072, China

<sup>2</sup>Department of Thoracic Surgery, Navy Military Medical University Affiliated Changhai Hospital, Shanghai 200433, China

<sup>3</sup>Department of Pancreatic and Hepatobiliary Surgery, Cancer Hospital, Fudan University Shanghai Cancer Center, Shanghai 200032, China

<sup>4</sup>Central Laboratory for Medical Research, Shanghai Tenth People's Hospital, Tongji University School of Medicine, Shanghai 200072, China

Correspondence should be addressed to Geng-Xi Jiang; [jiang9909@hotmail.com](mailto:jiang9909@hotmail.com), Da Fu; [fu800da900@126.com](mailto:fu800da900@126.com), and Fei Yu; [yufei021@sina.com](mailto:yufei021@sina.com)

Received 3 November 2020; Revised 1 December 2020; Accepted 18 December 2020; Published 6 January 2021

Academic Editor: Andrea Maugeri

Copyright © 2021 Jia-Jia Zhang et al. This is an open access article distributed under the Creative Commons Attribution License, which permits unrestricted use, distribution, and reproduction in any medium, provided the original work is properly cited.

Non-small-cell lung cancer (NSCLC) is one of the most devastating diseases worldwide. The study is aimed at identifying reliable prognostic biomarkers and to improve understanding of cancer initiation and progression mechanisms. RNA-Seq data were downloaded from The Cancer Genome Atlas (TCGA) database. Subsequently, comprehensive bioinformatics analysis incorporating gene ontology (GO), Kyoto Encyclopedia of Genes and Genomes (KEGG), and the protein-protein interaction (PPI) network was conducted to identify differentially expressed genes (DEGs) closely associated with NSCLC. Eight hub genes were screened out using Molecular Complex Detection (MCODE) and cytoHubba. The prognostic and diagnostic values of the hub genes were further confirmed by survival analysis and receiver operating characteristic (ROC) curve analysis. Hub genes were validated by other datasets, such as the Oncomine, Human Protein Atlas, and cBioPortal databases. Ultimately, logistic regression analysis was conducted to evaluate the diagnostic potential of the two identified biomarkers. Screening removed 1,411 DEGs, including 1,362 upregulated and 49 downregulated genes. Pathway enrichment analysis of the DEGs examined the Ras signaling pathway, alcoholism, and other factors. Ultimately, eight prioritized genes (GNGT1, GNG4, NMU, GCG, TAC1, GAST, GCGR1, and NPSR1) were identified as hub genes. High hub gene expression was significantly associated with worse overall survival in patients with NSCLC. The ROC curves showed that these hub genes had diagnostic value. The mRNA expressions of GNGT1 and NMU were low in the Oncomine database. Their protein expressions and genetic alterations were also revealed. Finally, logistic regression analysis indicated that combining the two biomarkers substantially improved the ability to discriminate NSCLC. GNGT1 and NMU identified in the current study may empower further discovery of the molecular mechanisms underlying NSCLC's initiation and progression.

## 1. Introduction

As one of the most devastating diseases worldwide, lung cancer causes nearly 1.6 million mortalities each year [1–3]. Approximately 85% of lung cancers are characterized as

non-small-cell lung cancer (NSCLC) [4–6], which is typically classified into two subtypes, squamous cell carcinoma (SCC) and adenocarcinoma (AD), using standard pathology methods [7–10]. Tobacco smoking is the most common risk factor for lung cancer. Smoking is also associated with

multiple risks, including worse tolerance of treatment, higher risk of failure and second primary tumors, and poorer quality of life. Indeed, it has become clear that the significant reduction in tobacco consumption would result in the prevention of a large fraction of lung cancer cases and other smoking-related diseases [11–13].

In addition, other factors such as air pollution, poor diet, occupational exposure, and hereditary factors have been reported in association with NSCLC in nonsmokers [14–16]. Over the past few years, newly developed cytotoxic agents, including paclitaxel, gemcitabine, and vinorelbine, have emerged to offer multiple therapeutic choices for patients with LUAD [17–20]. However, chemotherapy for advanced NSCLC is often considered ineffective or excessively toxic [21–23].

In an attempt to improve treatments for NSCLC, new therapeutic strategies, such as the development of noncytotoxic targeted agents, have emerged [24–27]. Moreover, the targeted therapies have significantly improved clinical outcomes in a subset of lung cancer patients whose tumors harbor EGFR [28], ALK [29, 30], and HER2 alterations [31–33].

Despite recent advances in cancer treatment, unfortunately, the current five-year survival rate of NSCLC remains unsatisfactory [34–37]. Thus, it is imperative to identify potential biomarkers and explore NSCLC's underlying biological mechanisms.

In recent years, bioinformatics analysis has been utilized as a powerful tool to explore novel prognostic and therapeutic biomarkers and to unveil the potential mechanisms of NSCLC [38–41]. For instance, a novel model including seven genes was reported to indicate a promising prognostic biomarker for lung SCC patients using integrated bioinformatics methods [41–43]. In addition, studies used comprehensive bioinformatics analysis to show that the cell cycle pathway may play a significant role in NSCLC in nonsmokers [44–47].

In the present study, RNA-Seq data were downloaded from The Cancer Genome Atlas (TCGA) database. Then, the EdgeR package was applied to uncover differentially expressed genes (DEGs) between NSCLC tissues and normal tissues. Using the resulting data, this study is aimed at unveiling the underlying molecular mechanism of NSCLC onset and progression through gene ontology (GO), Kyoto Encyclopedia of Genes and Genomes (KEGG) pathway enrichment analysis, and the protein-protein interaction (PPI) network. Subsequently, cytoHubba, a novel Cytoscape plugin, was used to reveal the hub genes from 12 topological analysis methods. Furthermore, the prognostic and diagnostic values of the hub genes were further confirmed by survival analysis and receiver operating characteristic (ROC) curve analysis.

The screening revealed two key genes, GNGT1 and NMU, and the protein expressions of these genes were validated by the Human Protein Atlas online database at the system level. Their genetic alteration and coexpression were also revealed. Finally, a logistic regression model was built to evaluate the combined diagnostic capability of GNGT1 and NMU.

## 2. Materials and Methods

**2.1. Downloading of TCGA Datasets and DEG Screening.** The mRNA expression data of NSCLC patients were downloaded

from the TCGA database (<https://cancergenome.nih.gov/>) [48]. The criteria used were as follows: primary site (lung), data category (Transcriptome Profiling), project ID (TCGA-LUAD and TCGA-LUSC), experimental strategy (RNA-Seq), and workflow type (HTSeq-counts). The other filters were kept as default. Practical Extraction and Reporting Language (Perl) was utilized to extract the sample information, generate the mRNA expression matrix, and annotate gene symbols. Finally, data from a cohort containing 1,145 samples were obtained from TCGA. Of these 1,145 samples, there were 108 normal tissue and 1,037 NSCLC samples, respectively. The EdgeR package from Bioconductor was used to screen the DEGs between normal tissue and NSCLC [49–51]. The adjusted  $P < 0.001$ , and fold change (FC)  $> 4$  were set as the cutoff criteria.

**2.2. DEG Functional Enrichment Analysis.** Gene ontology (GO) analysis provides a standardized description of gene products in terms of molecular function (MF), biological process (BP), and cellular component (CC) [52]. The Kyoto Encyclopedia of Genes and Genomes (KEGG) is a database offering gene functional meanings and expressed proteins [53]. GO and KEGG enrichment analyses were conducted using the powerful online tool DAVID (DAVID, <https://david.ncicrf.gov/>) and visualized by the R package “ggplot2” [54]. In addition,  $P < 0.05$  was considered to indicate statistical significance.

**2.3. Constructing the Protein-Protein Interaction Network.** The Search Tool for the Retrieval of Interacting Genes (STRING, <https://string-db.org/>) database, a database that integrates all functional interactions between proteins, was used to build the PPI network [55]. An interaction score of  $\geq 0.4$  was considered statistically significant.

**2.4. Hub Gene Selection and Analysis.** A Cytoscape plugin, Molecular Complex Detection (MCODE), was utilized to screen modules of PPI networks with a node score cutoff of 0.2, degree cutoff of 2,  $k$ -core of 2, and max depth of 100. A  $P$  value of  $< 0.05$  was considered statistically significant. Next, the DEGs were ranked by cytoHubba [56], which contains 12 algorithms: Maximal Clique Centrality, Edge Percolated Component, Betweenness, Density of Maximum Neighborhood Component, Degree, Bottleneck, Eccentricity, Closeness, Radiability, Maximum Neighborhood Component, Stress, and Clustering Coefficient. The MCODE and cytoHubba results were combined to identify the hub genes.

**2.5. Survival Analysis of Hub Genes.** Whether the expression level of hub genes was associated with overall survival was investigated using the Kaplan–Meier plotter (<http://www.kmplot.com/>). An online database is capable of assessing the effect of 54,675 genes on survival using 10,461 cancer samples, including samples from 2,437 lung cancer, 1,065 gastric cancer, 1,816 ovarian cancer, and 5,143 breast cancer patients.  $P < 0.05$  (Cox) was considered statistically significant.

**2.6. ROC Curve.** The ROC curve analysis was applied to evaluate the specificity and sensitivity of the hub genes. The area

under the curve (AUC) and  $P$  value were calculated.  $P < 0.05$  was considered to denote statistical significance.

**2.7. Validation of Hub Genes.** The expression level of hub genes in LUAD was validated by OncoPrint (https://www.oncoPrint.org/resource/login.html) [57]. The threshold was set as the following:  $P < 1E - 4$ , fold change  $> 2$ , and gene ranking in the top 10%.

**2.8. Human Protein Atlas.** The Human Protein Atlas (https://www.proteinatlas.org) is an online website that includes immunohistochemical data of nearly 20 types of tumors [58]. In our study, immunohistochemical images were used to directly compare the expression of biomarkers in normal and NSCLC tissues. The intensity of antibody staining indicated the protein expression of hub genes.

**2.9. Genetic Alteration of Hub Genes.** The cBio Cancer Genomics Portal (http://www.cbioportal.org/) is an open platform that provides visualization, analysis, and downloads of large-scale cancer genomic datasets for various cancer types [59]. Complex cancer genomic profiles can be easily obtained using the portal's query interface, enabling researchers to explore and compare genetic alterations across samples. cBioPortal was used to explore genetic alterations, coexpression, and overall survival of two hub genes, GNGT1 and NMU.

**2.10. Statistical Analysis.** SPSS version 23.0 (SPSS Inc., Chicago, IL, USA) was used to perform logistic regression analysis. ROC curves were generated to evaluate the diagnostic accuracy of GNGT1 and NMU, and AUC was used to evaluate sensitivity and specificity.

### 3. Results

**3.1. Identification of DEGs in NSCLC.** The workflow is shown in Figure 1(a). DEGs were identified using the criteria of  $P < 0.001$  and  $FC > 4$ . A total of 1,411 DEGs were screened out between NSCLC and normal samples, including 1,362 upregulated genes and 49 downregulated genes (Figures 1(b) and 1(c)).

**3.2. Functional and Pathway Analysis of DEGs.** To further investigate the specific function of these genes, all DEGs were uploaded to the online tool DAVID. GO analysis revealed that in terms of BP, the DEGs were associated with nucleosome assembly, transcription from RNA polymerase II promoter, telomere organization, flavonoid glucuronidation, and DNA replication-dependent nucleosome assembly.

When examined in terms of MF, DEGs were enriched in protein heterodimerization activity, retinoic acid-binding, hormone activity, glucuronosyltransferase activity, and extracellular ligand-gated ion channel activity. Regarding CC, the DEGs were mainly enriched in the extracellular region, cornified envelope, nucleosome, extracellular space, and intermediate filament. KEGG analysis found that the DEGs were predominantly involved in the Ras signaling pathway, nicotine addiction, steroid hormone biosynthesis, alcoholism, and systemic lupus erythematosus (Figure 2(a)).

**3.3. PPI Network Construction, Module Analysis, and Hub Gene Selection.** The PPI network was constructed using the STRING database and visualized in Cytoscape. The PPI network consisted of 787 nodes and 2,104 edges, including 1,362 upregulated genes and 49 downregulated genes. The overlapping genes of different algorithms selected by cytoHubba were GNGT1, GNG4, NMU, GCG, TAC1, GAST, NPSR1, and GCGR (Figure 2(b)). The top modules were then extracted from the PPI network (Figure 2(c)).

**3.4. Survival Analysis.** The Kaplan–Meier plotter was used to predict the prognostic value of the six identified hub genes. The results demonstrated that high expressions of GNGT1 (HR = 1.17 (1.03 – 1.33), logrank  $P = 0.017$ ), GNG4 (HR = 1.42 (1.2 – 1.67), logrank  $P = 4.4e - 05$ ), NMU (HR = 1.48 (1.3 – 1.68), logrank  $P = 2.5e - 09$ ), GCG (HR = 1.15 (1.01 – 1.31), logrank  $P = 0.031$ ), TAC1 (HR = 1.23 (1.08 – 1.39), logrank  $P = 0.0017$ ), GAST (HR = 1.27 (1.12 – 1.44), logrank  $P = 0.00025$ ), GCGR (HR = 0.79 (0.69 – 0.89), logrank  $P = 0.00022$ ), and NPSR1 (HR = 1.21 (1.02 – 1.42), logrank  $P = 0.024$ ) were associated with worse overall survival for NSCLC patients (Figure 3).

**3.5. ROC Curve.** According to ROC curve analysis, the AUCs of GNGT1, GNG4, NMU, GCG, TAC1, GAST, GCGR1, and NPSR1 were 0.9027 ( $P < 0.0001$ ), 0.8729 ( $P < 0.0001$ ), 0.9323 ( $P < 0.0001$ ), 0.559 ( $P < 0.0432$ ), 0.6822 ( $P < 0.0001$ ), 0.7426 ( $P < 0.0001$ ), 0.816 ( $P < 0.0001$ ), and NPSR1 0.8949 ( $P < 0.0001$ ), respectively (Figure 4(a)).

**3.6. Validating Hub Gene Expression.** The OncoPrint database was used to validate the expression of hub genes. The results demonstrated that GNGT1 had high expression in LUAD ( $P: 0.024$ , FC: 1.877) and LUSC ( $P: 9.77E-6$ , FC: 3.358). In Bhattacharjee's study, NMU showed high expression in LUAD ( $P: 0.007$ , FC: 5.186) and LUSC ( $P: 0.012$ , FC: 2.378) (Figure 4(b)).

**3.7. Human Protein Atlas.** After studying the mRNA expression of hub genes in NSCLC, we tried to explore the protein expression of hub genes using the Human Protein Atlas. The results revealed that NMU protein was not expressed in normal lung tissues, whereas medium expression of NMU protein was observed in the NSCLC tissues. However, GNGT1 was not detected in either normal lung tissues or NSCLC tissues (Figure 4(c)).

**3.8. Genetic Alteration of Hub Genes.** The two hub genes altered in 22 (4%) of the 584 patients, and the frequency of alteration of each hub gene, are shown in Figure 5(a). GNGT1 and NMU were altered most often (2.7% and 1.7%, respectively), with mutation, amplification, and mRNA upregulation as the main types of alterations observed (Figure 5(b)). The expression of GNGT1 was correlated with NMU (Spearman: 0.13,  $P = 2.415e - 3$ ; Pearson = 0.13,  $P = 4.821e - 3$ ) (Figure 5(c)). Patients with CYP1A2 and GSTA3 alteration had worse overall survival than patients without CYP1A2 and GSTA3 alteration ( $P = 0.465$ ) (Figure 5(d)).

Notably, according to the ROC curve analysis, the AUC of GNGT1 was 0.903 ( $P < 0.0001$ ). For NMU, the AUC was

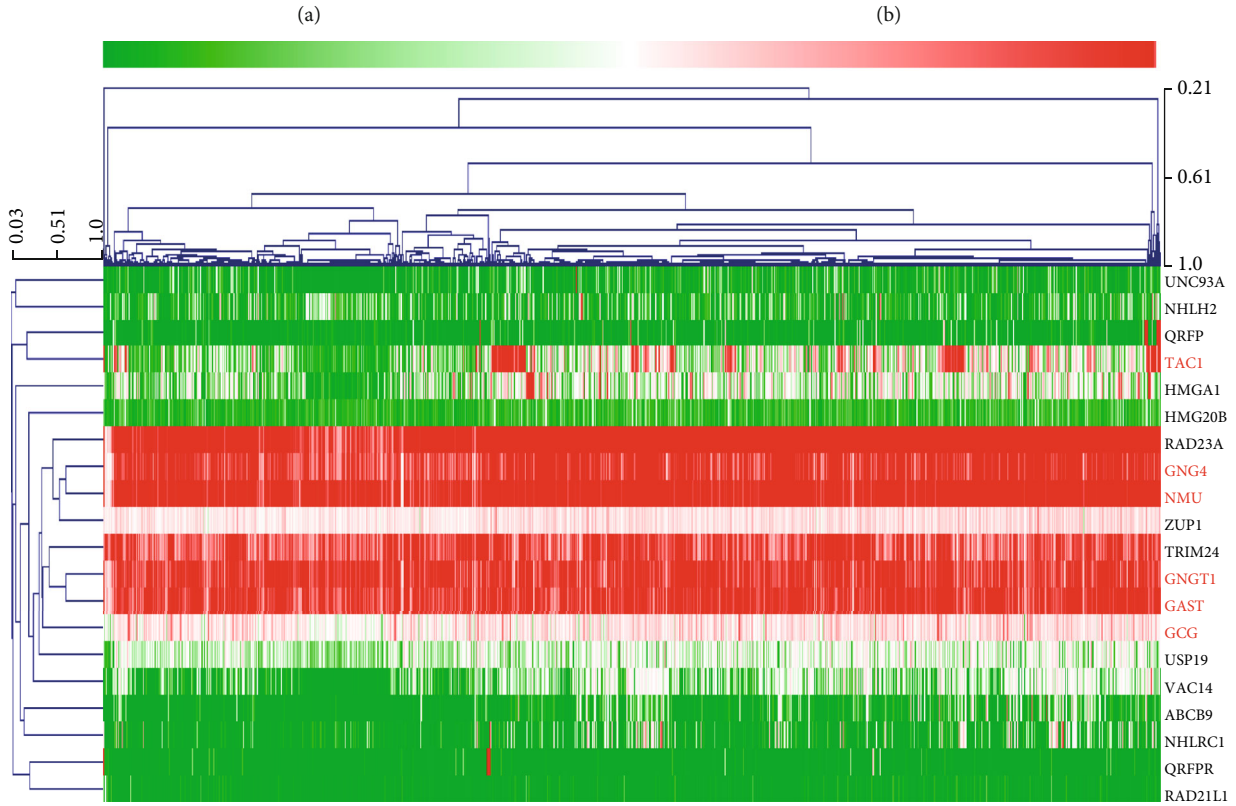
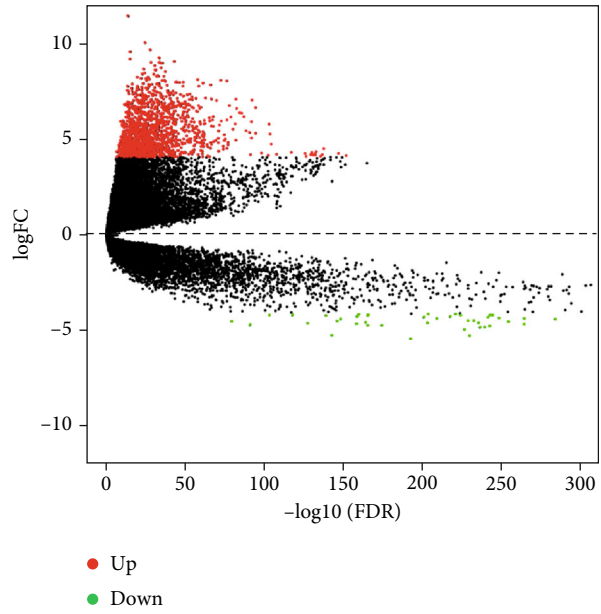
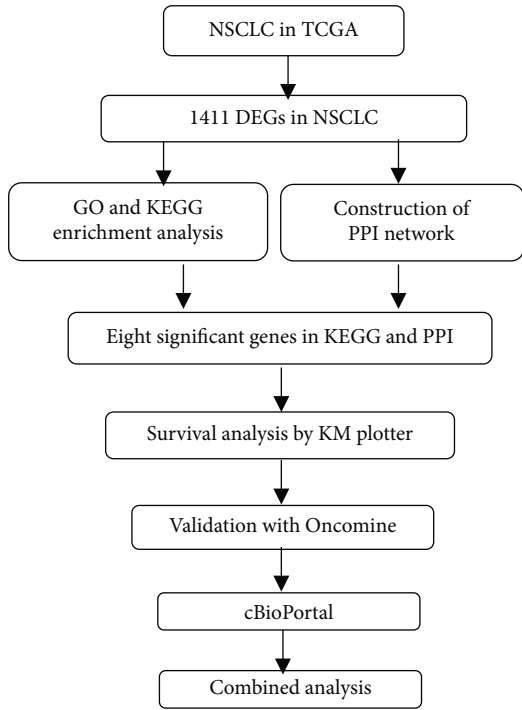


FIGURE 1: Identification of DEGs in NSCLC. (a) Workflow for the identification of key pathways and genes between non-small-cell lung cancer and normal samples. (b) DEGs between LUAD tissue and normal tissue. The volcano plot showed 1,411 DEGs. The red dots represented the upregulated genes, while the green dots represented downregulated genes. DEGs: differentially expressed genes. (c) Heatmap of the 20 upregulated and downregulated DEGs. The red color represents high expression, and the blue color represents low expression.

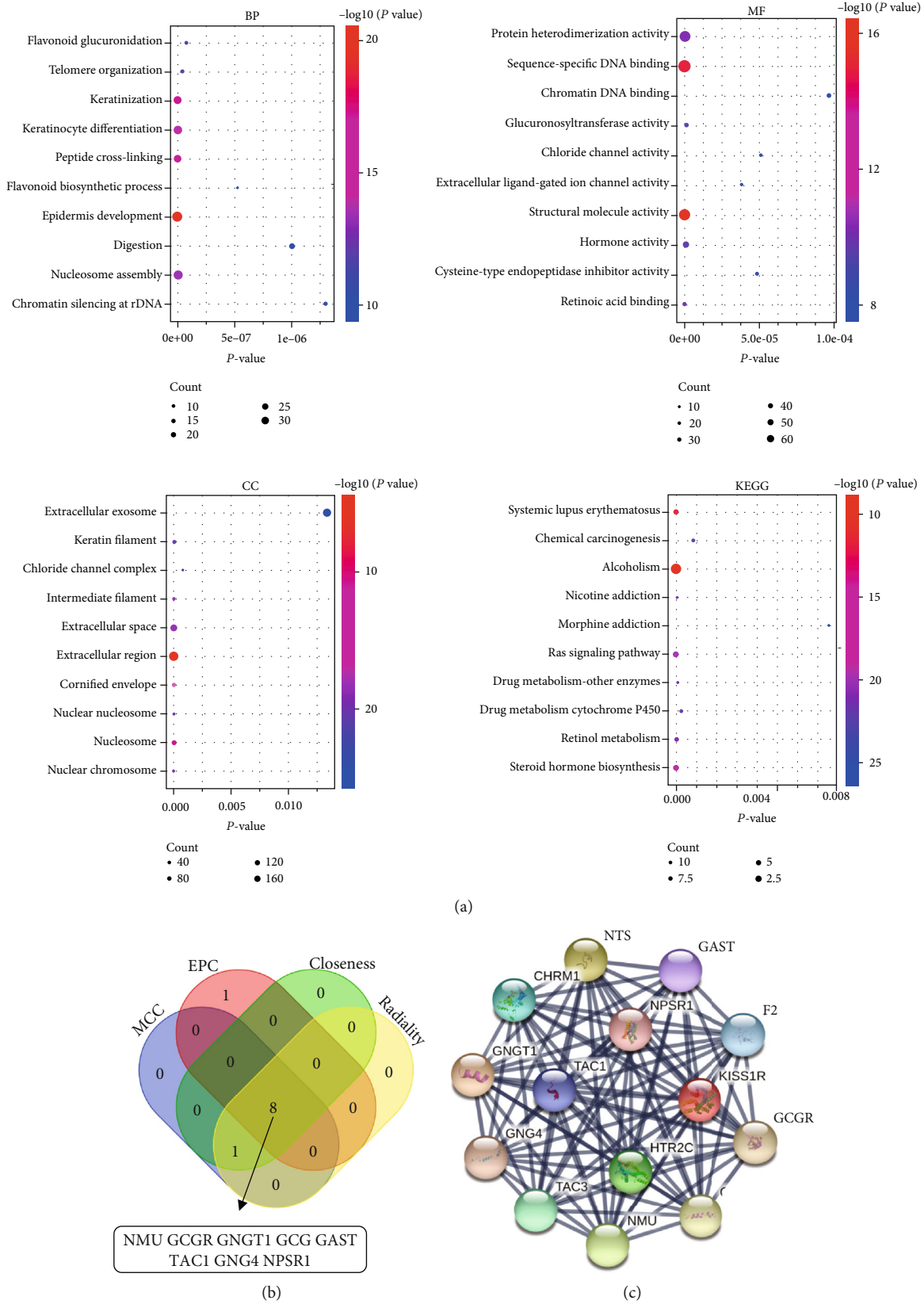


FIGURE 2: Functional and pathway analysis of DEGs. (a) GO and KEGG analysis of DEGs. *P* value is displayed on the *x*-axis, and GO function enrichment and KEGG pathway are shown on the *y*-axis. GO: gene ontology. KEGG: Kyoto Encyclopedia of Genes and Genomes. (b) The overlapping genes of different algorithms selected by cytoHubba. (c) The most significant modules obtained from the PPI network. PPI: protein-protein interaction.

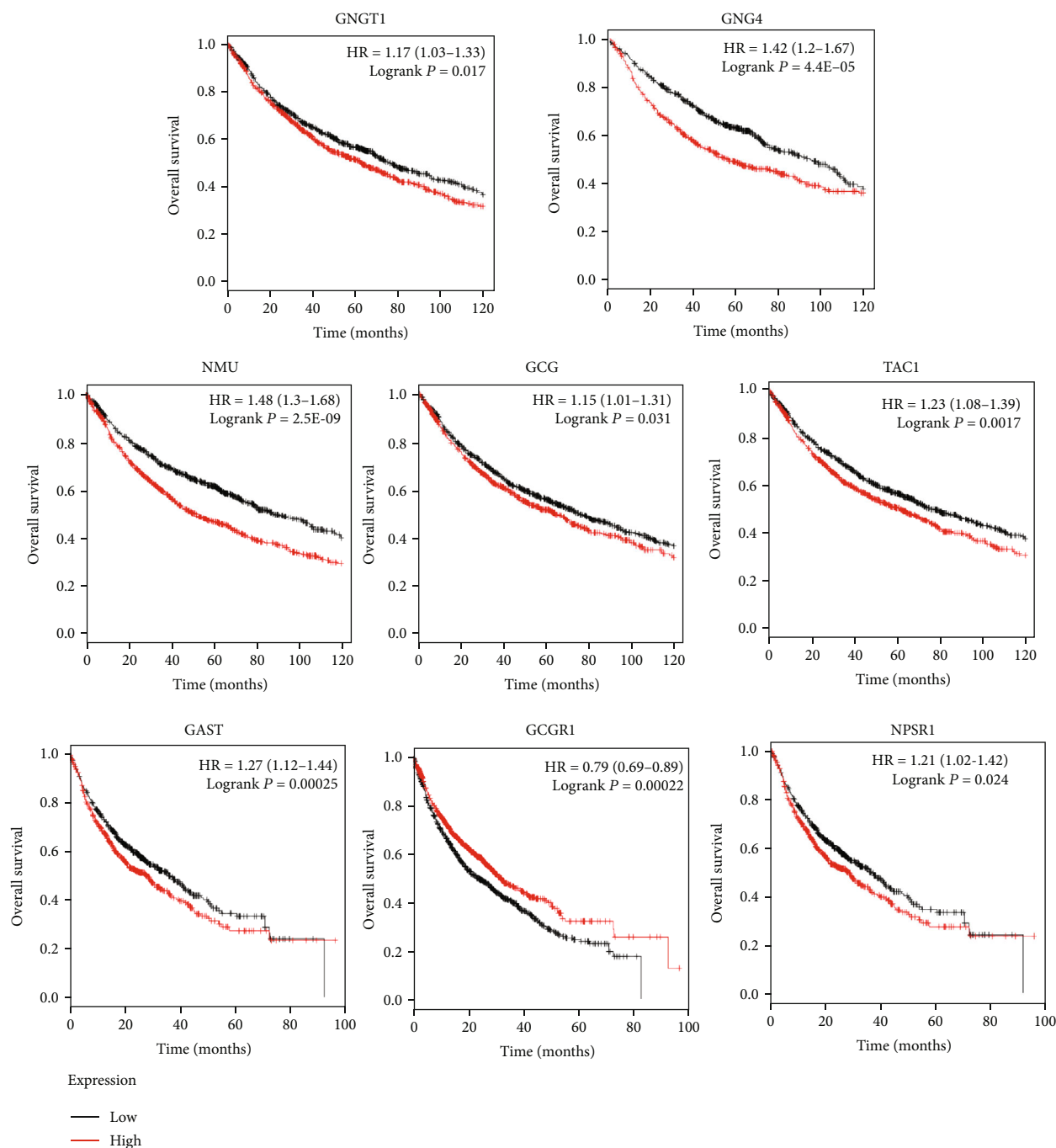


FIGURE 3: The prognostic value of hub genes in NSCLC patients. Kaplan–Meier curve analysis between hub gene expression and prognosis in NSCLC patients from the KM plotter database.

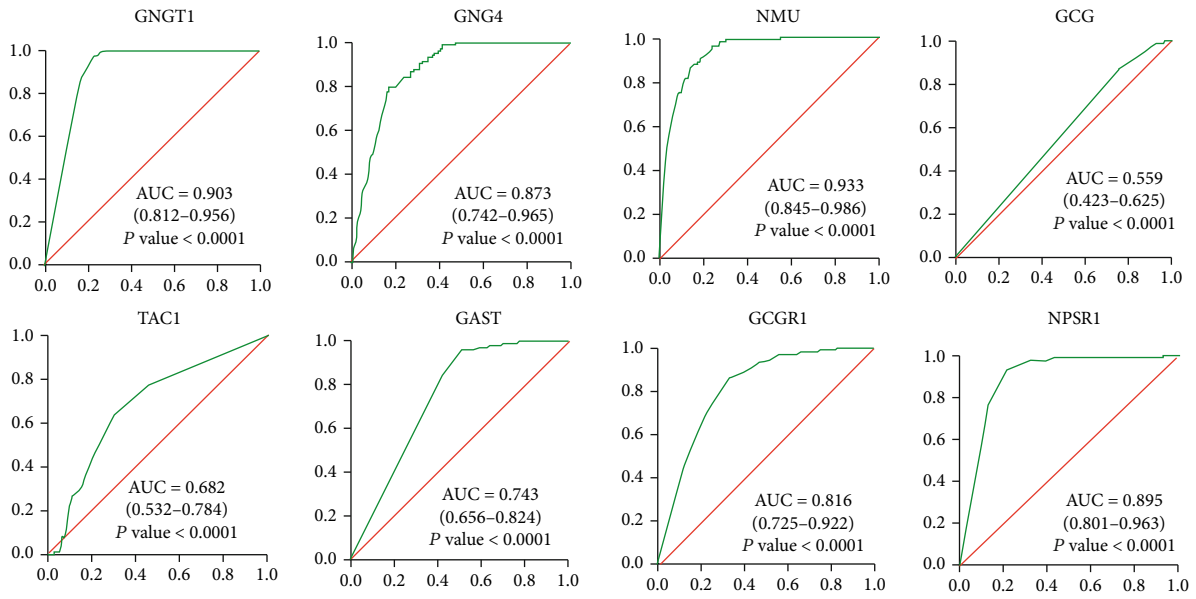
0.932 ( $P < 0.0001$ ). The AUC was largest when GNGT1 was combined with NMU (AUC = 0.969,  $P < 0.0001$ ) (Figure 5(e)).

#### 4. Discussion

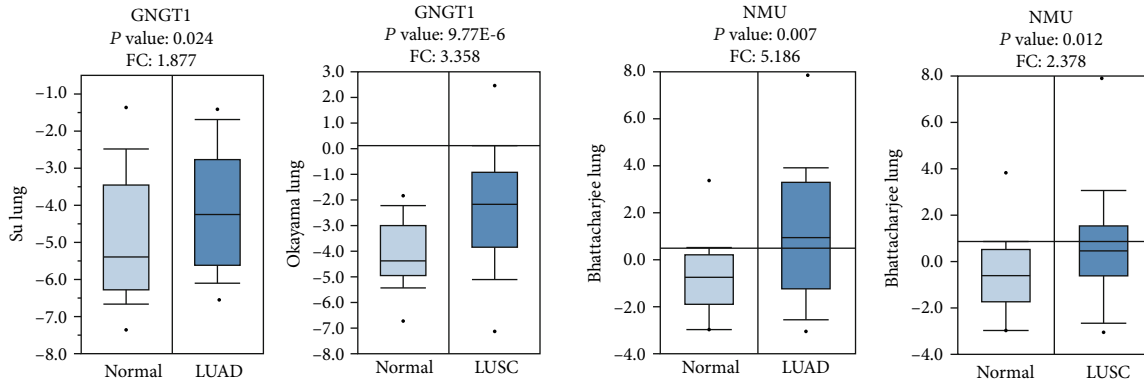
Elucidating the molecular mechanisms of the initiation and development of NSCLC would benefit the early diagnosis and targeted therapy efforts [60–63]. In this study, we identified 1,362 upregulated genes and 49 downregulated genes

and selected GNGT1, GNG4, NMU, GCG, TAC1, GAST, NPSR1, and GCGR as hub genes using Molecular Complex Detection (MCODE) and cytoHubba. These genes were primarily enriched in terms of the Ras signaling pathway, steroid hormone biosynthesis, nicotine addiction, alcoholism, steroid hormone biosynthesis, and systemic lupus erythematosus.

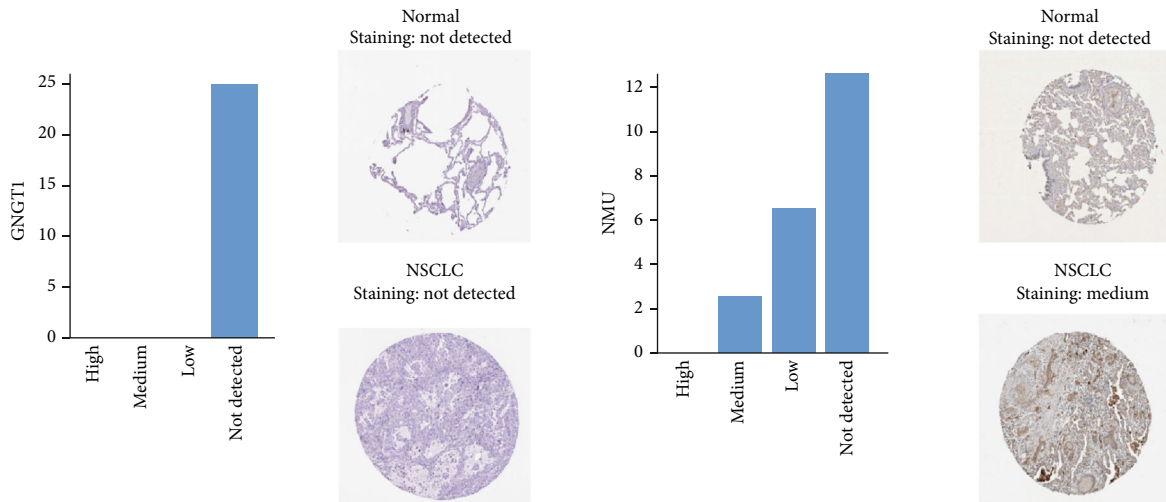
The Ras signaling pathway is closely related to the occurrence and progression of most human tumors [64–67]. The activation of RAS-RAF-MEK-MAPK in gene transcription



(a)



(b)



(c)

FIGURE 4: The expression and prognostic value of four hub genes in NSCLC patients. (a) The ROC curves of hub genes. AUC and *P* values of each hub gene are displayed in the plot. ROC: receiver operating characteristic. AUC: area under the curve. (b) Expression levels of significant genes compared between different types of NSCLC and normal tissues from the Oncomine platform. Fold changes and *P* values of each hub gene are displayed in the plot. (c) Immunohistochemical analysis of GNGT1 and NMU in normal tissues and NSCLC tissues from the Human Protein Atlas.

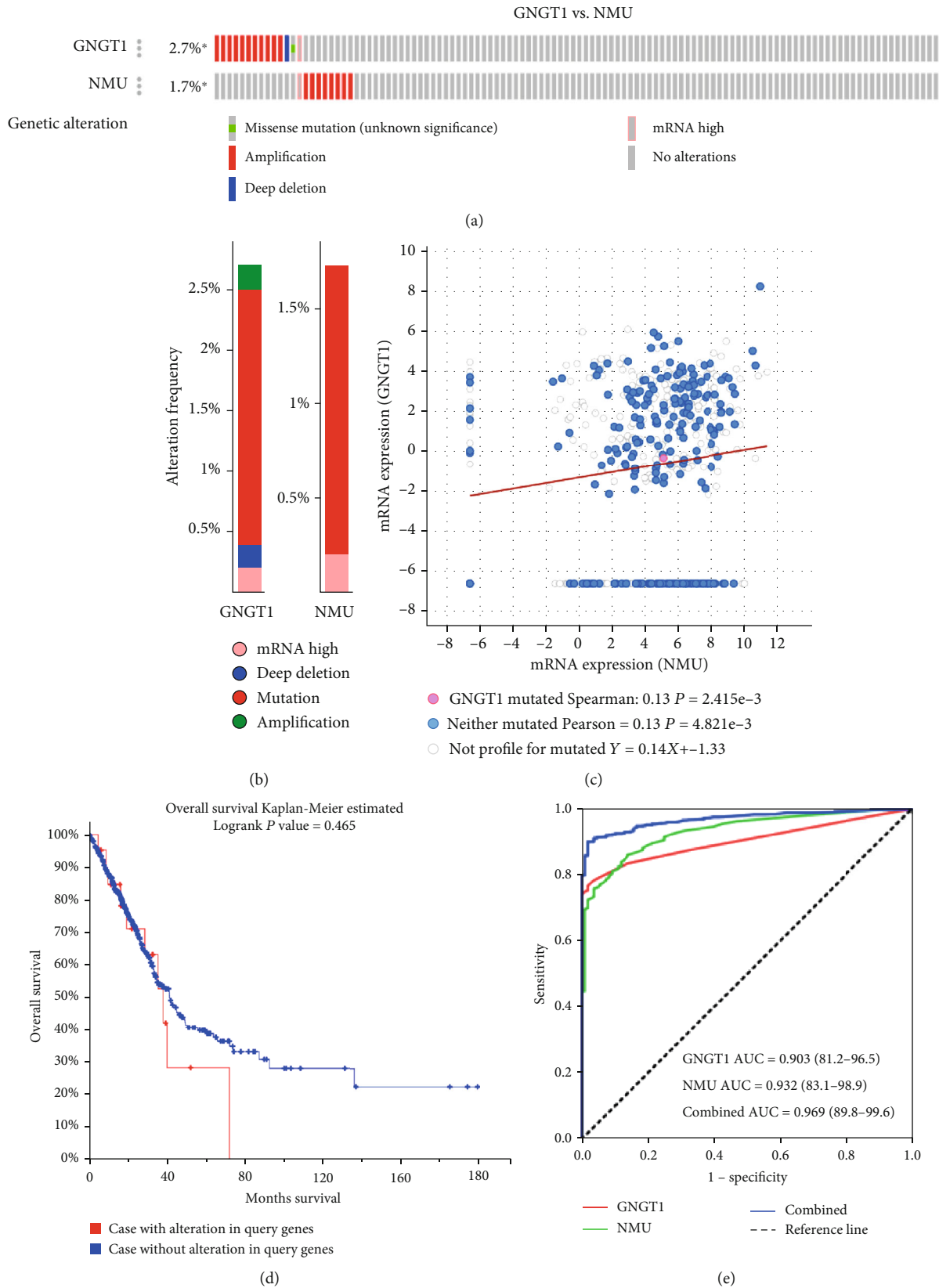


FIGURE 5: The expression and prognostic value of GNGT1 and NMU in NSCLC patients. (a) Genetic alteration of GNGT1 and NMU genes in NSCLC patients. (b) Illustration of the alteration frequency of GNGT1 and NMU genes in NSCLC patients. (c) Coexpression between GNGT1 and NMU. (d) Overall survival analysis for GNGT1 and NMU genes in NSCLC patients. (e) Combined diagnosis of GNGT1 and NMU genes in NSCLC patients.

regulation can promote proliferation, migration, and angiogenesis of cancer cells [68–70]. RAS-PI3K interaction is an important signaling node and potential therapeutic target in EGFR-mutant lung cancer [71–73]. In addition, steroid hormones were not previously considered to be involved with lung function [74–76]. However, numerous studies have reported that steroid hormones are important in normal lung development and function [77], as well as in the pathogenesis of pulmonary diseases, including lung cancer [78–81].

Cigarette smoking is a well-known risk factor for the occurrence and progression of malignant diseases [82–85]. Nicotine, the major constituent in cigarette smoke, plays key roles in cancer progression [86–89]. Nicotine likely promotes lung cancer cell proliferation by upregulating HIF-1 $\alpha$  and SOCC components [90–93]. It was demonstrated that nicotine increased NSCLC cell proliferation through nicotinic acetylcholine receptor-mediated signals [94–97]. Nicotine can also induce the expression of embryonic stem cell factor Sox2, which is indispensable for self-renewal and the maintenance of stem cell properties in NSCLC cells [98–100].

Several studies have been conducted to investigate the association between alcohol and lung cancer. Some studies have reported that alcohol is linked to a number of human diseases, including cancers [101–103]. Interestingly, another report shows that alcohol has nothing to do with lung cancer [104]. Thus, conducting further experiments is necessary to confirm whether lung cancer is attributable to alcohol abuse. All in all, the findings of these studies are consistent with our results.

In the current study, the expressions of GNGT1 and NMU were low both in the Oncomine and TCGA databases, indicating that GNGT1 and NMU may play a role as oncogenes. The transducin  $\gamma$ -subunit gene (GNGT1) has been localized to human chromosome 7 [104] and is associated with various forms of cancer [105–108]. GNGT1 exerts effects in different tissues regulating cell proliferation, migration, adhesion, and apoptosis [109–111]. One study showed that GNGT1 could serve as a marker of medulloblastoma [112]. GNGT1 can be utilized to differentiate gastrointestinal stromal tumor and leiomyosarcoma, two cancers that have very similar histopathology, but require very different treatments [113–115]. In the current study, GNGT1 was significantly upregulated and high mRNA expression of GNGT1 was associated with poor overall survival in NSCLC patients. Furthermore, KEGG analysis showed that GNGT1 was involved in the Ras signaling pathway. Therefore, it is reasonable to regard GNGT1 as a hub gene of NSCLC. Further studies are needed to better understand GNGT1's association with NSCLC.

Neuromedin U (NMU) has been reported to exhibit early alterations associated with cancer, including lung cancer, pancreatic cancer, breast cancer, renal cancer, and endometrioid endometrial carcinoma, through promoting migration, invasion, glycolysis, a mesenchymal phenotype, a stem cell phenotype of cancer cells, and resistance to the antitumor immune response [116–118]. It is overexpressed in pancreatic cancer and increases the cancer invasiveness through the hepatocyte growth factor c-Met pathway [119–121]. A role has also been implicated for NMU in human breast can-

cer and endometrial cancer [122–124]. The protein encoded by NMU can amplify ILC2 to drive allergic lung inflammation [125]. NMU is regulated by RhoGDI2, a metastasis inhibitor, which can be used as a target for lung metastasis. The expression of NMU is negatively correlated with prognosis in most types of cancer [126–128]. In the present study, the higher mRNA and protein expression of NMU were negatively correlated with overall survival. Therefore, our results are in line with these previous studies, which indicated that NMU may be directly or indirectly important in NSCLC development.

Moreover, to explore the predictive ability of GNGT1 and NMU, logistic regression analysis was performed. The logistic regression analysis showed a probabilistic nonlinear regression, which has functions in discrimination and prediction. Notably, according to logistic regression analysis, the AUC of the ROC curve of GNGT1 was 0.903 ( $P < 0.0001$ ), and the AUC of NMU was 0.932 ( $P < 0.0001$ ). Combining the two biomarkers enabled a relatively high capacity for discrimination between NSCLC and normal patients, with an AUC of 0.969, indicating that the combined test of GNGT1 combined with NMU was superior to testing for either gene individually, with better clinical accuracy and higher diagnostic value. Therefore, it is of high scientific value to use a logistic regression model as a diagnostic model for NSCLC.

In conclusion, our results identified two hub genes, GNGT1 and NMU, as prognostic target genes, and highlighted their probable role in NSCLC. Nevertheless, a few limitations to this study should be acknowledged. Because all the data analyzed in the current study were retrieved from the online databases, further independent experiments are required to validate our findings and to explore the molecular mechanism of the hub genes in NSCLC development and progression.

## Data Availability

All data generated or analyzed during this study are included in this article.

## Additional Points

*Impact Statement.* GNGT1 and NMU identified in the current study may empower further discovery of the molecular mechanisms underlying NSCLC's initiation and progression.

## Conflicts of Interest

The authors declared no potential conflicts of interest with respect to the research, authorship, and/or publication of this article.

## Authors' Contributions

Y.-S.M., D.F., and F.Y. designed the study. All authors collected data, performed the statistical analyses, and interpreted the data. J.-J.Z., D.F., and F.Y. wrote the manuscript. J.-J.Z., J.H., and Y.-S.M. contributed equally to this work.

All authors contributed to the final version of the manuscript and approved the final manuscript. Jia-Jia Zhang, Jiang Hong, and Yu-Shui Ma contributed equally to this work.

## Acknowledgments

This study was supported partly by grants from the National Natural Science Foundation of China (81972214, 81772932, 82071956, 81472202, and 81302065), Shanghai Talents Development Foundation (2017103), Shanghai Science and Technology Commission (18441903500, 14DZ1940606), Shanghai Academic/Technology Research Leader (18XD1403000), and National Key R&D Program of China (2016YFC0104303).

## References

- [1] F. Yu, J. B. Liu, Z. J. Wu et al., "Tumor suppressive microRNA-124a inhibits stemness and enhances gefitinib sensitivity of non-small cell lung cancer cells by targeting ubiquitin-specific protease 14," *Cancer Letters*, vol. 427, pp. 74–84, 2018.
- [2] L. Guo, Y. Zhang, R. Wei, C. Wang, and M. Feng, "Lipopoly-saccharide-anchored macrophages hijack tumor microtubule networks for selective drug transport and augmentation of antitumor effects in orthotopic lung cancer," *Theranostics*, vol. 9, pp. 6936–6948, 2019.
- [3] J. Ferlay, M. Colombet, I. Soerjomataram et al., "Cancer incidence and mortality patterns in Europe: estimates for 40 countries and 25 major cancers in 2018," *European Journal of Cancer*, vol. 103, pp. 356–387, 2018.
- [4] Z. Wang, S. Fu, J. Zhao et al., "Transbronchoscopic patient biopsy-derived xenografts as a preclinical model to explore chemorefractory-associated pathways and biomarkers for small-cell lung cancer," *Cancer letters*, vol. 440, pp. 180–188, 2019.
- [5] Y. Han, W. Guo, T. Ren et al., "Tumor-associated macrophages promote lung metastasis and induce epithelial-mesenchymal transition in osteosarcoma by activating the COX-2/STAT3 axis," *Cancer letters*, vol. 440, pp. 116–125, 2019.
- [6] S. K. Hong, H. Lee, O. S. Kwon et al., "Large-scale pharmacogenomics based drug discovery for ITGB3 dependent chemoresistance in mesenchymal lung cancer," *Molecular Cancer*, vol. 17, no. 1, p. 175, 2018.
- [7] C. Bouclier, M. Simon, G. Laconde et al., "Stapled peptide targeting the CDK4/Cyclin D interface combined with Abemaciclib inhibits KRAS mutant lung cancer growth," *Theranostics*, vol. 10, pp. 2008–2028, 2020.
- [8] O. B. Garbuzenko, A. Kuzmov, O. Taratula, S. R. Pine, and T. Minko, "Strategy to enhance lung cancer treatment by five essential elements: inhalation delivery, nanotechnology, tumor-receptor targeting, chemo- and gene therapy," *Theranostics*, vol. 9, no. 26, pp. 8362–8376, 2019.
- [9] M. Shen, X. Zhao, L. Zhao et al., "Met is involved in TIGAR-regulated metastasis of non-small-cell lung cancer," *Molecular Cancer*, vol. 17, p. 88, 2018.
- [10] A. Lin, T. Wei, H. Meng, P. Luo, and J. Zhang, "Role of the dynamic tumor microenvironment in controversies regarding immune checkpoint inhibitors for the treatment of non-small cell lung cancer (NSCLC) with EGFR mutations," *Molecular Cancer*, vol. 18, p. 139, 2019.
- [11] J. Zhu, W. C. Huang, B. Huang et al., "Clinical characteristics and prognosis of COVID-19 patients with initial presentation of lung lesions confined to a single pulmonary lobe," *American Journal of Translational Research*, vol. 12, no. 11, pp. 7501–7509, 2020.
- [12] M. Reda, W. Ngamcherdtrakul, S. Gu et al., "PLK1 and EGFR targeted nanoparticle as a radiation sensitizer for non-small cell lung cancer," *Cancer Letters*, vol. 467, pp. 9–18, 2019.
- [13] J. Gasparello, M. Lomazzi, C. Papi et al., "Efficient delivery of microRNA and anti-miRNA molecules using an argininocalix [4] arene macrocycle," *Molecular Therapy-Nucleic Acids*, vol. 18, pp. 748–763, 2019.
- [14] J. Nong, Y. Gong, Y. Guan et al., "Circulating tumor DNA analysis depicts subclonal architecture and genomic evolution of small cell lung cancer," *Nature Communications*, vol. 9, no. 1, p. 3114, 2018.
- [15] C. M. Dowling, H. Zhang, T. N. Chonghaile, and K.-K. Wong, "Shining a light on metabolic vulnerabilities in non-small cell lung cancer," *Biochimica et Biophysica Acta (BBA)-Reviews on Cancer*, vol. 1875, no. 1, Article ID 188462, 2021.
- [16] Z. Hu, X. Zheng, D. Jiao et al., "LunX-CAR T cells as targeted therapy for non-small cell lung cancer," *Molecular Therapy-Oncolytics*, vol. 17, pp. 361–370, 2020.
- [17] Y. Hu, J. Yu, Q. Wang et al., "Tartrate-resistant acid phosphatase 5/ACP5 interacts with p53 to control the expression of SMAD3 in lung adenocarcinoma," *Molecular Therapy-Oncolytics*, vol. 16, pp. 272–288, 2020.
- [18] M. V. Giulietti, A. Vespa, M. Ottaviani et al., "Personality (at intrapsychic and interpersonal level) associated with quality of life in patients with cancer (lung and colon)," *Cancer Control*, vol. 26, 2019.
- [19] Y. Li, Z. Yin, J. Fan, S. Zhang, and W. Yang, "The roles of exosomal miRNAs and lncRNAs in lung diseases," *Signal transduction and targeted therapy*, vol. 4, p. 47, 2019.
- [20] A. Taschauer, W. Polzer, F. Alioglu et al., "Peptide-targeted polyplexes for aerosol-mediated gene delivery to CD49f-overexpressing tumor lesions in lung," *Molecular Therapy-Nucleic Acids*, vol. 18, pp. 774–786, 2019.
- [21] W. J. Christian, N. L. Vanderford, J. McDowell et al., "Spatio-temporal analysis of lung cancer histological types in Kentucky, 1995-2014," *Cancer Control*, vol. 26, article 1073274819845873, 2019.
- [22] J. M. Matés, J. A. Campos-Sandoval, J. L. Santos-Jiménez, and J. Márquez, "Dysregulation of glutaminase and glutamine synthetase in cancer," *Cancer Letters*, vol. 467, pp. 29–39, 2019.
- [23] R. K. Dutta, S. Chinnapaiyan, and H. Unwalla, "Aberrant microRNAomics in pulmonary complications: implications in lung health and diseases," *Molecular Therapy-Nucleic Acids*, vol. 18, pp. 413–431, 2019.
- [24] H. R. Choi, I. A. Song, and T. K. Oh, "Association of opioid use in the week before death among patients with advanced lung cancer having sepsis," *Cancer Control*, vol. 26, article 1073274819871326, 2019.
- [25] C. P. Santiago, C. J. Keuthan, S. L. Boye, S. E. Boye, A. A. Imam, and J. D. Ash, "A drug-tunable gene therapy for broad-spectrum protection against retinal degeneration," *Molecular Therapy*, vol. 26, pp. 2407–2417, 2018.

- [26] F. Bianchini, E. Portioli, F. Ferlenghi et al., "Cell-targeted c(AmpRGD)-sunitinib molecular conjugates impair tumor growth of melanoma," *Cancer Letters*, vol. 446, pp. 25–37, 2019.
- [27] M. Caine, T. Chung, H. Kilpatrick et al., "Evaluation of novel formulations for transarterial chemoembolization: combining elements of Lipiodol emulsions with drug-eluting beads," *Theranostics*, vol. 9, no. 19, pp. 5626–5641, 2019.
- [28] C. Zhou, C. Yi, Y. Yi et al., "lncRNA PVT1 promotes tumorigenesis of colorectal cancer by stabilizing miR-16-5p and interacting with the VEGFA/VEGFR1/AKT axis," *Molecular Therapy-Nucleic Acids*, vol. 20, pp. 438–450, 2020.
- [29] N. Zhang, A. Nan, L. Chen et al., "Circular RNA circSATB2 promotes progression of non-small cell lung cancer cells," *Molecular Cancer*, vol. 19, no. 1, p. 101, 2020.
- [30] M. Chen, Y. Xu, J. Zhao et al., "Concurrent driver gene mutations as negative predictive factors in epidermal growth factor receptor-positive non-small cell lung cancer. EBioMedicine 2019;42:304-310. Nicot C. RNA-Seq reveal the circular RNAs landscape of lung cancer," *Molecular Cancer*, vol. 18, p. 183, 2019.
- [31] S. H. Vellanki, R. G. B. Cruz, H. Jahns et al., "Natural compound Tetrocarcin-A downregulates Junctional Adhesion Molecule-A inconjunction with HER2 and inhibitor of apoptosis proteins and inhibits tumorcell growth," *Cancer Letters*, vol. 440, pp. 23–34, 2019.
- [32] S. Yu, J. Zhang, Y. Yan et al., "A novel asymmetrical anti-HER2/CD3 bispecific antibody exhibits potent cytotoxicity for HER2-positive tumor cells," *Journal of Experimental & Clinical Cancer Research*, vol. 38, p. 355, 2019.
- [33] B. Yuan, J. Zhao, C. Zhou et al., "Co-occurring alterations of ERBB2 exon 20 insertion in non-small cell lung cancer (NSCLC) and the potential indicator of response to afatinib," *Frontiers in Oncology*, vol. 10, p. 729, 2020.
- [34] Y. He, D. Chen, Y. Yi et al., "Histone deacetylase inhibitor sensitizes ERCC1-high non-small-cell lung cancer cells to cisplatin via regulating miR-149," *Molecular Therapy-Oncolytics*, vol. 17, pp. 448–459, 2020.
- [35] W. Zhou, J. Yang, G. Saren et al., "HDAC6-specific inhibitor suppresses Th17 cell function via the HIF-1 $\alpha$  pathway in acute lung allograft rejection in mice," *Theranostics*, vol. 10, no. 15, pp. 6790–6805, 2020.
- [36] P. Chen, Q. Wu, J. Feng et al., "Erianin, a novel dibenzyl compound in *Dendrobium* extract, inhibits lung cancer cell growth and migration via calcium/calmodulin-dependent ferroptosis," *Signal Transduction and Targeted Therapy*, vol. 5, p. 51, 2020.
- [37] T. Li, Y. Liu, W. Zhang et al., "A rapid liquid biopsy of lung cancer by separation and detection of exfoliated tumor cells from bronchoalveolar lavage fluid with a dual-layer "PER-FECT" filter system," *Theranostics*, vol. 10, pp. 6517–6529, 2020.
- [38] H. Wang, Q. Deng, Z. Lv et al., "N6-methyladenosine induced miR-143-3p promotes the brain metastasis of lung cancer via regulation of VASH1," *Molecular Cancer*, vol. 18, p. 181, 2019.
- [39] Z. Hu, X. Zheng, D. Jiao et al., "LunX-CAR T Cells as a targeted therapy for non-small cell lung cancer," *Molecular Therapy-Oncolytics*, vol. 17, pp. 361–370, 2020.
- [40] X. Chen, Z. Wang, F. Tong, X. Dong, G. Wu, and R. Zhang, "lncRNA UCA1 promotes gefitinib resistance as a ceRNA to target FOSL2 by sponging miR-143 in non-small cell lung cancer," *Molecular Therapy-Nucleic Acids*, vol. 19, pp. 643–653, 2020.
- [41] M. Zhang, L. Zhang, Y. Li et al., "Exome sequencing identifies somatic mutations in novel driver genes in non-small cell lung cancer," *Aging (Albany NY)*, vol. 12, no. 13, pp. 13701–13715, 2020.
- [42] X. H. Huang, X. Yan, Q. H. Zhang et al., "Direct targeting of HSP90 with daurisolone destabilizes  $\beta$ -catenin to suppress lung cancer tumorigenesis," *Cancer Letters*, vol. 489, pp. 66–78, 2020.
- [43] Y. de Man, F. Atsma, M. G. Oosterveld-Vlug et al., "The intensity of hospital care utilization by Dutch patients with lung or colorectal cancer in their final months of life," *Cancer Control*, vol. 26, article 1073274819846574, 2019.
- [44] G. Yang, Q. Chen, J. Xiao, H. Zhang, Z. Wang, and X. Lin, "Identification of genes and analysis of prognostic values in nonsmoking females with non-small cell lung carcinoma by bioinformatics analyses," *Cancer Management and Research*, vol. Volume 10, pp. 4287–4295, 2018.
- [45] H. Wang, B. Lu, S. Ren et al., "Long Noncoding RNA LINC01116 contributes to gefitinib resistance in non-small cell lung cancer through regulating IFI44," *Molecular Therapy-Nucleic Acids*, vol. 19, pp. 218–227, 2020.
- [46] Z. Wu, Z. Liu, X. Jiang et al., "Depleting PTOV1 sensitizes non-small cell lung cancer cells to chemotherapy through attenuating cancer stem cell traits," *Journal of Experimental & Clinical Cancer Research*, vol. 38, p. 341, 2019.
- [47] Cancer Genome Atlas Research Network, "Comprehensive molecular profiling of lung adenocarcinoma," *Nature*, vol. 511, no. 7511, pp. 543–550, 2014.
- [48] H. G. Xiong, H. Li, Y. Xiao et al., "Long noncoding RNA MYOSLID promotes invasion and metastasis by modulating the partial epithelial-mesenchymal transition program in head and neck squamous cell carcinoma," *Journal of Experimental & Clinical Cancer Research*, vol. 38, p. 278, 2019.
- [49] Z. Gao, P. Fu, Z. Yu, F. X. Zhen, and Y. H. Yanhong Gu, "Comprehensive analysis of lncRNA-miRNA- mRNA network ascertains prognostic factors in patients with colon cancer," *Technology in Cancer Research & Treatment*, vol. 18, article 1533033819853237, 2019.
- [50] M. D. Robinson, D. J. McCarthy, and G. K. Smyth, "edgeR: a bioconductor package for differential expression analysis of digital gene expression data," *Bioinformatics*, vol. 26, pp. 139–140, 2010.
- [51] M. Ashburner, C. A. Ball, J. A. Blake et al., "Gene ontology: tool for the unification of biology," *Nature genetics*, vol. 25, pp. 25–29, 2000.
- [52] H. Ogata, S. Goto, K. Sato, W. Fujibuchi, H. Bono, and M. Kanehisa, "KEGG: Kyoto Encyclopedia of Genes and Genomes," *Nucleic Acids Research*, vol. 27, pp. 29–34, 1999.
- [53] X. Sun, K. Wu, and D. Cook, "PKgraph: an R package for graphically diagnosing population pharmacokinetic models," *Computer Methods and Programs in Biomedicine*, vol. 104, no. 3, pp. 461–471, 2011.
- [54] C. Perez-Iratxeta, P. Bork, and M. A. Andrade-Navarro, "Update of the G2D tool for prioritization of gene candidates to inherited diseases," *Nucleic Acids Research*, vol. 35, pp. W212–W216, 2007.
- [55] C. H. Chin, S. H. Chen, H. H. Wu, C. W. Ho, M. T. Ko, and C. Y. Lin, "cytoHubba: identifying hub objects and sub-

- networks from complex interactome,” *BMC systems biology*, vol. 8, p. S11, 2014.
- [56] D. R. Rhodes, J. Yu, K. Shanker et al., “ONCOMINE: a cancer microarray database and integrated data-mining platform,” *Neoplasia*, vol. 6, no. 1, pp. 1–6, 2004.
- [57] X. Q. Xie, M. J. Wang, Y. Li et al., “miR-124 intensified oxaliplatin-based chemotherapy by targeting CAPN2 in colorectal cancer,” *Molecular Therapy-Oncolytics*, vol. 17, pp. 320–331, 2020.
- [58] N. Hoshikawa, A. Sakai, S. Takai, and H. Suzuki, “Targeting extracellular miR-21-TLR7 signaling provides long-lasting analgesia in osteoarthritis,” *Molecular Therapy-Nucleic Acids*, vol. 19, pp. 199–207, 2020.
- [59] C. Gao, X. Sun, Z. Wu et al., “A novel benzofuran derivative Moracin N induces autophagy and apoptosis through ROS generation in lung cancer,” *Frontiers in Pharmacology*, vol. 11, p. 391, 2020.
- [60] N. C. Demircan, T. Akın Telli, T. Başoğlu Tüylü et al., “QT interval prolongation related to afatinib treatment in a patient with metastatic non-small-cell lung cancer,” *Current Problems in Cancer*, vol. 27, p. 100594, 2020.
- [61] A. Malinina, D. Dikeman, R. Westbrook et al., “IL10 deficiency promotes alveolar enlargement and lymphoid dysmorphogenesis in the aged murine lung,” *Aging Cell*, vol. 19, article e13130, 2020.
- [62] S. Xiong, Z. Hong, L. S. Huang et al., “IL-1 $\beta$  suppression of VE-cadherin transcription underlies sepsis-induced inflammatory lung injury,” *The Journal of Clinical Investigation*, vol. 8, p. 136908, 2020.
- [63] K. Xu, D. Park, A. T. Magis et al., “Small molecule KRAS agonist for mutant KRAS cancer therapy,” *Molecular Cancer*, vol. 18, p. 85, 2019.
- [64] P. Chen, X. Li, R. Zhang et al., “Combinative treatment of  $\beta$ -elemene and cetuximab is sensitive to KRAS mutant colorectal cancer cells by inducing ferroptosis and inhibiting epithelial-mesenchymal transformation,” *Theranostics*, vol. 10, no. 11, pp. 5107–5119, 2020.
- [65] G. Shan, B. Shao, Q. Liu et al., “circFMN2 sponges miR-1238 to promote the expression of LIM-homeobox gene 2 in prostate cancer cells,” *Molecular Therapy-Nucleic Acids*, vol. 21, pp. 133–146, 2020.
- [66] H. Jin, Y. Jang, N. Cheng et al., “Restoration of mutant K-Ras repressed miR-199b inhibits K-Ras mutant non-small cell lung cancer progression,” *Journal of Experimental & Clinical Cancer Research*, vol. 38, no. 1, p. 165, 2019.
- [67] Y. Jin, M. Liu, R. Sa, H. Fu, L. Cheng, and L. Chen, “Mouse models of thyroid cancer: bridging pathogenesis and novel therapeutics,” *Cancer Letters*, vol. 469, pp. 35–53, 2020.
- [68] C. Wu, E. Guo, J. Ming et al., “Radiation-induced DNMT3B promotes radioresistance in nasopharyngeal carcinoma through methylation of p53 and p21,” *Molecular Therapy-Oncolytics*, vol. 17, pp. 306–319, 2020.
- [69] R. Hu, Q. Han, and J. Zhang, “STAT3: a key signaling molecule for converting cold to hot tumors,” *Cancer Letters*, vol. 489, pp. 29–40, 2020.
- [70] C. Han, B. K. Choi, S. H. Kim et al., “Polymorphic region-specific antibody for evaluation of affinity-associated profile of chimeric antigen receptor,” *Molecular Therapy-Oncolytics*, vol. 17, pp. 293–305, 2020.
- [71] Y. J. Kim, D. S. Baek, S. Lee et al., “Dual-targeting of EGFR and Neuropilin-1 attenuates resistance to EGFR-targeted antibody therapy in KRAS-mutant non-small cell lung cancer,” *Cancer Letters*, vol. 466, pp. 23–34, 2019.
- [72] A. Casal-Mouriño, A. Ruano-Ravina, M. Torres-Durán et al., “Lung cancer survival in never-smokers and exposure to residential radon: results of the LCRINS study,” *Cancer Letters*, vol. 487, pp. 21–26, 2020.
- [73] F. Xu, J. X. Chen, X. B. Yang et al., “Analysis of lung adenocarcinoma subtypes based on immune signatures identifies clinical implications for cancer therapy,” *Molecular Therapy-Oncolytics*, vol. 17, pp. 241–249, 2020.
- [74] W. Lin, Y. Xu, X. Chen et al., “Radiation-induced small extracellular vesicles as “carriages” promote tumor antigen release and trigger antitumor immunity,” *Theranostics*, vol. 10, no. 11, pp. 4871–4884, 2020.
- [75] J. Xie, W. Zhang, X. Liang et al., “RPL32 promotes lung cancer progression by facilitating p53 degradation,” *Molecular Therapy-Nucleic Acids*, vol. 21, pp. 75–85, 2020.
- [76] M. Keller, F. Dubois, S. Teulier et al., “NDR2 kinase contributes to cell invasion and cytokinesis defects induced by the inactivation of RASSF1A tumor-suppressor gene in lung cancer cells,” *Journal of Experimental & Clinical Cancer Research*, vol. 38, p. 158, 2019.
- [77] A. van Waarde, A. A. Rybczynska, N. K. Ramakrishnan, K. Ishiwata, P. H. Elsinga, and R. A. Dierckx, “Potential applications for sigma receptor ligands in cancer diagnosis and therapy,” *Biochimica et Biophysica Acta*, vol. 1848, pp. 2703–2714, 2015.
- [78] L. Jiang, R. Wang, L. Fang et al., “HCP5 is a SMAD3-responsive long non-coding RNA that promotes lung adenocarcinoma metastasis via miR-203/SNAI axis,” *Theranostics*, vol. 9, no. 9, pp. 2460–2474, 2019.
- [79] C. Chen, W. R. Liu, B. Zhang et al., “LncRNA H19 downregulation confers erlotinib resistance through upregulation of PKM2 and phosphorylation of AKT in EGFR-mutant lung cancers,” *Cancer Letters*, vol. 486, pp. 58–70, 2020.
- [80] E. Fernandes, J. Sores, S. Cotton et al., “Esophageal, gastric and colorectal cancers: looking beyond classical serological biomarkers towards glycoproteomics-assisted precision oncology,” *Theranostics*, vol. 10, pp. 4903–4928, 2020.
- [81] M. Shen, Z. Xu, W. Xu et al., “Inhibition of ATM reverses EMT and decreases metastatic potential of cisplatin-resistant lung cancer cells through JAK/STAT3/PD-L1 pathway,” *Journal of Experimental & Clinical Cancer Research*, vol. 38, p. 149, 2019.
- [82] J. Kang, S. H. Jeong, K. Lee et al., “Exacerbation of symptomatic arthritis by cigarette smoke in experimental arthritis,” *PLoS One*, vol. 15, no. 3, article e0230719, 2020.
- [83] S. Galland, P. Martin, G. Fregni, I. Letovanec, and I. Stamenkovic, “Attenuation of the pro-inflammatory signature of lung cancer-derived mesenchymal stromal cells by statins,” *Cancer Letters*, vol. 484, pp. 50–64, 2020.
- [84] H. Liu, Y. C. Xue, H. Deng et al., “MicroRNA modification of Cocksackievirus B3 decreases its toxicity, while retaining oncolytic potency against lung cancer,” *Molecular Therapy-Oncolytics*, vol. 16, pp. 207–218, 2020.
- [85] Y. Qiao, Z. Wang, F. Tan et al., “Enhancer reprogramming within pre-existing topologically associated domains promotes TGF- $\beta$ -induced EMT and cancer metastasis,” *Molecular Therapy*, vol. 28, pp. 2083–2095, 2020.
- [86] Q. Huang, Q. Wang, D. Li et al., “Co-administration of 20(S)-protopanaxatriol (g-PPT) and EGFR-TKI overcomes EGFR-

- TKI resistance by decreasing SCD1 induced lipid accumulation in non-small cell lung cancer,” *Journal of Experimental & Clinical Cancer Research*, vol. 38, p. 129, 2019.
- [87] M. Fan, Y. Han, S. Gao et al., “Ultrasmall gold nanoparticles in cancer diagnosis and therapy,” *Theranostics*, vol. 10, no. 11, pp. 4944–4957, 2020.
- [88] S. Duan, J. Li, J. Tian et al., “Crosstalk between let-7a-5p and BCL-xL in the initiation of toxic autophagy in lung cancer,” *Molecular Therapy-Oncolytics*, vol. 15, pp. 69–78, 2019.
- [89] Q. Ben, W. An, Y. Sun et al., “A nicotine-induced positive feedback loop between HIF1A and YAP1 contributes to epithelial-to-mesenchymal transition in pancreatic ductal adenocarcinoma,” *Journal of Experimental & Clinical Cancer Research*, vol. 39, no. 1, p. 181, 2020.
- [90] Y. Xiong, L. He, C. Shay et al., “Nck-associated protein 1 associates with HSP90 to drive metastasis in human non-small-cell lung cancer,” *Journal of Experimental & Clinical Cancer Research*, vol. 38, no. 1, p. 122, 2019.
- [91] J. Chen, A. Liu, Z. Lin et al., “Downregulation of the circadian rhythm regulator HLF promotes multiple-organ distant metastases in non-small cell lung cancer through PPAR/NF- $\kappa$ b signaling,” *Cancer Letters*, vol. 482, pp. 56–71, 2020.
- [92] Z. Li, C. Zeng, Q. Nong et al., “Exosomal leucine-rich-Alpha2-glycoprotein 1 derived from non-small-cell lung cancer cells promotes angiogenesis via TGF- $\beta$  signal pathway,” *Molecular Therapy-Oncolytics*, vol. 4, pp. 313–322, 2019.
- [93] L. Zhou, Y. Jiang, Q. Luo, L. Li, and L. Jia, “Neddylation: a novel modulator of the tumor microenvironment,” *Molecular Cancer*, vol. 18, no. 1, p. 77, 2019.
- [94] Z. Zhao, N. Zhang, A. Li et al., “Insulin-like growth factor-1 receptor induces immunosuppression in lung cancer by upregulating B7-H4 expression through the MEK/ERK signaling pathway,” *Cancer Letters*, vol. 485, pp. 14–26, 2020.
- [95] S. Kim, J. Y. Maeng, S. J. Hyun et al., “Extracellular vesicles from human umbilical cord blood plasma modulate interleukin-2 signaling of T cells to ameliorate experimental autoimmune encephalomyelitis,” *Theranostics*, vol. 10, pp. 5011–5028, 2020.
- [96] X. Chen, Y. Jia, Y. Zhang, D. Zhou, H. Sun, and X. Ma, “ $\alpha$ 5-nAChR contributes to epithelial-mesenchymal transition and metastasis by regulating Jab1/Csn5 signalling in lung cancer,” *Journal of Cellular and Molecular Medicine*, vol. 24, no. 4, pp. 2497–2506, 2020.
- [97] L. Fang, D. Ly, S. S. Wang et al., “Targeting late-stage non-small cell lung cancer with a combination of DNT cellular therapy and PD-1 checkpoint blockade,” *Journal of Experimental & Clinical Cancer Research*, vol. 38, p. 123, 2019.
- [98] W. Zhou, Y. Liu, Y. Gao et al., “MICAL2 is a novel nucleocytoplasmic shuttling protein promoting cancer invasion and growth of lung adenocarcinoma,” *Cancer Letters*, vol. 483, pp. 75–86, 2020.
- [99] C. Wei, X. Dong, H. Lu et al., “LPCAT1 promotes brain metastasis of lung adenocarcinoma by up-regulating PI3K/AKT/MYC pathway,” *Journal of Experimental & Clinical Cancer Research*, vol. 38, p. 95, 2019.
- [100] C. Wei, X. Dong, H. Lu et al., “Novel lncRNA-IUR suppresses Bcr-Abl-induced tumorigenesis through regulation of STAT5-CD71 pathway,” *Molecular Cancer*, vol. 18, p. 84, 2019.
- [101] M. Tian, X. Wu, T. Lu et al., “Phytochemical analysis, antioxidant, antibacterial, cytotoxic, and enzyme inhibitory activities of *Hedychium flavum* rhizome,” *Frontiers in Pharmacology*, vol. 11, p. 572659, 2020.
- [102] H. Lee, Y. S. Son, M. O. Lee et al., “Low-dose interleukin-2 alleviates dextran sodium sulfate-induced colitis in mice by recovering intestinal integrity and inhibiting AKT-dependent pathways,” *Theranostics*, vol. 10, no. 11, pp. 5048–5063, 2020.
- [103] X. Luo, N. Li, X. Zhao et al., “DHRS2 mediates cell growth inhibition induced by Trichothecin in nasopharyngeal carcinoma,” *Journal of Experimental & Clinical Cancer Research*, vol. 38, p. 300, 2019.
- [104] S. W. Scherer, D. S. Feinstein, L. Oliveira, L. C. Tsui, and S. J. Pittler, “Gene structure and chromosome localization to 7q21.3 of the human rod photoreceptor transducin gamma-subunit gene (GNGT1),” *Genomics*, vol. 35, no. 1, pp. 241–243, 1996.
- [105] O. C. Ong, K. Hu, H. Rong, R. H. Lee, and B. K. Fung, “Gene structure and chromosome localization of the GycSubunit of human cone G-protein (GNGT2),” *Genomics*, vol. 44, no. 1, pp. 101–109, 1997.
- [106] H. Chen, T. Leung, K. E. Giger et al., “Expression of the G protein gammaT1 subunit during zebrafish development,” *Gene Expression Patterns*, vol. 7, pp. 574–583, 2007.
- [107] D. Lagman, A. Callado-Pérez, I. E. Franzén, D. Larhammar, and X. M. Abalo, “Transducin duplicates in the zebrafish retina and pineal complex:differential specialisation after the teleost tetraploidisation,” *PLoS One*, vol. 10, article e0121330, 2015.
- [108] L. E. Sucheston-Campbell, A. I. Clay-Gilmour, W. E. Barlow et al., “Genome-wide meta-analyses identifies novel taxane-induced peripheral neuropathy-associated loci,” *Pharmacogenetics and Genomics*, vol. 28, no. 2, pp. 49–55, 2018.
- [109] T. Mulligan and S. A. Farber, “Central and C-terminal domains of heterotrimeric G protein gamma subunits differentially influence the signaling necessary for primordial germ cell migration,” *Cellular Signalling*, vol. 23, no. 10, pp. 1617–1624, 2011.
- [110] J. L. Zhang, M. Liu, C. N. Zhang, E. C. Li, M. Z. Fan, and M. X. Huang, “Transcriptomic analyses of tributyltin-induced sexual dimorphisms in rare minnow (*Gobiocypris rarus*) brains,” *Ecotoxicology and Environmental Safety*, vol. 156, pp. 18–24, 2018.
- [111] E. J. Mucaki, J. Z. L. Zhao, D. J. Lizotte, and P. K. Rogan, “Predicting responses to platinum chemotherapy agents with biochemically-inspired machine learning,” *Signal Transduction and Targeted Therapy*, vol. 4, no. 1, p. 1, 2019.
- [112] R. Zou, D. Zhang, L. Lv et al., “Bioinformatic gene analysis for potential biomarkers and therapeutic targets of atrial fibrillation-related stroke,” *Journal of Translational Medicine*, vol. 17, no. 1, p. 45, 2019.
- [113] B. X. Liu, G. J. Huang, and H. B. Cheng, “Comprehensive analysis of core genes and potential mechanisms in rectal cancer,” *Journal of Computational Biology*, vol. 26, no. 11, pp. 1262–1277, 2019.
- [114] A. de-la-Torre, C. T. Silva-Aldana, J. Muñoz-Ortiz et al., “Uveitis and multiple sclerosis: potential common causal mutations,” *Molecular Neurobiology*, vol. 56, pp. 8008–8017, 2019.

- [115] S. K. Harten, M. A. Esteban, D. Shukla, M. Ashcroft, and P. H. Maxwell, "Inactivation of the von Hippel-Lindau tumour suppressor gene induces Neuromedin U expression in renal cancer cells," *Molecular Cancer*, vol. 10, p. 89, 2011.
- [116] M. Fruzangohar, E. Ebrahimie, and D. L. Adelson, "A novel hypothesis-unbiased method for Gene Ontology enrichment based on transcriptome data," *PLoS One*, vol. 12, article e0170486, 2017.
- [117] J. Lee, E. R. Snyder, Y. Liu et al., "Reconstituting development of pancreatic intraepithelial neoplasia from primary human pancreas duct cells," *Nature Communications*, vol. 8, p. 14686, 2017.
- [118] V. G. Martinez, J. Crown, R. K. Porter, and L. O'Driscoll, "Neuromedin U alters bioenergetics and expands the cancer stem cell phenotype in HER2-positive breast cancer," *International Journal of Cancer*, vol. 140, pp. 2771–2784, 2017.
- [119] T. Ensho, K. Maruyama, K. Mori et al., "Neuromedin U precursor-related peptide (NURP) exerts neuromedin U-like sympathetic nerve action in the rat," *Biochemical and Biophysical Research Communications*, vol. 492, no. 3, pp. 412–418, 2017.
- [120] X. Yang, C. C. Wang, W. Y. W. Lee, J. Trovik, T. K. H. Chung, and J. Kwong, "Long non-coding RNA HAND2-AS1 inhibits invasion and metastasis in endometrioid endometrial carcinoma through inactivating neuromedin U," *Cancer Letters*, vol. 413, pp. 23–34, 2018.
- [121] X. G. Chen, L. Ma, and J. X. Xu, "Abnormal DNA methylation may contribute to the progression of osteosarcoma," *Molecular Medicine Reports*, vol. 17, pp. 193–199, 2018.
- [122] J. Watteyne, K. Peymen, P. Van der Auwera et al., "Neuromedin U signaling regulates retrieval of learned salt avoidance in a *C. elegans* gustatory circuit," *Nature Communications*, vol. 11, p. 2076, 2020.
- [123] A. C. Kaushik, A. Mehmood, D. Q. Wei, and X. Dai, "Systems biology integration and screening of reliable prognostic markers to create synergies in the control of lung cancer patients," *Frontiers in Molecular Biosciences*, vol. 7, p. 47, 2020.
- [124] G. M. Jowett and J. F. Neves, "Commentary: neuronal regulation of type 2 innate lymphoid cells via neuromedin U," *Frontiers in Pharmacology*, vol. 9, p. 230, 2018.
- [125] S. Peng, Y. Lu, P. Li et al., "The short interference RNA (siRNA) targeting NMUR2 relieves nociception in a bone cancer pain model of rat through PKC-ERK and PI3K-AKT pathways," *Biochemical and Biophysical Research Communications*, vol. 512, pp. 616–622, 2019.
- [126] L. Lu, R. Wang, and M. Luo, "An optical brain-to-brain interface supports rapid information transmission for precise locomotion control," *Science China. Life Sciences*, vol. 63, pp. 875–885, 2020.
- [127] K. Maruyama, H. Kaiya, M. Miyazato, N. Murakami, K. Nakahara, and K. Matsuda, "Purification and identification of native forms of goldfish neuromedin U from brain and gut," *Biochemical and Biophysical Research Communications*, vol. 517, no. 3, pp. 433–438, 2019.
- [128] L. Lu, Y. Ren, T. Yu et al., "Control of locomotor speed, arousal, and hippocampal theta rhythms by the nucleus incertus," *Nature Communications*, vol. 11, no. 1, p. 262, 2020.